8-18-2015 12:00 AM

Hierarchical Organization in Auditory Cortex of the Cat Using High-Field Functional Magnetic Resonance Imaging

Amee J. Hall, *The University of Western Ontario*

Supervisor: Stephen G Lomber, *The University of Western Ontario*

A thesis submitted in partial fulfillment of the requirements for the Doctor of Philosophy degree in Anatomy and Cell Biology

HIERARCHICAL ORGANIZATION IN AUDITORY CORTEX OF THE CAT USING HIGH-FIELD FUNCTIONAL MAGNETIC RESONANCE IMAGING

(Thesis format: Integrated Article)

by

Amee Joy Hall

Graduate Program in Anatomy and Cell Biology

A thesis submitted in partial fulfillment
of the requirements for the degree of
Doctorate of Philosophy

The School of Graduate and Postdoctoral Studies
The University of Western Ontario
London, Ontario, Canada

Abstract

Sensory localization within cortex is a widely accepted and documented principle. Within cortices dedicated to specific sensory information there is further organization. For example, in visual cortices a more detailed functional division and hierarchical organization has been recorded in detail. This organization starts with areas dedicated to analysis of simple visual stimuli. Areas higher in the organization are specialized for processing of progressively more complex stimuli. A similar hierarchical organization has been proposed within auditory cortex and a wealth of evidence supports this hypothesis. In the cat, the initial processing of simple auditory stimuli, such as pure tones, has been well documented in primary auditory cortex (A1) which is also the recipient of the largest projection from the thalamus. This indicates that at least the initial stages of a hierarchy exist within auditory cortex. Until now it has been difficult to investigate the remaining hierarchy in its entirety because of methodological limitations. In the present set of investigations the use of functional magnetic resonance imaging (fMRI) facilitated the investigation of auditory cortex of the cat in its entirety. Results from these investigations support the proposed hierarchy in auditory cortex in the cat with lower cortical areas selectively responding to more simple stimuli while higher areas are progressively more responsive to complex stimuli.

Keywords

fMRI, 7T, High-Field, Cat, Sparse, Continuous, Tonotopy, Complex, Auditory, Cortex, Hierarchy

Dedication

To any graduate student who may find this thesis in the future. Pressure creates diamonds and turbulent water smooth's rough edges but the potential was always there. Keep working, keep writing, you can do it!

Co-Authorship Statement

All research conducted in this thesis was in collaboration with my supervisor, Dr. Stephen G. Lomber. Contributions of additional authors are detailed below.

Chapter 2 – This initial project was the first of its kind which necessitated consultation with experts in multiple fields. Dr. Trecia A Brown assisted with data collection and provided advice for data analysis. Dr. Jessica A Grahn assisted in the use of SPM for analysis of animal data, provided advice on additional data analysis, and was involved in editing the final manuscript. Joseph S Gati, Pam L Nixon, Sarah M Hughes and Dr. Ravi S Menon provided technical assistance with respect to MRI acquisition and animal care.

Chapter 4 – Dr. Blake E Butler developed an average cat brain template which was used in analysis of all data for this chapter. Dr. Butler also assisted in preparation of the manuscript for publication.

Acknowledgments

There is, quite literally, an army of people who have supported me and this work academically, emotionally, physically and spiritually. While I am going to give specific credit to a few, it does not diminish the impact of those I did not name.

First and foremost, I would like to thank my supervisor, Dr Stephen Lomber, who made this whole experience possible. He has served as an outstanding mentor for more than 10 years. I owe my graduate degree and my enthusiasm for neuroscience completely to Dr Lomber. I am honored to have studied under an academic powerhouse.

I also owe a huge debt of gratitude to my fellow lab members. Dr Shveta Malhotra was an inspiration and mentor in my early ventures as an undergraduate volunteer in the lab. Dr Trecia Brown who provided technical support but more importantly a constant reassurance that "It will all work out". Dr Nicole Chabot who, in addition to technical help, taught me by example about the kind of person I want to be. Dr Melanie Kok, my comrade-in-arms, commiserating and celebrating together as we each passed hurdles at the same time. Dr Blake Butler who, along with his professional knowledge, shared many laughs keeping me sane through some of the hardest parts. Lastly, this work would not have been possible without Pam Nixon whose expertise and open door were invaluable.

I will also be eternally grateful to my advisory committee, Dr Jody Culham, Dr Ewan Macpherson, and Dr Vania Prado. While they were incredibly encouraging they also tempered my goals which were, at times, overly ambitious. Their input, reassurance, and honesty were instrumental to the completion of this work.

This whole process would not have been possible without the support of my family. They were, and still are, an unmovable rock during the floods, and sometimes tsunami's, of life. My parents have been an inspiration and support my whole life and this was no exception. My brother and his family have been a beacon of light helping me to keep my priorities straight. My niece and nephew offered their love and laughter keeping my spirits up. Last, but nowhere near least, my son who provided a daily reminder to keep pressing forward. I love you all, you are all my heroes.

Table of Contents

List of Tables

List of Figures

List of Abbreviations

2DG	2-deoxy-D-[^{14}C]glucose
7T	7-Tesla
A1	primary auditory cortex
A2	second auditory cortex
AAF	anterior auditory field
AC	auditory cortex
aes	anterior ectosylvian sulcus
AL	anterolateral division of belt auditory cortex
BBN	broadband noise
BOLD	blood-oxygen level dependent
CL	caudolateral division of belt auditory cortex
CM	caudomedial division of belt auditory cortex
CPB	caudal parabelt
dB	decibel
dPE	dorsal posterior ectosylvian
DTI	diffusion tensor imaging
DZ	dorsal zone
EEG	electroencephalogram
EPI	echo planar imaging
FAES	auditory field of the anterior ectosylvian sulcus
FM	frequency modulated
fMRI	functional magnetic resonance imaging
HG	Heschyl's gyrus
HRF	hemodynamic response function
IC	inferior colliculus
IN	insular area
ILD	interaural level difference
iPE	inferior posterior ectosylvian
ITD	interaural time difference
kHz	kilohertz
LFP	local field potential

LS	lateral sulcus
MEG	magnetoencephalography
MGB	medial geniculate body
MGd	dorsal division of the medial geniculate body
MGm	medial division of the medial geniculate body
MGv	ventral division of the medial geniculate body
ML	middle lateral division of belt auditory cortex
MM	middle medial division of belt auditory cortex
MRI	magnetic resonance imaging
NBN	narrow band noise
NHP	non-human primate
PAF	posterior auditory field
PSC	percent signal change
pes	posterior ectosylvian sulcus
R	rostral division of core auditory cortex
RM	rostromedial division of the belt auditory cortex
ROI	region of interest
RPB	rostral parabelt
RT	rostrotemporal division of core auditory cortex
RTL	rostrotemporal lateral division of belt auditory cortex
RTM	rostrotemporal medial division of belt auditory cortex
SPL	sound pressure level
ss	suprasylvian sulcus
STS	superior temporal sulcus
T	temporal area
TA	acquisition time
TR	repetition time
V1	primary visual cortex
VAF	ventral auditory field
VPAF	ventral posterior auditory field
vPE	ventral posterior ectosylvian

Chapter 1 – Introduction

The transition from theological or mythical beliefs to analysis through logic and experience that began around the 6th century B.C. revolutionized how we looked at the world around us. It was during this time that the connection between the brain and our senses was made, by Alcmaeon. One of the first to perform dissections, Alcmaeon noted a physical connection between the back of the eye and the brain and theorized that similar connections existed for the organs of all of the other senses (Wickens, 2015). Since this time, there has been a dramatic advancement in our understanding of the brain's connection to, and processing of, our senses. For example, we now know that not only are senses connected to the brain but that specific regions of the brain are dedicated to processing of individual senses. Also, these sensory cortices can be further subdivided into areas of functional specificity. The cortices responsive to visual stimuli, for example, are subdivided into areas which specifically process visual features like faces (Taylor and Downing, 2011), spatial location (Land, 2014), and motion (Lui and Rosa, 2015). It has been proposed that similar areal specialization within auditory cortices, located on the lateral aspect of the cerebrum, also exists.

In this chapter, the methods used to define cortical areas in general will first be discussed in order to give context to our current understanding of auditory cortex. Next, the present knowledge surrounding the anatomy, organization, and function of auditory cortex will be outlined. Then, the use of functional magnetic resonance imaging (fMRI) for investigations of auditory cortex will be discussed. Finally, the necessity and hypotheses for each of the three experiments included in this thesis, will be specified.

1.1 Defining Cortical Areas

Major landmarks are commonly used to describe gross anatomical organization. For example, lobes of the human cerebrum and general location of sensory cortices are both described using major sulci and gyri (Bear et al., 2007). Although the general location of sensory cortices can be described this way, sub-divisions within each sense cannot. There are many different methods for defining cortical subdivisions and, usually, these

methods agree. Sometimes, however, methods do disagree and it is important, in these instances, to have a working knowledge of the methods in question. This section is dedicated to outlining major methods of delineation and their respective strengths and weaknesses.

1.1.1 Structural

In the early 20th century Korbinian Brodmann divided the human cortex into 52 discrete cortical regions (Brodmann, 1909). To do this, Brodmann processed tissue with stains which enabled the visualization of cytoarchitectural, cellular organization, differences among the layers of cortex. The most common method for cytoarchitectural assessment of this sort is the Nissl stain. The Nissl stain enables the visualization of neuronal cell bodies by staining the nucleus and surrounding material (Bear et al., 2007). The densities of cell bodies are then used to demonstrate six distinct layers of cortex. While the full thickness of cortex is relatively constant throughout the cerebrum, the distribution of layers does change. It is these variations in laminar distribution that provide the basis for the earliest proposed cortical subdivisions, such as those suggested by Brodmann.

A more recently developed cytoarchitectural method uses SMI-32 immunoreactivity which stains non-phosphorylated neurofilament proteins (Sternberger and Sternberger, 1983). When used in conjunction with cortical tissue this results in pyramidal cells in layers III and V being selectively stained (van der Gucht et al., 2001). Pyramidal neurons in these layers are known to project to subcortical structures or to distant cortical regions. Since individual areas within cortex will have different projection patterns it stands to reason that there will be differences in SMI-32 staining between areas. As expected, differences in the quality, diversity, density, and distribution of stained cells contribute to the demarcation of cortical areas (van der Gucht et al., 2001). SMI-32 has been successfully used to delineate finer subdivisions within visual cortex of the old world monkey (Lewis and Van Essen, 2000) and cat (van der Gucht et al., 2001) and auditory cortex of the cat (Mellott et al., 2010).

Techniques using cytoarchitecture to define cortical boundaries, such as Nissl and SMI-32, are useful but do not provide a complete picture. They can provide little

information about the functional properties for areas that are defined. Also, they cannot provide information about connections, and their effects, of individual areas to and from other cortical regions or subcortical structures.

Patterns of connections can also be used to demarcate cortical areas and define their position within a hierarchical organization. Substances, designed to travel along neuronal axons, are injected into cortex. Cortical tissue is then processed in order to visualize the substance and trace projections to or from the site of injection. Retrograde tracers, such as wheat germ agglutinin conjugated to horse radish peroxidase (WGA-HRP), are taken up at axon terminals and fill the axon back towards the cell bodies. After tissue is processed, it is then analyzed for cell bodies. The areal and laminar distribution of cell bodies provides information about cortical and subcortical structures which provide input to the injected region. Anterograde tracers, such as biotinylated dextrose amine (BDA), are taken up at cell bodies and transported towards the axon terminals. After being processed, tissue is examined for labeled terminal boutons. The areal and laminar distribution of boutons provides information about cortical and subcortical structures that the injected area is projecting to.

Retrograde and anterograde tracing techniques can each provide important information separately. Without both, however, there is important missing information. One neuron can have hundreds of synaptic contacts or just a handful. Therefore, the number of cell bodies at the origin of a projection, using retrograde transport, does not accurately predict the effect on the cortical terminus. Similarly, the number of boutons at the terminus of a projection, using anterograde transport, does not accurately predict the number of contributing neurons at the origin. Both sets of data are needed to form a complete anatomical picture with regard to connectivity between cortical areas.

Using both retrograde and anterograde tracing techniques, Felleman and Van Essen (1991) described three patterns of connection between cortical areas relating to their position within a processing hierarchy. Using their criteria, each projection can be classified as ascending (feed forward), lateral (equivalent processing levels), or descending (feedback). Felleman and Van Essen (1991) then used these classifications to

describe a hierarchical organization within the visual, somatosensory and motor cortices of the old world monkey and visual cortex of the cat.

All previous methods are invasive and many, especially tract tracing, cannot be performed in human subjects. Recently, a technique called diffusion tensor imaging (DTI) has enabled tract tracing in humans. As water molecules diffuse along axons they experience different magnetic fields and by measuring these changes the length of a tract can be traced (Huettel et al., 2009). This method, however, cannot infer direction (anterograde vs retrograde) or even how many neurons participate in the tract, only that it exists.

Cytoarchitectural and tract tracing methods result in a wealth of information about cortical subdivisions. Using cytoarchitecture, boundaries between subdivisions can be clearly delineated. Tract tracing provides information about strength of connection between cortical areas and even their place within a processing hierarchy. This information can give rise to theories about effects of one area on another and functional division of processing. However, neither can confirm functional properties of individual areas and, in fact, functional properties of cortical areas can also define borders.

1.1.2 Functional

A method bridging the structural and functional delineation of cortex was developed in the 1970's. A radioactive substance, 2-deoxy-D-[^{14}C]glucose (2DG), competes with glucose, using the same mechanism to cross the blood-brain barrier (Sokoloff et al., 1977). Once across the barrier, 2DG is then processed using the same pathway as glucose. Unlike glucose, however, the products of 2DG processing are not cleared from the cell. Neural tissue uses glucose to produce the energy that is needed and, therefore, consumes more glucose when active. As a result, when 2DG is administered systemically, neurons that are more active contain more of the radioactive products. Tissue can then be processed and, based on the amount of radioactivity present, function can be assigned to specific cortical areas. Using this technique, Tootell and colleagues (1982) were not only able to distinguish primary visual cortex (V1) from surrounding cortices but also demonstrate a functional map of the visual field within V1.

The action potential and changes in electrical potential also provide functional information that can be used to differentiate cortical areas. For example, a map of the visual field, which is directly replicated on the retina, is maintained up to visual cortex. Using electrical stimulation or recording from cortex, at least three complete maps of visual space can be charted, designating different areas of cortex, in multiple species (Dobelle et al., 1979; Hubel and Wiesel, 1965; Tiao and Blakemore, 1976). Similarly, multiple somatosensory (Whitsel et al., 1969; Woolsey and Fairman, 1946) and tonotopic (Merzenich et al., 1976; Reale and Imig, 1980; Romani et al., 1982) maps exist within cortex. In addition to mapping, differences between areas can also be functionally demonstrated using: changes in response when surrounding cortex is damaged or deactivated (Carrasco and Lomber, 2009a, b; Kaas and Krubitzer, 1992; Kok et al., 2015), response latency (Carrasco and Lomber, 2011; Nowak et al., 1995; Raiguel et al., 1989), and specificity for different stimuli (Fattori et al., 2009).

Functional delineation can also be done using deactivation or lesion techniques combined with psychophysical testing. By either temporarily deactivating or permanently destroying specific cortical areas, deficits or changes in the ability to perform specific tasks reveal the functional effects of that area. This technique has been used many times to investigate cortical function in the auditory (Lomber and Malhotra, 2008; Malhotra et al., 2004; Malhotra and Lomber, 2007), visual (Nguyen et al., 2004; Silvanto et al., 2005) and somatosensory (Garraghty et al., 1990; Glassman, 1994) systems as well as higher level cognition (Lajoie and Drew, 2007; Petrides, 2000; Urgesi et al., 2007).

Most of the techniques previously detailed are invasive and are rarely possible in human subjects. When they are performed, it's usually because a pre-existing neurological condition allows for it. For this reason, non-invasive techniques like magnetoencephalography (MEG), electroencephalography (EEG), and functional magnetic resonance imaging (fMRI) have been developed.

Both MEG and EEG are based on a similar neural principal called a local field potential (LFP Bear et al., 2007). A LFP is generated when hundreds of neurons are

firing in synchrony, the more cells which are involved the stronger the signal. MEG measures changes in the magnetic field generated orthogonal to the electrical current. EEG measures the voltage fluctuations, via electrodes placed on the scalp, resulting from the same electrical current. While both of these methods are relatively non-invasive they have a limited field of view. MEG has difficulty resolving any activity finer than 5mm, and EEG is limited by the number and placement of electrodes.

The fMRI technique takes advantage of the local change in blood oxygenation while neurons are active (Huettel et al., 2009). Active neurons require more oxygen than those at rest which results in an initial local increase in deoxygenated blood. The systemic response overcompensates and floods the area with oxygenated blood. Inside of a magnetic field oxygenated and deoxygenated blood responds differently to radio frequency pulses which can be recorded in an image. This blood-oxygen-level-dependent (BOLD) signal is then analyzed for changes in response to different stimuli. Using this technique, cortical areas have been delineated using visual (Dougherty et al., 2003; Fize et al., 2003; Wong and Sharpe, 1999) and auditory (Da Costa et al., 2015; Langers et al., 2014; Petkov et al., 2006; Schönwiesner et al., 2014; Woods et al., 2010) maps, specificity for stimuli or stimulus features (d'Avossa et al., 2007; Liu et al., 2010; Ortiz-Rios et al., 2015; Petkov et al., 2008; von Kriegstein et al., 2008; Woods et al., 2010) and higher order cognitive tasks (Kim et al., 2015).

In summary, functional delineations within cortex can be made using cellular metabolism, measuring action potentials and changes in electrical potential, and lesion or deactivation techniques. Most of these, however, are invasive and only rarely used in human studies. Techniques such as fMRI are used for non-invasive delineation of cortical areas but cannot provide information about processes taking place at a cellular level. Structural techniques can provide direct information about cortical subdivisions, and can also provide information about potential functional influences of individual cortical areas on each other. Overall, each technique has limitations as to how much information it can provide. However, in concert, structural and functional techniques can provide a global understanding of the sub-division of the cortices examined.

1.2 Auditory Cortex

Auditory cortex has been the subject of investigation for decades. As a result, much is known about its subdivisions. The ability to use more invasive techniques has resulted in more detailed understanding of cat and monkey cortices in comparison to that of human cortex. The current understanding of auditory cortex subdivisions in the cat, monkey and human are outlined in Fig 1.1. In this section, what is currently known, and how it was determined, about cat, monkey and human auditory cortex will be detailed followed by current understanding and theories underlying hierarchical processing.

1.2.1 Human and Monkey Auditory Cortex

The delineation of human auditory cortex has proven difficult but most investigations agree that it is contained within the lateral (Sylvian) fissure. The most current understanding of human auditory cortex, that is consistent across investigations, is that there is a core-like region of cortex (Fig 1.1C, red). This region is located on Heschl's gyrus (HG) in area 41 of Brodmann's cytoarchitectural map deep within the Sylvian fissure in both hemispheres, and can be functionally subdivided into multiple areas.

Early anatomists, such as Brodmann (1909), divided cortex in this region into multiple numbered areas (Fig 1.1C). Area 41, on HG, has been the focus of most human auditory research because of its gross anatomical similarity to core auditory cortex found in the monkey. Investigations using DTI have demonstrated a strong connection between the medial geniculate body (MGB) of the thalamus and Heschl's gyrus (Berman et al., 2013; Javad et al., 2014; Keifer et al., 2015). In the monkey, the strongest thalamic connection to the core auditory cortex is the ventral division of the MGB (de la Mothe et al., 2006; Hackett, 2008; Pandya and Rosene, 1993). This means that the connection between the MGB and HG observed in the human closely resembles that of the monkey.

Beyond imaging techniques, which will be addressed in the next section, there are very few functional investigations of human auditory cortex. When electrophysiological investigations have been conducted, there is a pre-existing condition, usually epilepsy, which necessitated the invasive procedure (Brugge et al., 2008; Nourski et al., 2013; Steinschneider et al., 2014). Regardless, these studies have identified a region on HG

with similar characteristics, such as tonotopy, to that of core auditory cortex in the monkey.

Auditory cortex of the monkey is known in much more detail (Fig 1.1B). Subdivisions of auditory cortex include a central region, or core (Fig 1.1B, red) which is further segmented into three areas. The core is surrounded on all sides by another region, or belt (Fig 1.1B, orange) which is also subdivided into multiple areas. Lateral to the belt there is a third region, or parabelt (Fig 1.1B, green), which is subdivided into two areas.

Knowledge about subdivisions of auditory cortex in the monkey starts with the pattern of thalamic input. Auditory cortex of the monkey receives inputs from three distinct divisions of the MGB (Hackett, 2015); ventral (MGv), medial (MGm), and dorsal (MGd). The main source of input to core auditory cortex, including its subdivisions, is MGv (de la Mothe et al., 2006; Morel et al., 1993; Morel and Kaas, 1992). The MGv contains a tonotopic map, an organization which is maintained up to the level of cortex. The most robust thalamic input to belt or parabelt areas is from MGd (de la Mothe et al., 2006; Hackett et al., 1998b) only a portion of which is tonotopic.

Early investigations of monkey auditory cortex focused primarily on the core. Imig and colleagues (1977) identified five cortical divisions. Two of which, the primary auditory field (A1) and rostral field (R), correspond to what is now known as the core region (Fig 1.1B). They made this distinction based on anatomy as well as tonotopic maps using electrophysiology. In A1, higher frequencies were found to be represented caudo-medially progressing to lower frequencies rostro-laterally at the border of R (Imig et al., 1977; Merzenich and Brugge, 1973). At the border of R, the tonotopic gradient was then reversed and progressed back to high frequency representations at the lateral most borders of R. Later, a second reversal, and third tonotopic gradient, was observed at the lateral border of R (Morel and Kaas, 1992). Anatomical investigations would later confirm that a third division, the rostrotemporal field (RT), is also part of the core (Hackett et al., 1998a).

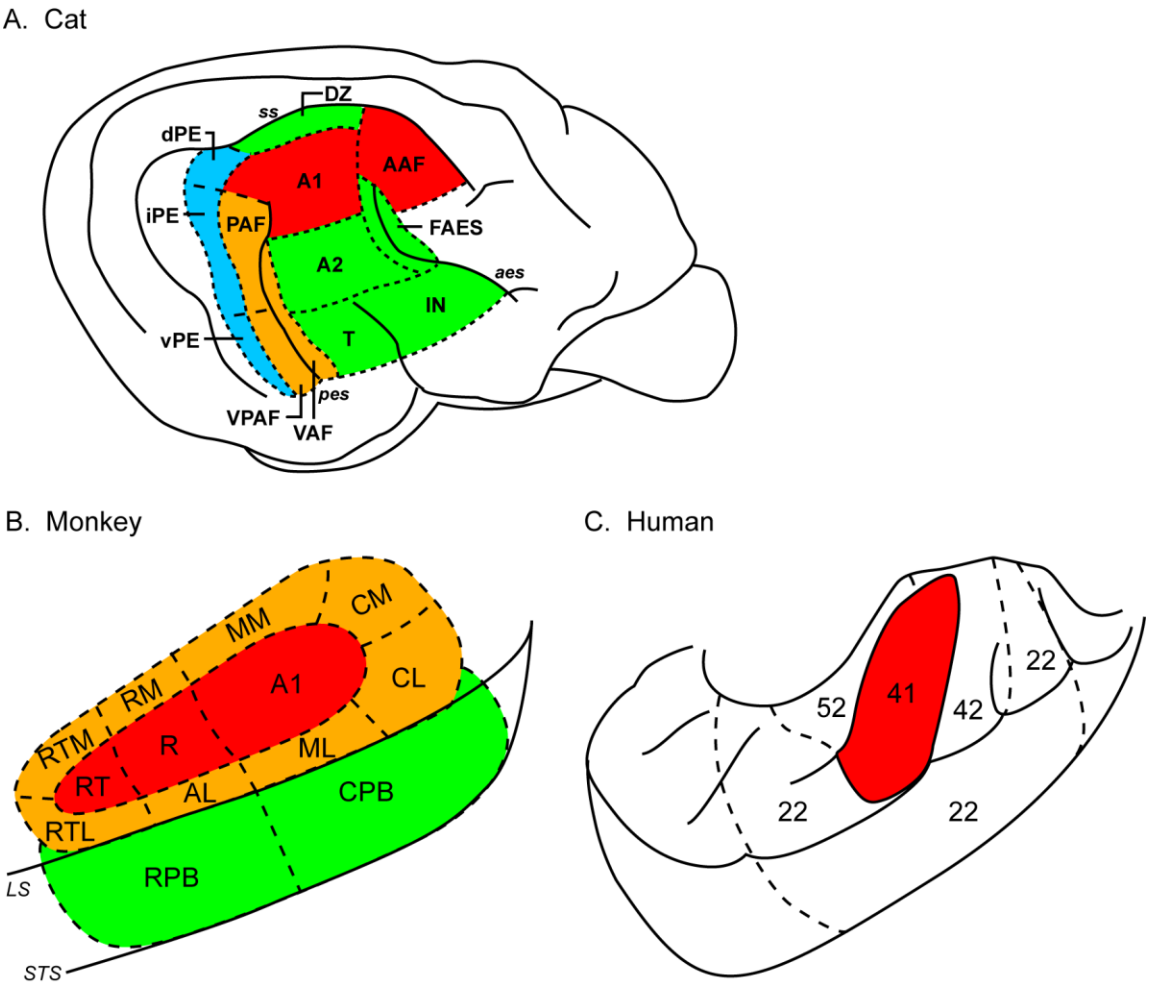

Figure 1.1 Auditory Cortex of Cat, Monkey, and Human

A) Thirteen subdivisions of the auditory cortex of the cat. B) Thirteen subdivisions of the auditory cortex of the monkey. C) Subdivisions of human auditory cortex determined by Brodmann. Core (red), tonotopic non-core (orange), non-tonotopic (green), and multisensory (blue) areas are indicated in each model using functional methods. For abbreviations refer to the list of definitions preceding this chapter.

The three other fields that Imig and colleagues (1977) identified were some of the earliest documentations of the belt region (Fig 1.1B). They identified caudomedial (CM), posterolateral, and anterolateral fields within the belt region. The posterolateral and anterolateral fields consist of the posterior or anterior half of the lateral belt, respectively. Further investigations using anatomical tracers and electrophysiological recording using pure tone stimuli revealed a much more extensive subdivision of the belt region (Galaburda and Pandya, 1983; Morel and Kaas, 1992). Morel and Kaas (1992) identified seven divisions of the belt region which are still recognized today. Medial belt areas included CM as well as rostromedial (RM), medial rostrotemporal (RTM), and a caudal area that wraps around the posterior border of A1. Lateral belt areas included mediolateral (ML), rostrolateral (RL), and rostrotemporal lateral (RTL) areas. Areas outside of core auditory cortex were not consistently responsive to pure tones and more complex stimuli were soon employed. Investigators began using more complex stimuli, such as bandpassed noise bursts, frequency modulated (FM) sweeps, and conspecific vocalizations, to elucidate further subdivisions of the belt region (Rauschecker, 1997; Rauschecker et al., 1995). Belt areas are more consistently driven using these more complex stimuli and were found to be selective to specific stimulus features. For example, neurons in the lateral belt were found to be selective for specific speed and direction of FM sweep stimuli (Rauschecker, 1997). Also, using band passed noise stimuli centered at different frequencies, a tonotopic organization was identified in the belt region progressing along an anterior-posterior axis (Kaas et al., 1999; Kosaki et al., 1997; Rauschecker, 1997).

The rostral parabelt (RPB) and caudal parabelt (CPB) receive direct inputs from the rostral or caudal belt regions, respectively, but receive no input from the core (Hackett et al., 1998a). The RPB responds well to complex stimuli, such as white noise, but pure tones cannot evoke activity (Kaas et al., 1999). The CPB, however, responds to pure tones over a wide range of frequencies, has been shown to selectively respond to motion and direction and, on rare occasions, has multisensory responses. Also, connections to cortical areas outside of auditory cortex, such as prefrontal and adjacent temporal cortices, largely originate from the parabelt (Hackett et al., 1999; Romanski et al., 1999a).

1.2.2 Cat Auditory Cortex

Early investigations of cat auditory cortex utilized lesions of the cochlea (Walzl and Woolsey, 1946) or large swathes of cortex (Kaas et al., 1967; Meyer and Woolsey, 1952) and measured cortical and behavioral responses to pure tones. Using these methods it was not possible to delineate finer subdivisions of auditory cortex. They were, however, able to demonstrate that the extent of auditory cortex is bounded by the suprasylvian sulcus (ss). Also, these early investigations demonstrated a strong connection to the medial geniculate body (MGB) through neural degeneration in response to cortical lesions. These early studies provided the foundation for future investigations of the auditory cortex of the cat.

The present understanding and knowledge of cat auditory cortex (Fig 1.1) includes 13 subdivisions based on structure and function. Similar to the monkey, areal delineation of cat auditory cortex can first be seen through the pattern of thalamic innervation. The largest source of thalamic input to tonotopically organized cortex, namely the primary auditory cortex (A1), anterior auditory field (AAF), posterior auditory field (PAF), vetral posterior auditory field (VPAF) and ventral auditory field (VAF), is from the ventral division of the MGB (Lee and Winer, 2008a). In contrast, the second auditory area (A2), the auditory field of the anterior ectosylvian sulcus (FAES), the dorsal zone (DZ), and temporal (T) area receive most of their thalamic input from the dorsal division of the MGB (Lee and Winer, 2008a). The remaining areas of auditory cortex are evenly innervated by different portions of the MGB and other thalamic neuclei.

Delineation of auditory cortex of the cat is also demonstrated based on corticocortical connections and structural methods. Excluding the dorsal posterior ectosylvian (dPE), intermediate posterior ectosylvian (iPE), and ventral posterior ectosylvian (vPE) areas, all subdivisions of cat auditory cortex have been successfully defined using SMI32 (Mellott et al., 2010). The SMI32 derived borders and tonotopic maps of A1 and AAF closely match, providing evidence that SMI32 accurately delineates areas of auditory cortex. Retrograde tracers, injected into each of the thirteen areas, unveils a unique pattern of connectivity between areas of auditory cortex (Lee and Winer, 2008b). Areas known to be tonotopically organized are strongly interconnected. For

each of these areas, the three largest inputs (~40% of all ipsilateral cortical input) originate from the other tonotopic areas (Lee and Winer, 2008b, 2011). Interestingly, AAF provides the largest cortical input to A1 but provides minimal input to any other tonotopically organized area. Similarly, non-tonotopic auditory cortex of the cat is highly interconnected, in particular A2, T and IN. Multisensory areas dPE, iPE, and vPE are highly interconnected and are also innervated strongly by IN and T. While there are general patterns for each of the tonotopic, non-tonotopic, and multisensory groups, each individual area has a distinct pattern of innervation.

Investigations have also demonstrated that subdivisions of the auditory cortex of the cat can also be functionally defined. The earliest recordings from auditory cortex of the cat documented a tonotopic progression across the gyrus dorsal of the dorsal tips of the anterior ectosylvian sulcus (aes) and posterior ectosylvian sulcus (pes; (Evans and Whitfield, 1964). Since then, multiple tonotopic progressions have been identified (Reale and Imig, 1980). Low frequencies are represented at the antero-ventral most border of AAF, which progresses to higher frequencies at the A1 border. A reversal in the gradient then occurs at the AAF/ A1 border progressing back down to lower frequencies leading to the PAF border. Similar reversals occur at the A1/PAF and PAF/VPAF borders. Tonotopy is so distinctive of these areas that it is commonly used in current investigations to identify these areas for use with other methods (Carrasco et al., 2015; Carrasco and Lomber, 2009b; Kok et al., 2015; Mellott et al., 2010).

The location of the external auditory meatus of the cat makes functional delineation difficult for most areas ventral to A2. For this reason, most functional investigations focus on dorsal areas A1, PAF, AAF, and DZ. A1 has a response latency of ~18ms and a complete tonotopic representation that is approximately evenly distributed (Carrasco and Lomber, 2009a). AAF is tonotopically organized and latency values are similar to that of A1. However, there is a marked under-representation of mid-range frequencies in AAF (Carrasco and Lomber, 2009a; Imaizumi et al., 2004). PAF also has a complete tonotopic map but has significantly longer latancies (~36ms) than A1 and AAF (Carrasco and Lomber, 2009b). Anatomical studies, which demonstrated that these tonotopically organized areas are highly interconnected (Lee and Winer, 2008b,

2011), led to investigations of functional effects on each other. Reversible deactivation of AAF resulted in lower response strength in A1 to frequencies outside of those being deactivated (Carrasco and Lomber, 2009a). Receptive fields and thresholds within A1 were also affected by AAF deactivation. However, latencies and characteristic frequency tuning within A1 were not affected. In comparison, deactivation of A1 resulted in minimal response changes in AAF (Carrasco and Lomber, 2009a). In contrast, responses in PAF after A1 deactivation were significantly impaired, though not completely abolished (Carrasco and Lomber, 2009b). Therefore, while A1 and AAF are processing stimuli simultaneously, as indicated by similar latencies, AAF has a much bigger effect on A1 than the reverse. A1, however, is not dependent on the input from AAF. In contrast, PAF is highly dependent on A1.

Behavioral investigations have also demonstrated functional differences among areas within auditory cortex of the cat. Unilateral reversible deactivation of A1, PAF, or FAES results in a contralateral localization deficit (Malhotra et al., 2004). Later, Malhotra and Lomber (2007) would confirm that bilateral deactivation of the same three areas results in a complete loss of accurate acoustic orienting. Similar deactivations also indicate that DZ plays a role in auditory orienting (Malhotra et al., 2008). However, the effects were a reduction in orienting accuracy rather than a complete loss. In contrast, while deactivation of AAF did not affect auditory localization it did significantly affect auditory discrimination (Lomber and Malhotra, 2008). The effects of deactivating either AAF or PAF on either discrimination or localization, but not both, supported a long standing theory of hierarchical processing within auditory cortex.

1.2.3 Hierarchical Organization

More than three decades ago, Mishkin and colleagues (1983) proposed a model of hierarchical organization within visual cortex consisting of two streams (Fig 1.2A). After initial processing by the primary visual cortex (V1) information was then sent to dorsal cortical areas, to be processed for location, or ventral cortical areas, to be processed for identification. These parallel processing streams, commonly referred to as ‘where’ and ‘what’, respectively are also thought to exist within auditory cortex as well (Rauschecker and Tian, 2000; Romanski et al., 1999b). In the monkey, the dorsal ‘where’ stream starts

in core area A1 which projects to dorsal belt areas CM and CL and pre-frontal cortex via the posterior parietal cortex (Rauschecker and Tian, 2000; Recanzone and Cohen, 2010). Conversely, the ventral 'what' stream starts in core areas R and RT which are then projected to the ventral belt areas RTL and AL, the parabelt, other ventral temporal areas and finally ventral prefrontal cortex.

A similar division of labor has been proposed in cat auditory cortex as well (Fig 1.2B (Carrasco and Lomber, 2009b; Hackett, 2011; Lee and Winer, 2011; Lomber and Malhotra, 2008). Based on comparable thalamic input (Lee and Winer, 2008a) and response properties (Carrasco and Lomber, 2009a), A1 and AAF have been proposed to operate as a core region similar to that found in the monkey. PAF is dependent on A1 (Carrasco and Lomber, 2009b) and, when deactivated, results in a deficit in localization of auditory stimuli (Malhotra et al., 2004; Malhotra and Lomber, 2007) but not discrimination (Lomber and Malhotra, 2008). This has led to the hypothesis that the 'where' stream, in auditory cortex of the cat, starts in A1 and proceeds through PAF to more ventral areas. Conversely, AAF is not dependent on A1 (Carrasco and Lomber, 2009a) and, when deactivated, results in a deficit in discrimination but not localization (Lomber and Malhotra, 2008). This has led to the hypothesis that the 'what' stream, in auditory cortex of the cat, begins with AAF. Taken together this evidence supports the theory of dual processing streams in auditory cortex of the cat.

1.3 fMRI and Audition

Early uses of fMRI in investigations of human cortex in response to auditory stimuli used speech sounds which resulted in activations outside of core auditory cortex (Binder et al., 1997; Binder et al., 1994; Le Bihan et al., 1995). To better elucidate cortex comparable to the core, belt, and parabelt areas of the monkey, however, investigators use more simple stimuli such as pure tones (Langers et al., 2007; Strainer et al., 1997; Yetkin et al., 2004). Tonotopy in different areas of auditory cortex is a common characteristic across species (Hackett, 2015). Therefore, demonstrating tonotopy and using it to delineate areas in human auditory cortex has become a common theme of fMRI investigations.

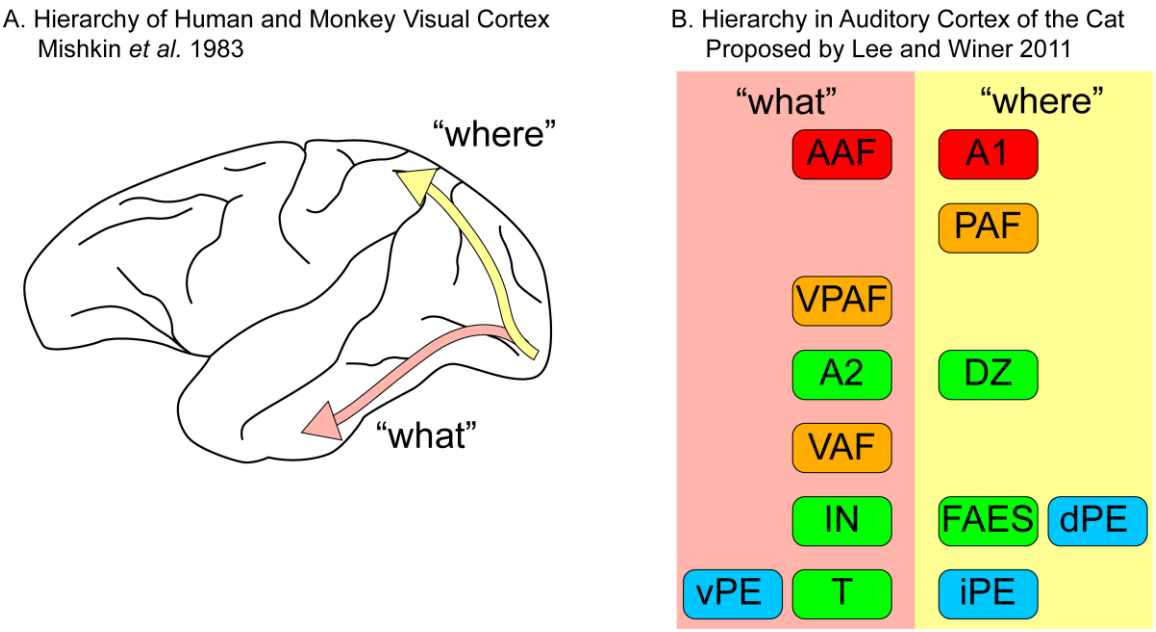

Figure 1.2 Dual processing streams in the visual and auditory systems.

Early fMRI investigations of tonotopy in human auditory cortex only used one or two frequencies (Bilecen et al., 1998; Wessinger et al., 1997). They noted that activations were located on HG and the higher frequency stimulus was represented medial to that of the lower frequency. Later studies used multiple frequencies and demonstrated that the progression from high to low frequencies is more gradual (Langers et al., 2007; Petkov et al., 2004). These studies, however, were only able to observe a single tonotopic progression, in human auditory cortex. It is well accepted, in multiple species, that core auditory cortex consists of multiple areas. For this reason, investigations used higher field fMRI, resulting in better resolution, to discover subdivisions of auditory cortex in human subjects. Although they disagree on the number, several studies have now demonstrated multiple tonotopic gradients, indicating the presence of more than one subdivision of auditory cortex (Formisano et al., 2003; Seifritz et al., 2006; Talavage et al., 2004; Woods et al., 2009).

An extensive number of human fMRI studies have been dedicated to speech processing. Spoken words, syllables, and sentence perceptions result in foci of activation in the ventral temporal cortices outside of core, belt or parabelt regions (Humphries et al., 2014; Rauschecker, 1997; von Kriegstein et al., 2010; Yue et al., 2013). This corresponds well with the hierarchical model in which the ventral 'what' stream is dedicated to identification of stimuli. Conversely, investigations of auditory localization concur that more dorsal areas are involved in spatial processing (Ahveninen et al., 2014; Kopco et al., 2012). Varying locations are simulated by creating interaural level differences (ILD) and interaural timing differences (ITD).

Electrophysiological investigations of core auditory cortices of the monkey have demonstrated three tonotopically organized areas. Using fMRI, three tonotopically organized regions have been identified in the monkey (Petkov et al., 2006, 2009; Schönwiesner et al., 2014). Surrounding the core, is a region of cortex that is more active in response to broadband noise (BBN) rather than pure tones (Petkov et al., 2006, 2009). Sensitivity to BBN provided a method to distinguish core from belt areas and multiple tonotopic gradients within this belt enables distinction between belt areas (Petkov et al., 2006).

Similar to human work, cortical activation in response to vocalizations was located in anterior belt areas, ventral temporal cortex and prefrontal cortex (Petkov et al., 2008). However, in an anesthetized preparation activations within core and belt areas disappeared (Petkov et al., 2008).

The use of fMRI to investigate auditory cortex of the cat is in early stages. In fact, a single study defining the HRF of auditory cortex is the only available literature prior to those contained in this investigation. Brown and colleagues (2013) found that the HRF, in auditory cortex of the cat, rose from the time of presentation, peaked at approximately 4s, and gradually returned to baseline levels. These results closely mirror that of the monkey which also peak at approximately 4 s (Baumann et al., 2010).

1.4 Current Investigation

The investigations presented in the next three chapters were designed to elucidate the hierarchical model of parallel processing within auditory cortex of the cat. First, methodological optimization of fMRI with the cat model was addressed. Next, it was demonstrated that known properties of four cortical areas of the cat could be discerned using fMRI. Finally, complex auditory stimuli were used to probe ventral cortical areas, for which very little is known, for specificity in higher levels of processing.

1.4.1 Chapter 2: There's more than one way to scan a cat: Imaging cat auditory cortex with high-field fMRI using continuous or sparse sampling.

There are several different methods of image acquisition for the purpose of fMRI. The two most common methods are called sparse and continuous scanning. The BOLD signal used for fMRI rises and falls on the order of seconds. This resulting curve is called the hemodynamic response function (HRF) and serves as the basis for sparse scanning. Image acquisition is delayed, during sparse scanning, based on when the peak HRF should occur following stimulus onset. This allows stimuli to be presented between acquisitions and in quieter conditions. Benefits of sparse scanning include; the absence of potential confounding scanner noise at the time of stimulus presentation, data collected will be done at peak values, and transverse magnetization will fully recover before the

next acquisition resulting in better contrasts. Drawbacks to the sparse scanning method include: lengthened run time due to insertion of silent period which can be problematic with an anesthetized preparation; and, lower number of images acquired, because of lengthened trial times, could result in poorer statistical strength of the data.

Continuous scanning, like its name implies, takes images continuously throughout the run with no breaks between acquisitions. This method records the HRF in its entirety instead of selectively sampling at or near its peak like sparse scanning does. Benefits to continuous scanning include: a larger amount of data can be collected in a shorter amount of time; and, due to the larger amount of data, the statistical strength of resulting activity will be strengthened.

The investigation in chapter 2 uses the same stimuli with both methods to identify which is optimal for fMRI of cat auditory cortex. Both methods have been successfully used in fMRI investigations of auditory cortex in the monkey and human. We hypothesized that, given the statistical and time benefits, continuous sampling would be the optimal method for using fMRI to investigate auditory cortex of the cat.

1.4.2 Chapter 3: High-field fMRI reveals tonotopically organized and core auditory cortex in the cat.

Results from electrophysiological investigations of cat auditory cortex have confirmed a tonotopic gradient across AAF, A1, PAF, and VPAF (Carrasco and Lomber, 2010; Reale and Imig, 1980). At each of the borders, between tonotopically organized areas, there is a reversal in tonotopic gradient. Since tonotopy has been successfully identified in human (Da Costa et al., 2015; Langers et al., 2014; Saenz and Langers, 2014; Wessinger et al., 1997) and monkey (Petkov et al., 2006, 2009) auditory cortex using fMRI, it was hypothesized that it would also be observed in the cat. It was also hypothesized that, the borders between these areas could be delineated based on the tonotopic organization in response to pure tones.

Core areas of the monkey are more responsive to pure tones than belt areas and vice versa for complex sounds such as broadband noise (Petkov et al., 2006, 2009). Since A1 and AAF are theorized to be similar to core areas (Carrasco and Lomber,

2009a; Lee and Winer, 2011), it was also hypothesized that A1 and AAF would respond best to pure tones while PAF and VPAF would respond best to broadband noise.

1.4.3 Chapter 4: The cat's meow: A high-field fMRI assessment of cortical activity in response to vocalizations and complex auditory stimuli.

Dual processing streams in auditory cortex have long been theorized. Investigations of human and monkey auditory cortex have provided evidence of separate 'what' and 'where' streams. In the cat, evidence of a division of labor in auditory cortex has also been observed (Lomber and Malhotra, 2008). Deficits in discrimination between, but not localization of, auditory stimuli were observed following deactivation of AAF. Conversely, localization of, but not discrimination between, auditory stimuli were observed following deactivation of PAF. Based on thalamocortical and corticocortical connectivity it is proposed that areas ventral to A1, AAF, and PAF are higher order areas specialized for more complex processing (Lee and Winer, 2011). However, because of the technical difficulty in recording from this area, exploration of ventral auditory cortical areas using functional methods is sparse at best. The use of fMRI removes these limitations and enables investigations of ventral areas. Based on this, it was hypothesized that individual areas towards the temporal pole would be selectively active in response to more complex stimuli.

1.5 References

Ahveninen, J, Kopco, N, Jaaskelainen, IP, 2014. Psychophysics and neuronal bases of sound localization in humans. Hear Res, 307, 86-97.

Baumann, S, Griffiths, TD, Rees, A, Hunter, D, Sun, L, Thiele, A, 2010. Characterisation of the BOLD response time course at different levels of the auditory pathway in non-human primates. Neuroimage, 50, 1099-1108.

Bear, MF, Connors, BW, Paradiso, MA, 2007. Neuroscience: exploring the brain, 3 ed. Lippincott Williams & Wilkins, Baltimore, MD.

Berman, JI, Lanza, MR, Blaskey, L, Edgar, JC, Roberts, TP, 2013. High angular resolution diffusion imaging probabilistic tractography of the auditory radiation. AJNR Am J Neuroradiol, 34, 1573-1578.

Bilecen, D, Scheffler, K, Schmid, N, Tschopp, K, Seelig, J, 1998. Tonotopic organization of the human auditory cortex as detected by BOLD-FMRI. Hear Res, 126, 19-27.

Binder, JR, Frost, JA, Hammeke, TA, Cox, RW, Rao, SM, Prieto, T, 1997. Human brain language areas identified by functional magnetic resonance imaging. J Neurosci, 17, 353-362.

Binder, JR, Rao, SM, Hammeke, TA, Yetkin, FZ, Jesmanowicz, A, Bandettini, PA, Wong, EC, Estkowski, LD, Goldstein, MD, Haughton, VM, et al., 1994. Functional magnetic resonance imaging of human auditory cortex. Ann Neurol, 35, 662-672.

Brodmann, K, 1909. Vergleichende lokalisationslehre der grosshirnrinde in ihren prinzipien dargestellt auf grund des zellenbaues. Barth.

Brown, TA, Joanisse, MF, Gati, JS, Hughes, SM, Nixon, PL, Menon, RS, Lomber, SG, 2013. Characterisation of the BOLD response in cat auditory cortex. Neuroimage, 64, 458-465.

Brugge, JF, Volkov, IO, Oya, H, Kawasaki, H, Reale, RA, Fenoy, A, Steinschneider, M, Howard, MA, 3rd, 2008. Functional localization of auditory cortical fields of human: click-train stimulation. Hear Res, 238, 12-24.

Carrasco, A, Kok, MA, Lomber, SG, 2015. Effects of core auditory cortex deactivation on neuronal response to simple and complex acoustic signals in the contralateral anterior auditory field. Cereb Cortex, 25, 84-96.

Carrasco, A, Lomber, SG, 2009a. Differential modulatory influences between primary auditory cortex and the anterior auditory field. J Neurosci, 29, 8350-8362.

Carrasco, A, Lomber, SG, 2009b. Evidence for Hierarchical Processing in Cat Auditory Cortex: Nonreciprocal Influence of Primary Auditory Cortex on the Posterior Auditory Field. J Neurosci, 29, 14323-14333.

Carrasco, A, Lomber, SG, 2010. Reciprocal modulatory influences between tonotopic and nontonotopic cortical fields in the cat. J Neurosci, 30, 1476-1487.

Carrasco, A, Lomber, SG, 2011. Neuronal activation times to simple, complex, and natural sounds in cat primary and nonprimary auditory cortex. J Neurophysiol, 106, 1166-1178.

d'Avossa, G, Tosetti, M, Crespi, S, Biagi, L, Burr, DC, Morrone, MC, 2007. Spatiotopic selectivity of BOLD responses to visual motion in human area MT. Nat Neurosci, 10, 249-255.

Da Costa, S, Saenz, M, Clarke, S, van der Zwaag, W, 2015. Tonotopic gradients in human primary auditory cortex: concurring evidence from high-resolution 7 t and 3 t FMRI. Brain Topogr, 28, 66-69.

de la Mothe, LA, Blumell, S, Kajikawa, Y, Hackett, TA, 2006. Thalamic connections of the auditory cortex in marmoset monkeys: core and medial belt regions. J Comp Neurol, 496, 72-96.

Dobelle, WH, Turkel, J, Henderson, DC, Evans, JR, 1979. Mapping the representation of the visual field by electrical stimulation of human visual cortex. Am J Ophthalmol, 88, 727-735.

Dougherty, RF, Koch, VM, Brewer, AA, Fischer, B, Modersitzki, J, Wandell, BA, 2003. Visual field representations and locations of visual areas V1/2/3 in human visual cortex. J Vis, 3, 586-598.

Evans, EF, Whitfield, IC, 1964. Classification of unit responses in the auditory cortex of the unanaesthetized and unrestrained cat. J Physiol, 171, 476-493.

Fattori, P, Pitzalis, S, Galletti, C, 2009. The cortical visual area V6 in macaque and human brains. J Physiol Paris, 103, 88-97.

Felleman, DJ, Van Essen, DC, 1991. Distributed hierarchical processing in the primate cerebral cortex. Cereb Cortex, 1, 1-47.

Fize, D, Vanduffel, W, Nelissen, K, Denys, K, Chef d'Hotel, C, Faugeras, O, Orban, GA, 2003. The retinotopic organization of primate dorsal V4 and surrounding areas: A functional magnetic resonance imaging study in awake monkeys. J Neurosci, 23, 7395-7406.

Formisano, E, Kim, DS, Di Salle, F, van de Moortele, PF, Ugurbil, K, Goebel, R, 2003. Mirror-symmetric tonotopic maps in human primary auditory cortex. Neuron, 40, 859-869.

Galaburda, AM, Pandya, DN, 1983. The intrinsic architectonic and connectional organization of the superior temporal region of the rhesus monkey. J Comp Neurol, 221, 169-184.

Garraghty, PE, Pons, TP, Kaas, JH, 1990. Ablations of areas 3b (SI proper) and 3a of somatosensory cortex in marmosets deactivate the second and parietal ventral somatosensory areas. Somatosens Mot Res, 7, 125-135.

Glassman, RB, 1994. Behavioral effects of SI versus SII cortex ablations on tactile orientation-localization and postural reflexes of rats. Exp Neurol, 125, 125-133.

Hackett, TA, 2008. Anatomical organization of the auditory cortex. Journal of the American Academy of Audiology, 19, 774-779.

Hackett, TA, 2011. Information flow in the auditory cortical network. Hear Res, 271, 133-146.

Hackett, TA, 2015. Anatomic organization of the auditory cortex. Handb Clin Neurol, 129, 27-53.

Hackett, TA, Stepniewska, I, Kaas, JH, 1998a. Subdivisions of auditory cortex and ipsilateral cortical connections of the parabelt auditory cortex in macaque monkeys. J Comp Neurol, 394, 475-495.

Hackett, TA, Stepniewska, I, Kaas, JH, 1998b. Thalamocortical connections of the parabelt auditory cortex in macaque monkeys. J Comp Neurol, 400, 271-286.

Hackett, TA, Stepniewska, I, Kaas, JH, 1999. Prefrontal connections of the parabelt auditory cortex in macaque monkeys. Brain Res, 817, 45-58.

Hubel, DH, Wiesel, TN, 1965. Receptive fields and functional aurchitecture in two nonstriate visual areas (18 and 19) of the cat. J Neurophysiol, 28, 229-289.

Huettel, SA, Song, AW, McCarthy, G, 2009. Functional magnetic resonance imaging, 2 ed. Sinauer Associates, Inc., Sunderland, MA.

Humphries, C, Sabri, M, Lewis, K, Liebenthal, E, 2014. Hierarchical organization of speech perception in human auditory cortex. Front Neurosci, 8, 406.

Imaizumi, K, Priebe, NJ, Crum, PA, Bedenbaugh, PH, Cheung, SW, Schreiner, CE, 2004. Modular functional organization of cat anterior auditory field. J Neurophysiol, 92, 444-457.

Imig, TJ, Ruggero, MA, Kitzes, LM, Javel, E, Brugge, JF, 1977. Organization of auditory cortex in the owl monkey (Aotus trivirgatus). J Comp Neurol, 171, 111-128.

Javad, F, Warren, JD, Micallef, C, Thornton, JS, Golay, X, Yousry, T, Mancini, L, 2014. Auditory tracts identified with combined fMRI and diffusion tractography. Neuroimage, 84, 562-574.

Kaas, J, Axelrod, S, Diamond, IT, 1967. An ablation study of the auditory cortex in the cat using binaural tonal patterns. J Neurophysiol, 30, 710-724.

Kaas, JH, Hackett, TA, Tramo, MJ, 1999. Auditory processing in primate cerebral cortex. Curr Opin Neurobiol, 9, 164-170.

Kaas, JH, Krubitzer, LA, 1992. Area 17 lesions deactivate area MT in owl monkeys. Vis Neurosci, 9, 399-407.

Keifer, OP, Jr., Gutman, DA, Hecht, EE, Keilholz, SD, Ressler, KJ, 2015. A comparative analysis of mouse and human medial geniculate nucleus connectivity: a DTI and anterograde tracing study. Neuroimage, 105, 53-66.

Kim, J, Schultz, J, Rohe, T, Wallraven, C, Lee, SW, Bulthoff, HH, 2015. Abstract representations of associated emotions in the human brain. J Neurosci, 35, 5655-5663.

Kok, MA, Stolzberg, D, Brown, TA, Lomber, SG, 2015. Dissociable influences of primary auditory cortex and the posterior auditory field on neuronal responses in the dorsal zone of auditory cortex. J Neurophysiol, 113, 475-486.

Kopco, N, Huang, S, Belliveau, JW, Raij, T, Tengshe, C, Ahveninen, J, 2012. Neuronal representations of distance in human auditory cortex. Proc Natl Acad Sci U S A, 109, 11019-11024.

Kosaki, H, Hashikawa, T, He, J, Jones, EG, 1997. Tonotopic organization of auditory cortical fields delineated by parvalbumin immunoreactivity in macaque monkeys. J Comp Neurol, 386, 304-316.

Lajoie, K, Drew, T, 2007. Lesions of area 5 of the posterior parietal cortex in the cat produce errors in the accuracy of paw placement during visually guided locomotion. J Neurophysiol, 97, 2339-2354.

Land, MF, 2014. Do we have an internal model of the outside world? Philos Trans R Soc Lond B Biol Sci, 369, 20130045.

Langers, DRM, Backes, WH, van Dijk, P, 2007. Representation of lateralization and tonotopy in primary versus secondary human auditory cortex. Neuroimage, 34, 264-273.

Langers, DRM, Krumbholz, K, Bowtell, RW, Hall, DA, 2014. Neuroimaging paradigms for tonotopic mapping (I): The influence of sound stimulus type. Neuroimage, 100, 650-662.

Le Bihan, D, Jezzard, P, Haxby, J, Sadato, N, Rueckert, L, Mattay, V, 1995. Functional magnetic resonance imaging of the brain. Ann Intern Med, 122, 296-303.

Lee, CC, Winer, JA, 2008a. Connections of cat auditory cortex: I. Thalamocortical system. J Comp Neurol, 507, 1879-1900.

Lee, CC, Winer, JA, 2008b. Connections of cat auditory cortex: III. Corticocortical system. J Comp Neurol, 507, 1920-1943.

Lee, CC, Winer, JA, 2011. Convergence of thalamic and cortical pathways in cat auditory cortex. Hear Res, 274, 85-94.

Lewis, JW, Van Essen, DC, 2000. Mapping of architectonic subdivisions in the macaque monkey, with emphasis on parieto-occipital cortex. J Comp Neurol, 428, 79-111.

Liu, J, Harris, A, Kanwisher, N, 2010. Perception of face parts and face configurations: an FMRI study. J Cogn Neurosci, 22, 203-211.

Lomber, SG, Malhotra, S, 2008. Double dissociation of 'what' and 'where' processing in auditory cortex. Nat Neurosci, 11, 609-616.

Lui, LL, Rosa, MG, 2015. Structure and function of the middle temporal visual area (MT) in the marmoset: Comparisons with the macaque monkey. Neurosci Res, 93, 62-71.

Malhotra, S, Hall, AJ, Lomber, SG, 2004. Cortical control of sound localization in the cat: Unilateral cooling deactivation of 19 cerebral areas. J Neurophysiol, 92, 1625-1643.

Malhotra, S, Lomber, SG, 2007. Sound localization during homotopic and heterotopic bilateral cooling deactivation of primary and nonprimary auditory cortical areas in the cat. J Neurophysiol, 97, 26-43.

Malhotra, S, Stecker, GC, Middlebrooks, JC, Lomber, SG, 2008. Sound localization deficits during reversible deactivation of primary auditory cortex and/or the dorsal zone. J Neurophysiol, 99, 1628-1642.

Mellott, JG, Van der Gucht, E, Lee, CC, Carrasco, A, Winer, JA, Lomber, SG, 2010. Areas of cat auditory cortex as defined by neurofilament proteins expressing SMI-32. Hear Res, 267, 119-136.

Merzenich, MM, Brugge, JF, 1973. Representation of the cochlear partition on the superior temporal plane of the macaque monkey. Brain Res, 50, 275-296.

Merzenich, MM, Kaas, JH, Roth, GL, 1976. Auditory cortex in the grey squirrel: tonotopic organization and architectonic fields. J Comp Neurol, 166, 387-401.

Meyer, DR, Woolsey, CN, 1952. Effects of localized cortical destruction on auditory discriminative conditioning in cat. J Neurophysiol, 15, 149-162.

Mishkin, M, Ungerleider, LG, Macko, KA, 1983. Object vision and spatial vision - 2 cortical pathways. Trends Neurosci, 6, 414-417.

Morel, A, Garraghty, PE, Kaas, JH, 1993. Tonotopic organization, architectonic fields, and connections of auditory cortex in macaque monkeys. J Comp Neurol, 335, 437-459.

Morel, A, Kaas, JH, 1992. Subdivisions and connections of auditory cortex in owl monkeys. J Comp Neurol, 318, 27-63.

Nguyen, AP, Spetch, ML, Crowder, NA, Winship, IR, Hurd, PL, Wylie, DR, 2004. A dissociation of motion and spatial-pattern vision in the avian telencephalon: implications for the evolution of "visual streams". J Neurosci, 24, 4962-4970.

Nourski, KV, Etler, CP, Brugge, JF, Oya, H, Kawasaki, H, Reale, RA, Abbas, PJ, Brown, CJ, Howard, MA, 3rd, 2013. Direct recordings from the auditory cortex in a cochlear implant user. J Assoc Res Otolaryngol, 14, 435-450.

Nowak, LG, Munk, MH, Girard, P, Bullier, J, 1995. Visual latencies in areas V1 and V2 of the macaque monkey. Vis Neurosci, 12, 371-384.

Ortiz-Rios, M, Kusmierek, P, DeWitt, I, Archakov, D, Azevedo, FA, Sams, M, Jaaskelainen, IP, Keliris, GA, Rauschecker, JP, 2015. Functional MRI of the vocalization-processing network in the macaque brain. Front Neurosci, 9, 113.

Pandya, DN, Rosene, DL, 1993. Laminar termination patterns of thalamic, callosal, and association afferents in the primary auditory area of the rhesus monkey. Exp Neurol, 119, 220-234.

Petkov, CI, Kang, X, Alho, K, Bertrand, O, Yund, EW, Woods, DL, 2004. Attentional modulation of human auditory cortex. Nat Neurosci, 7, 658-663.

Petkov, CI, Kayser, C, Augath, M, Logothetis, NK, 2006. Functional imaging reveals numerous fields in the monkey auditory cortex. PLoS Biol, 4, 1213-1226.

Petkov, CI, Kayser, C, Augath, M, Logothetis, NK, 2009. Optimizing the imaging of the monkey auditory cortex: sparse vs. continuous fMRI. Magn Reson Imaging, 27, 1065-1073.

Petkov, CI, Kayser, C, Steudel, T, Whittingstall, K, Augath, M, Logothetis, NK, 2008. A voice region in the monkey brain. Nat Neurosci, 11, 367-374.

Petrides, M, 2000. Dissociable roles of mid-dorsolateral prefrontal and anterior inferotemporal cortex in visual working memory. J Neurosci, 20, 7496-7503.

Raiguel, SE, Lagae, L, Gulyas, B, Orban, GA, 1989. Response latencies of visual cells in macaque areas V1, V2 and V5. Brain Res, 493, 155-159.

Rauschecker, JP, 1997. Processing of complex sounds in the auditory cortex of cat, monkey, and man. Acta oto-laryngologica Supplementum, 532, 34-38.

Rauschecker, JP, Tian, B, 2000. Mechanisms and streams for processing of "what" and "where" in auditory cortex. Proc Natl Acad Sci U S A, 97, 11800-11806.

Rauschecker, JP, Tian, B, Hauser, M, 1995. Processing of complex sounds in the macaque nonprimary auditory cortex. Science, 268, 111-114.

Reale, RA, Imig, TJ, 1980. Tonotopic organization in auditory cortex of the cat. J Comp Neurol, 192, 265-291.

Recanzone, GH, Cohen, YE, 2010. Serial and parallel processing in the primate auditory cortex revisited. Behav Brain Res, 206, 1-7.

Romani, GL, Williamson, SJ, Kaufman, L, 1982. Tonotopic organization of the human auditory cortex. Science, 216, 1339-1340.

Romanski, LM, Bates, JF, Goldman-Rakic, PS, 1999a. Auditory belt and parabelt projections to the prefrontal cortex in the rhesus monkey. J Comp Neurol, 403, 141-157.

Romanski, LM, Tian, B, Fritz, J, Mishkin, M, Goldman-Rakic, PS, Rauschecker, JP, 1999b. Dual streams of auditory afferents target multiple domains in the primate prefrontal cortex. Nat Neurosci, 2, 1131-1136.

Saenz, M, Langers, DRM, 2014. Tonotopic mapping of human auditory cortex. Hear Res, 307, 42-52.

Schönwiesner, M, Dechent, P, Voit, D, Petkov, CI, Krumbholz, K, 2014. Parcellation of human and monkey core auditory cortex with fMRI pattern classification and objective detection of tonotopic gradient reversals. Cereb Cortex.

Seifritz, E, Di Salle, F, Esposito, F, Herdener, M, Neuhoff, JG, Scheffler, K, 2006. Enhancing BOLD response in the auditory system by neurophysiologically tuned fMRI sequence. Neuroimage, 29, 1013-1022.

Silvanto, J, Lavie, N, Walsh, V, 2005. Double dissociation of V1 and V5/MT activity in visual awareness. Cereb Cortex, 15, 1736-1741.

Sokoloff, L, Reivich, M, Kennedy, C, Des Rosiers, MH, Patlak, CS, Pettigrew, KD, Sakurada, O, Shinohara, M, 1977. The [14C]deoxyglucose method for the measurement of local cerebral glucose utilization: theory, procedure, and normal values in the conscious and anesthetized albino rat. J Neurochem, 28, 897-916.

Steinschneider, M, Nourski, KV, Rhone, AE, Kawasaki, H, Oya, H, Howard, MA, 3rd, 2014. Differential activation of human core, non-core and auditory-related cortex during speech categorization tasks as revealed by intracranial recordings. Front Neurosci, 8, 240.

Sternberger, LA, Sternberger, NH, 1983. Monoclonal antibodies distinguish phosphorylated and nonphosphorylated forms of neurofilaments in situ. Proc Natl Acad Sci U S A, 80, 6126-6130.

Strainer, JC, Ulmer, JL, Yetkin, FZ, Haughton, VM, Daniels, DL, Millen, SJ, 1997. Functional MR of the primary auditory cortex: an analysis of pure tone activation and tone discrimination. AJNR Am J Neuroradiol, 18, 601-610.

Talavage, TM, Sereno, MI, Melcher, JR, Ledden, PJ, Rosen, BR, Dale, AM, 2004. Tonotopic organization in human auditory cortex revealed by progressions of frequency sensitivity. J Neurophysiol, 91, 1282-1296.

Taylor, JC, Downing, PE, 2011. Division of labor between lateral and ventral extrastriate representations of faces, bodies, and objects. J Cogn Neurosci, 23, 4122-4137.

Tiao, YC, Blakemore, C, 1976. Functional organization in the visual cortex of the golden hamster. J Comp Neurol, 168, 459-481.

Tootell, RB, Silverman, MS, Switkes, E, De Valois, RL, 1982. Deoxyglucose analysis of retinotopic organization in primate striate cortex. Science, 218, 902-904.

Urgesi, C, Candidi, M, Ionta, S, Aglioti, SM, 2007. Representation of body identity and body actions in extrastriate body area and ventral premotor cortex. Nat Neurosci, 10, 30-31.

van der Gucht, E, Vandesande, F, Arckens, L, 2001. Neurofilament protein: a selective marker for the architectonic parcellation of the visual cortex in adult cat brain. J Comp Neurol, 441, 345-368.

von Kriegstein, K, Griffiths, TD, Thompson, SK, McAlpine, D, 2008. Responses to interaural time delay in human cortex. J Neurophysiol, 100, 2712-2718.

von Kriegstein, K, Smith, DR, Patterson, RD, Kiebel, SJ, Griffiths, TD, 2010. How the human brain recognizes speech in the context of changing speakers. J Neurosci, 30, 629-638.

Walzl, EM, Woolsey, CN, 1946. Effects of cochlear lesions on click responses in the auditory cortex of the cat. Bull Johns Hopkins Hosp, 79, 309-319.

Wessinger, CM, Buonocore, MH, Kussmaul, CL, Mangun, GR, 1997. Tonotopy in human auditory cortex examined with functional magnetic resonance imaging. Hum Brain Mapp, 5, 18-25.

Whitsel, BL, Petrucelli, LM, Werner, G, 1969. Symmetry and connectivity in the map of the body surface in somatosensory area II of primates. J Neurophysiol, 32, 170-183.

Wickens, AP, 2015. A History of the brain: From stone age surgery to modern neuroscience. Psychology Press, New York, NY.

Wong, AM, Sharpe, JA, 1999. Representation of the visual field in the human occipital cortex: a magnetic resonance imaging and perimetric correlation. Arch Ophthalmol, 117, 208-217.

Woods, DL, Herron, TJ, Cate, AD, Yund, EW, Stecker, GC, Rinne, T, Kang, X, 2010. Functional properties of human auditory cortical fields. Front Syst Neurosci, 4, 155.

Woods, DL, Stecker, GC, Rinne, T, Herron, TJ, Cate, AD, Yund, EW, Liao, I, Kang, XJ, 2009. Functional maps of human auditory cortex: effects of acoustic features and attention. PLoS One, 4, e5183.

Woolsey, CN, Fairman, D, 1946. Contralateral, ipsilateral, and bilateral representation of cutaneous receptors in somatic area-I and area-II of the cerebral cortex of pig, sheep, and other mammals. Surgery, 19, 684-702.

Yetkin, FZ, Roland, PS, Christensen, WF, Purdy, PD, 2004. Silent functional magnetic resonance imaging (FMRI) of tonotopicity and stimulus intensity coding in human primary auditory cortex. Laryngoscope, 114, 512-518.

Yue, Q, Zhang, L, Xu, G, Shu, H, Li, P, 2013. Task-modulated activation and functional connectivity of the temporal and frontal areas during speech comprehension. Neuroscience, 237, 87-95.

Chapter 2 – There's More Than One Way to Scan a Cat: Imaging Cat Auditory Cortex with High-Field fMRI using Continuous or Sparse Sampling[1]

2.1 Abstract

When conducting auditory investigations using functional magnetic resonance imaging (fMRI), there are inherent potential confounds that need to be considered. Traditional continuous fMRI acquisition methods produce sounds >90dB which compete with stimuli or produce neural activation masking evoked activity. Sparse scanning methods insert a period of reduced MRI-related noise, between image acquisitions, in which a stimulus can be presented without competition. In this study, we compared sparse and continuous scanning methods to identify the optimal approach to investigate acoustically-evoked cortical, thalamic and midbrain activity in the cat. Using a 7T magnet, we presented broadband noise, 10 kHz tones, or 0.5 kHz tones in a block design, interleaved with blocks in which no stimulus was presented. Continuous scanning resulted in larger clusters of activation and more peak voxels within the auditory cortex. However, no significant activation was observed within the thalamus. Also, there was no significant difference found, between continuous or sparse scanning, in activations of midbrain structures. Higher magnitude activations were identified in auditory cortex compared to the midbrain using both continuous and sparse scanning. These results indicate that continuous scanning is the preferred method for investigations of auditory cortex in the cat using fMRI. Also, choice of method for future investigations of midbrain activity should be driven by other experimental factors, such as stimulus intensity and task performance during scanning.

Key Words: Tonal stimulation, Broadband noise, Cortex, 7-Tesla, Thalamus, Inferior Colliculus

---

[1] A version of this chapter is published as:

Hall, AJ, Brown, TA, Grahn, JA, Gati, JS, Nixon, PL, Hughes, SM, Menon, RS, Lomber, SG, 2014. There's more than one way to scan a cat: Imaging cat auditory cortex with high-field fMRI using continuous or sparse sampling. J Neurosci Methods, 224, 96-106.

2.2 Introduction

Investigations of cortical, and subcortical, processing of acoustic information using the cat have provided a foundation for many of the current theories in auditory neuroscience. However, the invasive nature of techniques used such as electrophysiological recording, makes it necessary to use alternate techniques, such as functional magnetic resonance imaging (fMRI), when conducting clinical investigations. Therefore, it would be highly beneficial to future investigations if literature were available using fMRI in the cat to provide a more comparable link between these experimental approaches.

The use of fMRI to study the organization of auditory cortex has inherent obstacles that must be overcome. In particular, standard blood oxygen level dependent (BOLD) fMRI acquisition techniques using single shot echo planar imaging (EPI) may produce sound pressure levels (SPL) greater than 90dB SPL with peak SPLs occurring at approximately 1 kHz (Amaro et al., 2002; Peelle et al., 2010; Price et al., 2001). It has also been reported that magnets of higher field strength produce significantly higher levels of noise (Moelker and Pattynama, 2003; Price et al., 2001; Ravicz et al., 2000). Therefore, the potential confound of scanner noise increases with the current trend in research towards using higher field magnets to produce higher resolution images. The acoustic noise which accompanies acquisition presents several potential problems for conducting experiments using auditory stimuli including: 1. interactions at the basilar membrane between scanner noise and the intended stimuli; 2. the masking of intended stimulus evoked neural activity by the scanner noise; and 3. the reduction in responsiveness to subsequent presented stimuli (Amaro et al., 2002; Bandettini et al., 1998; Hall et al., 1999; Peelle et al., 2010; Petkov et al., 2009; Talavage et al., 1999). In studies of human subjects, scanner noise is attenuated by employing methods such as headphones, ear inserts, and highly sound-absorbent material placed around the head and covering the ears (Amaro et al., 2002). These methods, however, do not eliminate scanner noise and such noise may therefore potentially still confound the acquired data.

An approach referred to as sparse scanning (Hall et al., 1999), as also called clustered-volume acquisitions (Edmister et al., 1999), has been developed in an attempt to address some of the confounds present in auditory fMRI. Sparse scanning takes advantage of the delay in the hemodynamic response to neural activity by inserting a

pause between volume acquisitions. During this period, a stimulus may be presented without competition and the response to that stimulus can be recorded (Hall et al., 1999; Peelle et al., 2010). While the period between acquisitions is quieter, it would be remiss to think of it as silent. Ambient noise related to ventilation, cryogen pumping, and monitoring equipment are all present during this period and, without effective acoustic shielding, could also affect fMRI data (Moelker and Pattynama, 2003). To take advantage of this technique, the hemodynamic response function (HRF) must be defined so that acquisition is timed to take place at the peak. The HRF of auditory cortex, in response to short stimuli, peaks at approximately 4-6 seconds for humans (Backes and van Dijk, 2002; Belin et al., 1999) and monkeys (Baumann et al., 2010). The HRF has recently been defined for the cat (Brown et al., 2013) and also peaks at 3-5 seconds, making it possible to optimize sparse scanning for the cat.

Sparse scanning provides many advantages for the presentation of auditory stimuli. Sparse scanning samples the haemodynamic response function (HRF) at its peak resulting in a higher and more variable measured BOLD response. In contrast, continuous scanning samples across the HRF providing a more stable level of measured BOLD response. Moreover, sparse scanning lacks the effects of spin history which are present during continuous scanning (Woods et al., 2009) whiceh would result in better contrasts to baseline levels. Also, cortical habituation due to scanner noise is limited. However, there are also characteristics of the sparse scanning method that could be problematic. The addition of gaps in fMRI acquisition result in a lengthened trial time and reduces the number of acquired volumes during the same time period (Peelle et al., 2010). Also, the limited number of volumes may lead to a reduction of the statistical power in the acquisition.

There have only been a few studies which have directly compared the two techniques to assess their optimality. Petkov et al. (2009) showed data from macaque monkeys in which sparse scanning resulted in larger activations and tonotopic mapping. This study lengthened the acquisition time (TA) of the continuous volume to more closely match the repetition time (TR) of the sparse paradigm. In doing this, several of the advantages of continuous scanning, namely the larger amount of data which can be collected in a given time period and a better resolution of the hemodynamic response,

biased results towards sparse scanning. Peelle et al. (2010) did a similar study in humans using a similar TA for both sparse and continuous scanning. In this study, while the sparse technique generally resulted in a higher signal, continuous scanning resulted in better statistical power. Similarly, Woods et al. (2009) also found that sparse scanning resulted in larger magnitude activations when compared to continuous scanning. However, this study noted that, beyond magnitude, both methods resulted in similar activation patterns and locations.

The present study provides a fundamental investigation of both sparse and continuous scanning methods to identify the optimal method for auditory investigations of the cat cerebrum. There have been numerous investigations of the auditory system using either sparse (Davis and Johnsrude, 2003; Langers et al., 2007; Scarff et al., 2004; van den Noort et al., 2008; Vannest et al., 2009) or continuous scanning (Inan et al., 2004; Talavage et al., 2000; Wessinger et al., 1997) . Given that there are benefits and caveats to both techniques, it was not possible to predict which would be ideal for imaging acoustically-evoked activity.

2.3 Methods

Five adult (>6M) female domestic shorthair cats were selected for this project. All animals were obtained from a commercial laboratory animal breeding facility (Liberty Labs, Waverly, NY) and housed as a clowder. All procedures were approved by the University of Western Ontario's Animal Use Subcommittee of the University Council on Animal Care and were in accordance with the National Research Council's *Guidelines for the Care and Use of Mammals in Neuroscience and Behavioral Research* (Van Sluyters et al., 2003) and the Canadian Council on Animal Care's *Guide to the Care and Use of Experimental Animals* (Olfert et al., 1993).

2.3.1 Anesthesia and recovery

All animals were pre-medicated (intramuscular injection; i.m.) with a mixture of atropine (0.02 mg/kg) and acepromizine (0.02 mg/kg). This pre-medication protocol has been shown to reduce the amount of general anesthesia required (Dyson et al., 1988) and thus potentially reduce any suppressive cortical effects. After twenty minutes, a solution of ketamine (4 mg/kg) and dexdomitor (0.025 mg/kg) was administered (i.m.) to induce

anesthesia. This anesthetic regime has been previously used and found to be effective in measuring BOLD responses in the cat (Brown et al., 2013). Once anesthetized, as determined by lack of paw-pinch or ear reflex, the animals were then intubated and an indwelling feline catheter was placed in the saphenous vein to facilitate maintenance of anesthesia. Body temperature was maintained with heating discs and vital signs were continually monitored. Each cat was then placed in a custom made Plexiglas apparatus in a sternal (sphinx-like) position. The animal's head was inserted into a custom built RF coil and MRI compatible ear inserts, which contained sound attenuating buds and a tube to direct the auditory stimulus close to the tympanic membrane, were placed in each ear. Both sides of the head were stabilized with sound dampening foam padding which aided in the attenuation of scanner noise (Fig. 2.1). The cat and apparatus were then placed inside the bore of the magnet. Anesthesia was maintained through the continuous administration of ketamine (0.6-0.75 mg/kg/hr) intravenous (i.v.) and spontaneous inhalation of isofluorane (0.4-0.5%). In our experience, these levels resulted in the collection of optimal fMRI data. On average, sessions lasted 2 hours.

Following each scanning session, anesthesia was discontinued and the cat was monitored closely during recovery. The endotracheal tube was removed when the cat exhibited a gag reflex and increased jaw tone. The catheter remained in place until the cat exhibited voluntary head and limb movement. The cat was then placed in individual housing until fully recovered from the effects of anesthesia at which time it was returned to the clowder. Generally, animals exhibited normal behavior within 1h of anesthesia cessation.

2.3.2 Image acquisition

All data were acquired on an actively shielded 68 cm human head 7-Tesla horizontal bore scanner with a DirectDrive console (Agilent, Santa Clara, California) equipped with a Siemens AC84 gradient subsystem (Erlangen, Germany) operating at a slew rate of 280 mT/m/s. An in-house designed and manufactured conformal 3-channel transceive cat head RF coil was used for all experiments (Fig. 2.1). Magnetic field optimization (B0 shimming) was performed using an automated 3D mapping procedure (Klassen and Menon, 2004) over the specific imaging volume of interest.

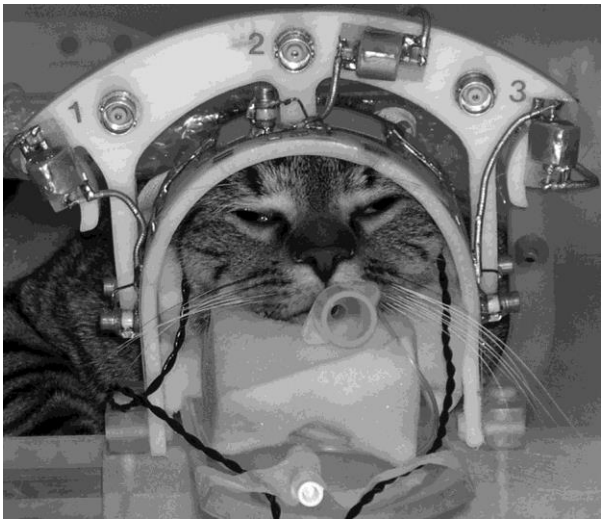

Figure 2.1 A photograph of an animal in the RF coil.

Braided black cords lateral to the animal's head terminate at ear buds inserted into each ear canal. The head is enveloped in foam to minimize movement and attenuate scanner noise. The animal is intubated (plastic tube ventral to nose) to permit administration of isofluorane anesthesia.

For each cat, functional volumes were collected using a segmented interleaved EPI acquisition (TR = 1000 ms; TE = 15 ms; 3 segments/plane; slices = 21 x 1 mm; matrix = 96 x 96; FOV = 72 x 72 mm; acquisition voxel size = 0.75 mm x 0.75 mm x 1.0 mm; acquisition time (TA) = 3 sec/volume). Images were corrected for physiological fluctuations using navigator echo correction (Hu and Kim, 1994). A high-resolution PD-weighted anatomical reference volume was acquired along the same orientation and field-of-view as the functional images using a FLASH imaging sequence (TR = 750 ms; TE = 8 ms; matrix = 256 x 256; acquisition voxel size = 281 μm x 281 μm x 1.0 mm). Functional imaging data sets were acquired for both continuous (120 continuous volumes) and sparse (53 volumes with 5 second delay between each volume) scanning paradigms during every session.

2.3.3 Stimulus presentation

The stimuli, used during both sparse and continuous scanning methods, consisted of a broadband noise (BBN; white noise), a 0.5 kHz tone and a 10 kHz tone. Each was presented, in bursts of 400ms with a 100ms interstimulus ("silent") interval, continuously for 4s or 30s for the sparse or continuous paradigms, respectively. Stimuli were generated using MatLab (MathWorks) and were presented using in-house custom software (Microsoft Visual Studio) on a Dell laptop through an external Roland Corporation soundcard (24-bit/96kHz ; Model UA-25EX), a PylePro power amplifier (Model PCAU11) and Sensimetrics MRI-compatible ear inserts (Model S14). Sound card and amplifier output levels were the same for all stimuli. Following data collection, speaker level measurements using an Etymotic Probe Microphone (Elk Grove Village, IL) and Tektronix oscilloscope (Beaverton, OR) confirmed presentation of all stimuli at levels 80-95 dB SPL out of the ear inserts.

Both sparse and continuous scanning methods were conducted using a block design of stimulus presentation (Fig. 2.2A). For sparse scans, a block of 4 volumes (TR= 8s and TA = 3s, resulting in a 5s gap between volume acquisitions) was collected every 32s (Fig. 2.2B) and, for continuous scans a block of 10 volumes (TR and TA = 3s) was collected every 30s (Fig. 2.2C). Two blocks for each stimulus type were collected per run interleaved with baseline blocks in which no stimulus was presented. This resulted in

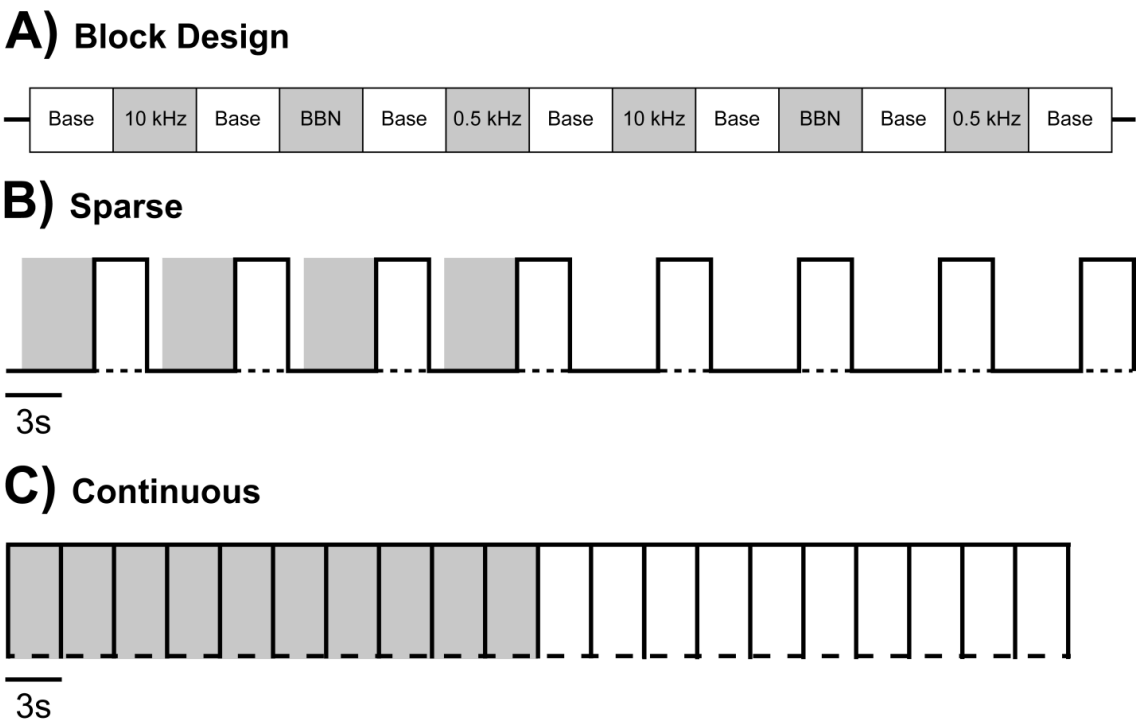

Figure 2.2 Schematic of the block design

Schematic of the block design (A) in which stimuli were presented. B) Two blocks, a stimulus presentation and a baseline, are diagramed for the sparse scanning method. Stimuli are presented during the relatively silent period between acquisitions. Four volumes of data are collected every 32 seconds using the sparse scanning method. Shading indicates presence of stimuli and the solid line indicates scanner acquisition activity. C) Two blocks, a stimulus presentation and baseline, are diagrammed for the continuous method. Stimuli were presented during acquisition allowing ten volumes of data to be collected every 30 seconds. Conventions same as in A.

a 6.9 or 6.5 minute time for a single sparse or continuous run, respectively.

During sparse scanning the following sequence was applied for each block: i) a 1s delay occurred after the start of each silent period; ii) the stimulus was played for 4s; iii) volume acquisition began at stimulus offset (Fig. 2.2B). Presentation of the stimulus for 4s allowed enough time for the hemodynamic response to peak (Brown et al., 2013) before acquisition and ensured maintenance of a maximal hemodynamic response throughout the acquisition period (3s). In contrast, the continuous paradigm included constant stimulus presentation during the entire block.

At the beginning of each session, a structural MRI was collected. Basic on-line analysis of activity was faster and provided higher statistical strength in a single run using continuous scanning. Therefore, following the structural scan, 2-3 continuous runs were performed and evaluated for activity. Once acoustically-evoked activity was confirmed, sparse scanning commenced. The initial induction of anesthesia uses an alpha-2 agonist, dexdomator, which has sedative, analgesic, and muscle relaxing effects and takes approximately 1h to be metabolized. Therefore, at the end of each session several continuous runs were collected to control for the effects of anesthesia. Two sessions with each subject were included in this study. A minimum of 40 volumes per stimulus for continuous and sparse scanning were required for a session to be included.

2.3.4 Data analysis

fMRI data from each animal was preprocessed and analyzed separately using SPM8 (Wellcome Trust Centre for Neuroimaging, UCL, London, UK) and MatLab (MathWorks) software. Initially, all images were reoriented and motion corrected (all translational and rotational movements were <0.5mm) and co-registered to the high resolution structural image from the same session. All sessions were then normalized to a single animal's structural image resulting in a 1mm isotropic voxel size and smoothed using a 2mm Gaussian full width at half maximum (FWHM) kernel.

Data were analyzed for each animal using a separate model for continuous and sparse scans. The last two runs of continuous data and the last 5 runs of sparse data from each session were included in further analysis. This ensured that volume numbers for both continuous and sparse scanning, for each stimulus, were equal. Analysis only

including the last two runs of sparse data was also included for comparison of time matched runs with continuous data. A correlational AR(1) model was used in conjunction with a high-pass filter of 128s and restricted maximum likelihood (ReML) model estimation was used (Friston et al., 2007). Following model estimation, a t-contrast was generated for each of the stimuli.

Hand drawn region of interest (ROI) masks were generated for auditory cortex, thalamus, and midbrain based on anatomy. These masks were used, in conjunction with small volume correction, to extract time-course data for significantly active voxels associated with each region.

Data from each animal were extracted separately. A voxelwise threshold of $p<0.001$ (uncorrected) and a cluster-level threshold of $p<0.05$ (FWE-corrected) were applied to all results. T-statistics and percent signal changes (PSC) were examined in order to compare variability and strength of activation. Time courses were extracted for all voxels within a 1mm radius sphere centered at each peak voxel for further analysis. Average PSC for each volume in a stimulus block was calculated by extracting PSC values for every volume in each block within an individual animal and then averaging across all blocks and animals. One-way analysis of variance (ANOVA) and Tukey's honestly-significant difference criteria were then performed to analyze differences between volumes in a block. Data from peak volumes were then extracted and two sample t-tests were run to make comparisons between the cortex, thalamus and midbrain activations.

2.4 Results

Data were inspected for significant activations in the auditory cortex, thalamus or midbrain. Sparse scanning data, time matched to continuous data, resulted in no significant activations. Significant activations were observed in the auditory cortex and midbrain (Fig. 2.3A,B) in data matched for number of volumes. However, no activations were observed within the thalamus. Magnitude of activation and statistical strength at peak voxels as well as extent of activation were analyzed, across cats, to address differences between sparse and continuous scanning methods within a block. Finally,

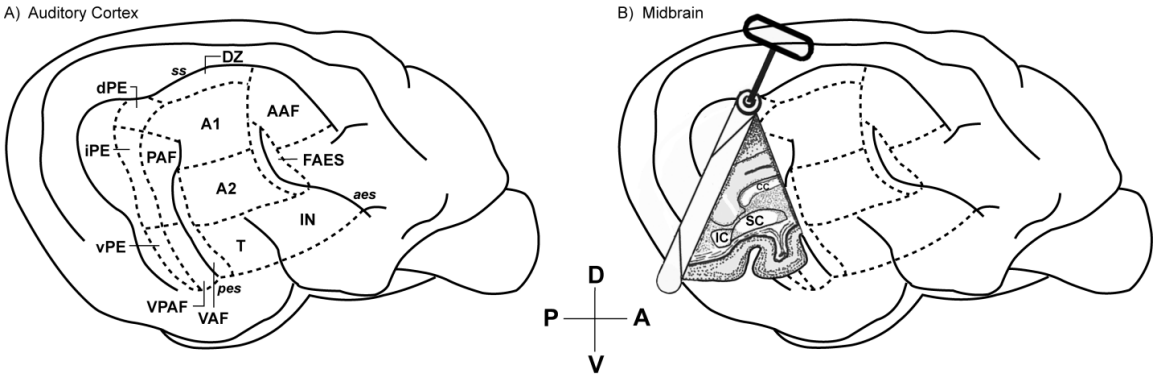

Figure 2.3 Activations were observed in the auditory cortex and midbrain.

A) The thirteen cortical areas are indicated: anterior auditory field, AAF; auditory field of the anterior ectosylvian sulcus, FAES; dorsal zone of the auditory cortex, DZ; insular region, IN; posterior auditory field, PAF; primary auditory cortex, A1; second auditory cortex, A2; temporal region, T; ventral auditory field, VAF; ventral posterior auditory field, VPAF. Sulci are indicated by italics: anterior ectosylvian sulcus, aes; posterior ectosylvian sulcus, pes;.suprasylvian sulcus, ss; B) Subcortical structures are indicated: superior colliculus (SC); inferior colliculus (IC); and corpus callosum (cc). Anterior (A), posterior (P), dorsal (D) and ventral (V) directions are indicated.

volumes within a block which elicited the strongest activation were further analyzed for comparison of cortical and midbrain activations.

2.4.1 Cortical activations

The auditory cortex of the cat lies on the lateral surface of the cerebrum and is functionally divided into 13 acoustically responsive areas (Fig. 2.3A). Activations within auditory cortex were observed through the full thickness of cortex for both continuous (Fig. 2.4A) and sparse (Fig. 2.4B) scanning methods. Peak voxels within clusters passing an FWE threshold of $p<0.05$ did not show a significant difference in statistical strength between sparse and continuous scanning for either the BBN or 0.5 kHz tone (Fig. 2.4C). The 10 kHz tone did not elicit a response during sparse scanning, and was only effective in two animals during continuous scanning, prohibiting a comparison between the two methods using this stimulus. Therefore, data are not shown for the 10 kHz tone.

Continuous scanning resulted in a significantly larger extent of activation for both the BBN and 0.5 kHz stimuli (Fig. 2.4D). This is also reflected in the number of peaks resulting from continuous scanning in each individual area (Table 2.1). Within each cortical area, a larger number of peaks resulting from the 0.5 kHz tone were found within known tonotopic areas such as the primary auditory cortex (A1), the posterior auditory field (PAF) and the ventral posterior auditory field (VPAF; Table 2.1). Conversely, the BBN resulted in a larger number of peaks appearing within non-tonotopically organized auditory cortices such as the second auditory cortex (A2), dorsal zone (DZ), insular (IN), ventral posterior ectosylvian gyrus (vPE), temporal (T) and ventral auditory field (VAF). While both continuous and sparse scanning demonstrated these organizational principles, it was more apparent using continuous as a result of the larger number of peaks.

2.4.2 Midbrain activations

Midbrain structures, including the superior and inferior colliculi, lie deep within the brain (Fig. 2.3B). Activations were identified in the midbrain using both continuous (Fig. 2.5A) and sparse (Fig. 2.5B) scanning methods. The data tended to be lateralized to either the right or the left using continuous scanning. Three of the animals had a bias to the left and one a bias to the right. No significant difference was observed for statistical

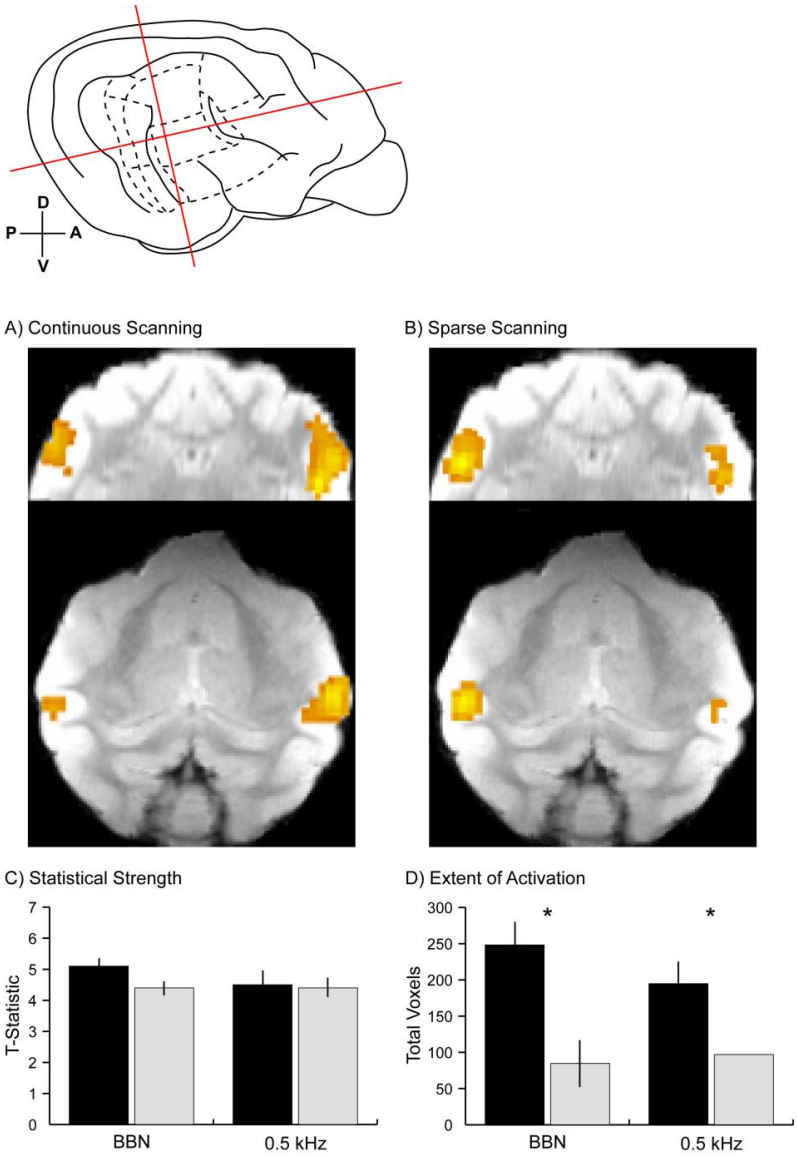

Figure 2.4 Activations within auditory cortex

A,B) Cortical activations, in a single animal in response to BBN, for continuous (A) or sparse (B) scanning methods. Cortical representation at top shows locations of coronal and horizontal slices shown in A and B. Activations passed $p<0.001$ uncorrected and cluster FWE thresholds. C) Average t-statistics at peak voxels within cortical activations are indicated for continuous (black bars) and sparse (grey bars) scanning. D) Extent of activation across cortex. Number of active voxels are indicated for continuous (black bars) and sparse (grey bars) scanning. Error bars represent S.E.M. * indicates t-test results of $p<0.01$ between continuous and sparse.

	A1		AAF		PAF		VPAF		DZ	
	BBN	0.5	BBN	0.5	BBN	0.5	BBN	0.5	BBN	0.5
Continuous	4	7	1	0	0	0	0	1	5	3
Sparse	2	1	0	0	0	2	0	1	2	1

	A2		IN		VPE		T		VAF		Total
	BBN	0.5	BBN	0.5	BBN	0.5	BBN	0.5	BBN	0.5	
Continuous	4	1	2	2	1	0	1	0	4	1	37
Sparse	2	0	2	0	0	0	0	0	3	0	16

Table 2.1 Number of peaks found within each of the cortical areas

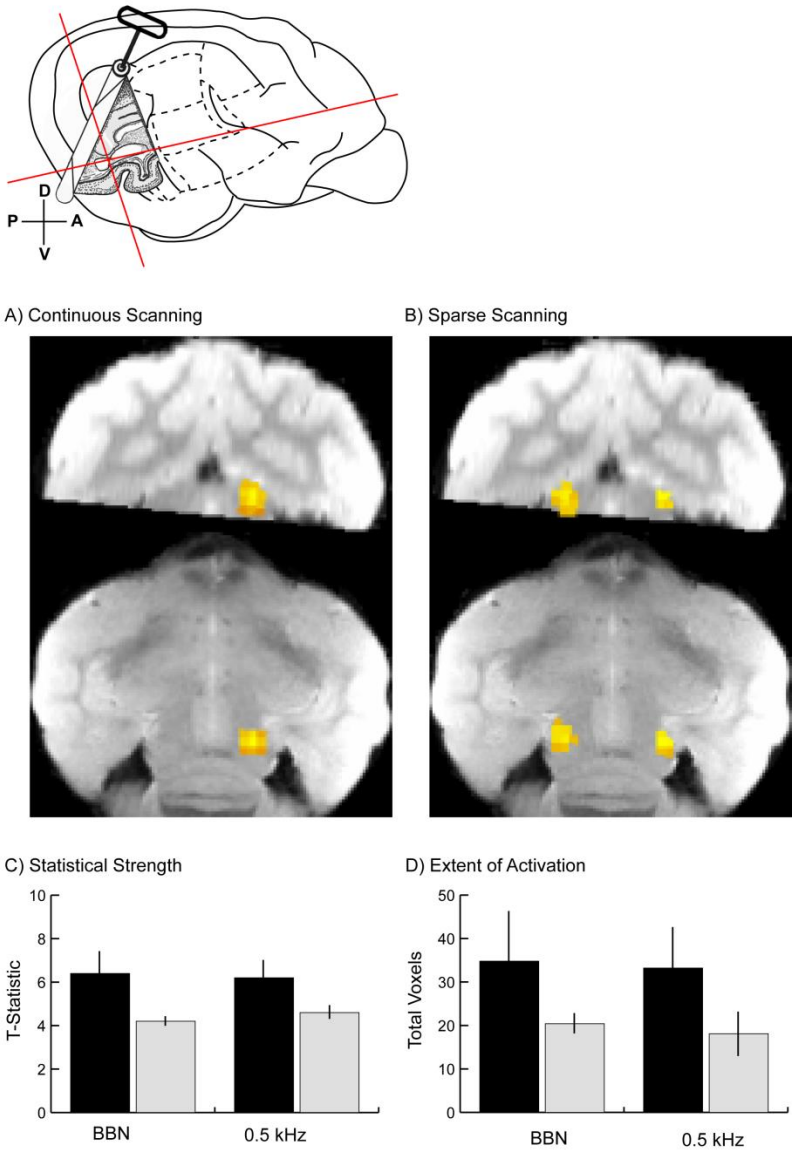

Figure 2.5 Activations in the midbrain.

A,B) Midbrain activations, in a single animal in response to 0.5 kHz tone, for continuous (A) or sparse (B) scanning methods. Subcortical representation at top shows locations of coronal and horizontal slices shown in A and B. Activations passed $p<0.001$ uncorrected and cluster FWE thresholds. C) Average t-statistics at peak voxels within midbrain activations are indicated for continuous (black bars) and sparse (grey bars) scanning. D) Extent of activation across the midbrain. Number of active voxels are indicated for continuous (black bars) and sparse (grey bars) scanning. Error bars represent S.E.M. * indicates t-test results of $p<0.01$ between continuous and sparse.

strength (Fig. 2.5C) or extent of activation (Fig. 2.5D) between continuous and sparse scanning.

2.4.3 Hemodynamic response

The difference in the stimulation sequence between continuous and sparse scanning, namely that the stimulus is presented continuously for 4 seconds during sparse scanning and for 30 seconds during continuous runs, could bias results. When considering the time from stimulus onset, the second volume of the continuous block (3-6s) best matches the first volume of the sparse block (4-7s). Analysis of these volumes separately showed no significant difference in the percent signal change (PSC) between continuous and sparse scanning in cortex (Fig. 2.6A) or midbrain for either BBN or 0.5 kHz stimuli (Fig. 2.6B). There was also no difference between the last volumes of the continuous and sparse blocks.

However, in cortex there was a significant increase in PSC between the second volume and the last volume of the continuous block for both stimuli (Fig. 2.6A). A similar pattern was also seen for sparse scanning, having a significant increase in PSC in the last volume of the block during stimulation with a 0.5kHz tone. A comparable difference was also observed in the midbrain activations using sparse scanning during 0.5 kHz stimulation.

Average PSC for each acquired volume within a block better illustrates the increasing trend for cortex (Fig. 2.7A) and midbrain (Fig. 2.7B). Cortical activations following the second volume show a significant increase in PSC during continuous scanning (Fig. 2.7Ai). Conversely, activations in the midbrain during continuous scanning (Fig. 2.7Bi) were, with a few exceptions during stimulation with the 0.5 kHz tone, generally not significantly different from the second volume. During sparse scanning, the timing of the stimulus onset was precisely placed so that each acquisition would be sampling at the peak of the hemodynamic response and was expected to result in a fairly flat PSC across a block. It is intriguing that data indicate that cortical activations during sparse scanning (Fig. 2.7Aii) also showed an upward trend through the block. Midbrain activations during sparse scanning (Fig. 2.7Bii) using the BBN more closely reflected the flat PSC across the block as was expected. However, midbrain

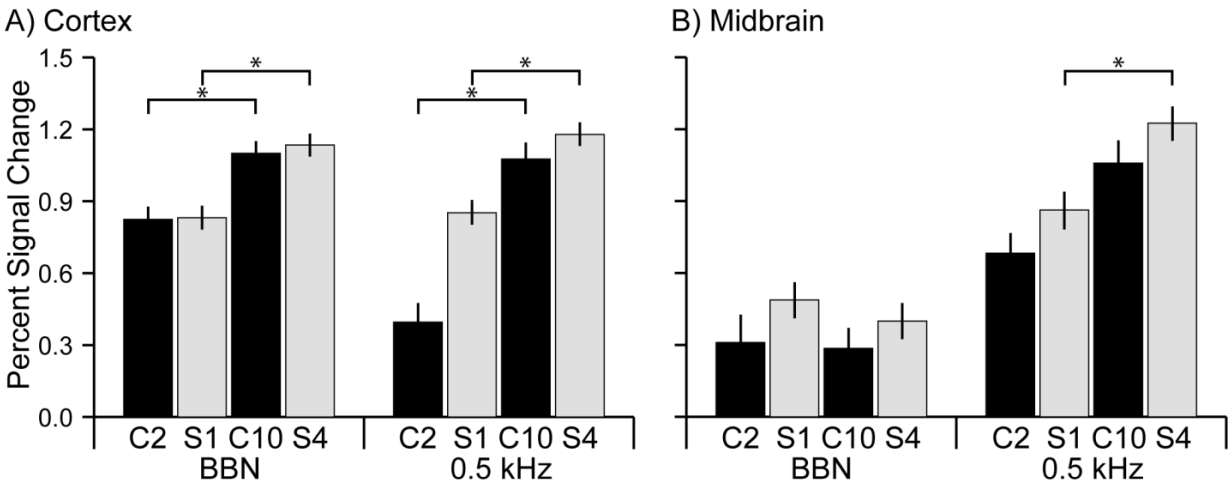

Figure 2.6 Stimulus presentation differences.

The second volume of the continuous runs (C2), an approximate time match for stimulus presentation to the first volume of the sparse runs (S1), is shown for both cortical (A) and midbrain (B) activations. The last volume for the continuous (C10) and sparse (S4) runs are also shown. Error bars represent S.E.M. * indicates t-test results of $p<0.01$ between continuous and sparse.

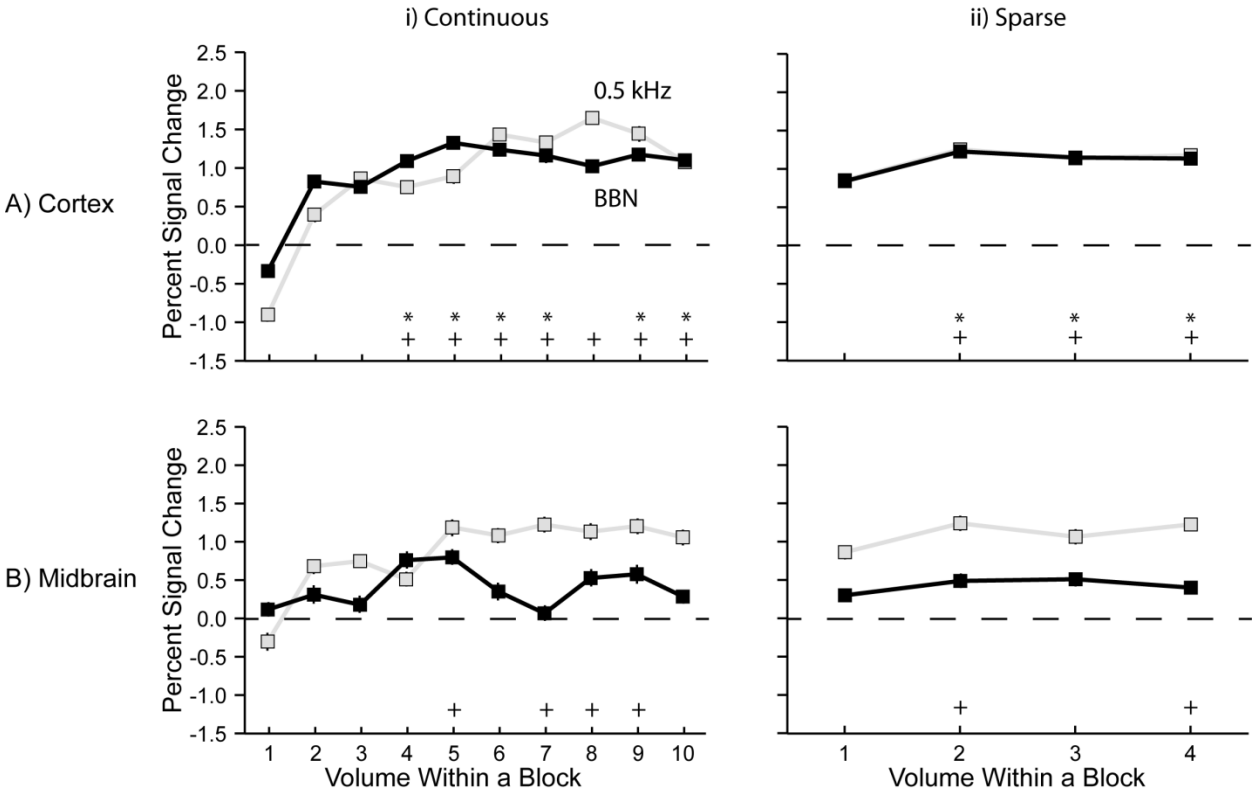

Figure 2.7 Hemodynamic time course

Mean percent signal change (PSC) in peak voxels for each volume in cortex (A) or midbrain (B) for both BBN (black lines) and 0.5 kHz (grey lines). i) Continuous scanning, significant differences from the second volume are indicated for both BBN (*) and 0.5 kHz (+) as indicated by ANOVA. ii) Sparse scanning, significant differences from the first volume for both BBN (*) and 0.5 kHz (+) as indicated by ANOVA. Error bars represent S.E.M. * or + indicates $p<0.01$.

activations during sparse scanning using the 0.5 kHz tone showed significantly higher PSC for two volumes, compared to the first.

2.4.4 Cortical and midbrain comparison

Time courses of volumes within a block eliciting the strongest activation (Fig. 2.7) were then compared for midbrain and cortical activations for each scanning method. The PSC at these peak volumes was significantly lower for midbrain activations during continuous scanning during presentation of each stimulus (Fig. 2.8A). Similarly, during sparse scanning (Fig. 2.8B), midbrain activations were significantly lower for the BBN stimulus. There were, however, no significant differences between cortical and midbrain activations using the 0.5 kHz stimulus during sparse scanning.

2.5 Discussion

In summary, activations of auditory cortex and midbrain structures resulted in similar statistical strengths and magnitudes for both continuous and sparse scanning. The differences between the two methods are best demonstrated in extent and location of cortical activation. Also, a rise in magnitude of activation was observed along a block for both continuous and sparse scanning. Finally, midbrain activations had significantly lower magnitude compared to cortical activations.

2.5.1 Continuous vs sparse scanning

The common use of sparse scanning in current fMRI investigations of acoustically-evoked activity would suggest that it is superior to the more traditional continuous method. In fact, previous human and non-human primate studies which have directly compared the two techniques, have indicated that sparse scanning resulted in larger magnitude and extent of activation (Hall et al., 1999; Peelle et al., 2010; Petkov et al., 2009; Schmidt et al., 2008; Woods et al., 2009). In contrast, results from the present study showed no difference in magnitude of activation between the two methods (Figs. 2.6, 2.7) and a significantly higher extent of cortical activation (Fig. 2.4D) using the continuous method. Variations between these studies and the present one could be attributed to differences in acquisition (Petkov et al., 2009), volume sampling (Hall et al., 1999), or stimulus presentation timing (Schmidt et al., 2008). For example,

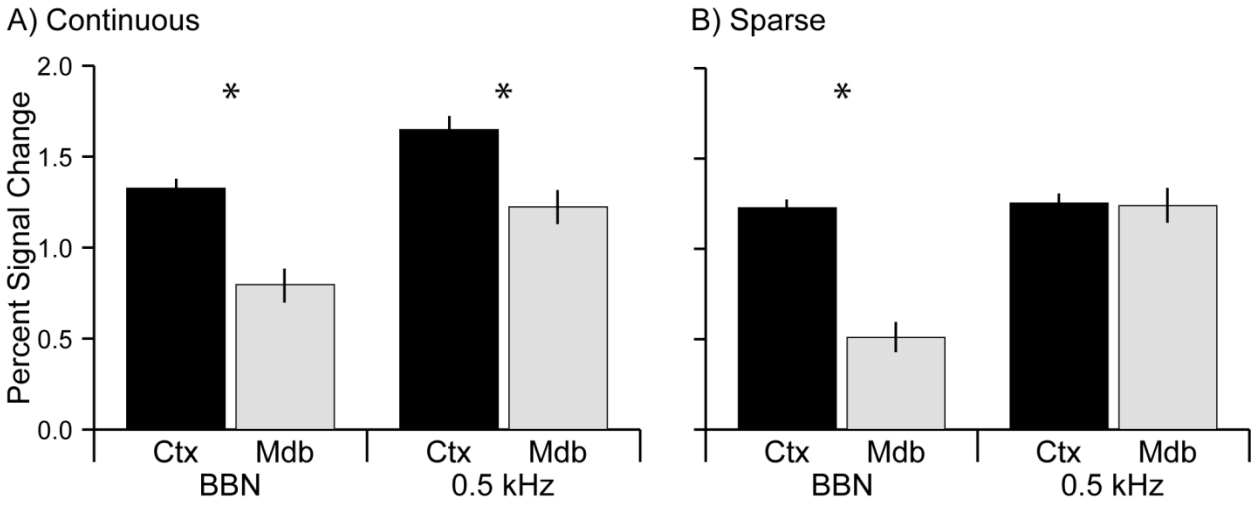

Figure 2.8 Comparison of cortical and midbrain activations

A) Activations at peak volumes and voxels for both cortex and midbrain using the continuous scanning method. B) Activations at peak volumes and voxels for both cortex and midbrain using the sparse scanning method. Error bars represent S.E.M. * indicates t-test results of $p<0.01$ between continuous and sparse.

Petkov et al. (2009) increased the acquisition time during continuous scanning in an attempt to temporally equalize the two methods. This may have introduced a greater degree of variability into each volume of continuous as a result of physiological movements, such as respiration or heartbeat, than was present in volumes acquired using sparse scanning. This could result in masking of neural-based BOLD responses by artifact induced by such movements.

Previous studies have also noted better statistics using continuous scanning (Peelle et al., 2010). Results from the present study did not find a significant difference in statistical power. However, to generate the fairest comparison between the two techniques, the number of volumes included in the analysis was equalized. One of the benefits of continuous scanning is the ability to collect larger amounts of data in a similar time frame. Taking into account time constraints, which are normally a factor in studies using fMRI, the larger amount of data which can be collected in the same amount of time would enhance statistical power using continuous scanning.

Previous work using continuous scanning has also resulted in similar, if not better, demonstrations of organizational principles such as primary versus non-primary cortex (Petkov et al., 2009) and functional maps (Woods et al., 2009). In agreement with previous studies, the present results show a better functional mapping of auditory cortex using continuous scanning. Cortical areas, such as A1, which are known to be tonotopic (Imig and Reale, 1980; Reale and Imig, 1980) show a larger number of peaks, using both continuous and sparse scanning, during tonal stimulation. Conversely, areas outside of primary auditory cortex show a larger number of peaks in response to BBN stimulation using both methods. However, this effect is magnified using continuous scanning, resulting in a larger number of peaks as well as peaks in areas that were not identified using sparse such as vPE and T.

The amplified laterality of activations using continuous, as opposed to sparse, scanning was surprising. It is well known, in humans, that there is a lateral weighting of acoustic activation in response to language but has not been noted for simpler stimuli. However, the present investigation did not involve vocalizations, human or conspecific, and for this laterality to be exaggerated in continuous scanning was not expected. The two paradigms, used during the present investigation, differed in their stimulus duration.

During sparse scanning, the stimulus was presented for 4s while it was presented for a full 30s during continuous scanning. Zaehle et al. (2004) found that there is a laterality associated with both tone and temporal changes, such as gap detection and information processing. The difference in the stimulation paradigms may provide an explanation not only for the existence of the laterality, but also for the differences in the laterality between the two methods.

In addition to the benefits of continuous over sparse scanning in volume matched data, time matched data also indicates continuous as the optimal method for fMRI in the cat using a 7T, high field, scanner. Using the same number of runs, meaning less data included for sparse scanning, resulted in no significant activations observed using sparse scanning. This indicates that in the same amount of time sparse scanning may not be able to collect enough data to be usable.

2.5.2 Duty Cycle

Length of stimulus presentation, or duty cycle, has been shown to affect both neural and hemodynamic responses (Birn and Bandettini, 2005; Eggermont, 1994). Therefore, differences noted between the two paradigms, in the present study, could have been a result of stimulation differences. Birn and Bandettini (2005) noted that the effects of duty cycle are most pronounced for stimuli which have durations less than 2s. Stimulus lengths in this study were both ≥4s. Therefore, effects of duty cycle were expected to be minimal. In the continuous run, the second volume starts 3s after stimulation begins and ends at 6s. This is the closest match to the sparse volumes which started 4s after stimulation begins and ends at 7s. If the duty cycle phenomenon was affecting the present data then the second volume of the continuous block and first volume of the sparse block should have been similar while the last volumes were different. Both comparisons were statistically the same (Fig. 2.6) and therefore effects of duty cycle were not observed in the present study.

2.5.3 Auditory pathway activations

A few studies have investigated BOLD responses at different stages of the auditory pathway in humans. Baumann et al. (2010) found similar time courses for the inferior colliculus (IC) and auditory cortex (AC) peaking at approximately 4s. The time course of

the medial geniculate body (MGB) of the thalamus however was slightly later peaking at approximately 5s. This study also noted that AC has the highest percent signal change in relation to IC and MGB activation. Also, with few exceptions, the IC has higher percent signal change than MGB. Similarly Backes et al. (2002) found no difference in the HRF time courses of the IC and AC. However, this study noted that in many of their subjects MGB activations were not identified. They also noted no significant difference in the percent signal change between IC and AC activations. In rats, Cheung et al. (2012) found that activations in subcortical regions were more robust than those in AC. However, this can be attributed to use of high levels of isofluorane as anesthesia which has been shown to alter cortical responsiveness to auditory stimuli (Cheung et al., 2001).

The poorer strength of significant thalamic activation observed during this investigation was not surprising given similar results in previous studies (Backes and van Dijk, 2002; Baumann et al., 2010). It is however, interesting that MGB activations were observed using continuous scanning while no significant activations could be elicited using sparse scanning. We can postulate that the timing of the volume collection along the HRF is most likely the culprit for this discrepancy. Currently there has not been an investigation published on the HRF of the MGB in the cat using fMRI. However, Bauman et al. (2010) found that the HRF peak for the MGB occurred later than AC and IC activations in non-human primates. If this were true, than the start of volume acquisition during sparse scanning, in the present investigation, was not optimally timed for capturing activations of the MGB.

The present investigation resulted in higher percent signal change in AC when compared to IC. The increased activation within AC could be a product of a couple factors: 1) vascularization differences and 2) neuronal processing differences. It has been noted that regions with larger capillary densities result in higher cerebral blood flow (Gerrits et al., 2000; Harrison et al., 2002; Song et al., 2011). The central nucleus of the IC is most likely the largest part of the activations observed in the present study since its microvasularization is significantly larger than the lateral and dorsal cortex of the IC (Song et al., 2011). The lack of MGB activation may be due to vascularization differences since it has lower recorded glucose utilization and blood flow (Baumann et al., 2010). No current literature directly compares capillary densities of AC and IC.

Therefore, further investigation would be necessary to determine if the vascularization is causing the differences seen in the present study. As noted previously, the central nucleus of the IC is most likely driving the activations seen in the present study because it is more vascular than the other two divisions of IC (Song et al., 2011). This nucleus receives mostly afferent projections, projects to the ventral MGB, and is tonotopic (Malmierca and Hackett, 2010; Schreiner and Langner, 1997). It is not surprising then that IC activation was more robust with tonal stimulation. Auditory cortex on the other hand is quite expansive comparatively. A few regions within AC are tonotopic but the majority of AC is not. This explains why activation in response to BBN was so much more robust in cortex (Fig. 2.8). Also, AC receives ascending input as well as lateral or descending input from other cortical areas and divisions of the MGB. This would result in heightened activity levels within AC and cause the larger percent signal change in AC compared to the IC.

2.5.4 Conclusions

In the present study we have successfully demonstrated that activations within the midbrain and cortex can be revealed using both fMRI techniques. When volume numbers were equalized, the extent of activation was larger using continuous scanning and resulted in a greater number of peaks. Also, it is likely that statistical power would also be greater for continuous scanning given the added benefit of more volumes in the same amount of time. Therefore, we conclude that, during passive stimulation in an anesthetized animal, continuous scanning is the preferred method for investigations of auditory cortex in the cat using fMRI. Also, choice of method for future investigations of midbrain activity should be driven by other experimental factors, such as stimulus intensity and task performance during scanning given no significant differences in activation exist between the two methods.

2.6 Acknowledgements

The authors would like to acknowledge the contributions of Kyle Gilbert, who designed the custom RF coil, and Kevin Barker, who designed the apparatus supporting the animals. This work was supported by the Canadian Institutes of Health Research

(CIHR), Natural Sciences and Engineering Research Council of Canada (NSERC), and Canada Foundation for Innovation (CFI).

2.7 References

Amaro, E, Williams, SCR, Shergill, SS, Fu, CHY, MacSweeney, M, Picchioni, MM, Brammer, MJ, McGuire, PK, 2002. Acoustic noise and functional magnetic resonance imaging: Current strategies and future prospects. J Magn Reson Imaging, 16, 497-510.

Backes, WH, van Dijk, P, 2002. Simultaneous sampling of event-related BOLD responses in auditory cortex and brainstem. Magn Reson Med, 47, 90-96.

Bandettini, PA, Jesmanowicz, A, Van Kylen, J, Birn, RM, Hyde, JS, 1998. Functional MRI of brain activation induced by scanner acoustic noise. Magn Reson Med, 39, 410-416.

Baumann, S, Griffiths, TD, Rees, A, Hunter, D, Sun, L, Thiele, A, 2010. Characterisation of the BOLD response time course at different levels of the auditory pathway in non-human primates. Neuroimage, 50, 1099-1108.

Belin, P, Zatorre, RJ, Hoge, R, Evans, AC, Pike, B, 1999. Event-related fMRI of the auditory cortex. Neuroimage, 10, 417-429.

Birn, RM, Bandettini, PA, 2005. The effect of stimulus duty cycle and "off" duration on BOLD response linearity. Neuroimage, 27, 70-82.

Brown, TA, Joanisse, MF, Gati, JS, Hughes, SM, Nixon, PL, Menon, RS, Lomber, SG, 2013. Characterisation of the BOLD response in cat auditory cortex. Neuroimage, 64, 458-465.

Cheung, MM, Lau, C, Zhou, IY, Chan, KC, Cheng, JS, Zhang, JW, Ho, LC, Wu, EX, 2012. BOLD fMRI investigation of the rat auditory pathway and tonotopic organization. Neuroimage, 60, 1205-1211.

Cheung, SW, Nagarajan, SS, Bedenbaugh, PH, Schreiner, CE, Wang, XQ, Wong, A, 2001. Auditory cortical neuron response differences under isoflurane versus pentobarbital anesthesia. Hear Res, 156, 115-127.

Davis, MH, Johnsrude, IS, 2003. Hierarchical processing in spoken language comprehension. J Neurosci, 23, 3423-3431.

Dyson, DH, Allen, DG, Ingwersen, W, Pascoe, PJ, 1988. Evaluation of acepromazine meperidine atropine premedication followed by thiopental anesthesia in the cat. Can J Vet Res-Rev Can Rech Vet, 52, 419-422.

Edmister, WB, Talavage, TM, Ledden, PJ, Weisskoff, RM, 1999. Improved auditory cortex imaging using clustered volume acquisitions. Hum Brain Mapp, 7, 89-97.

Eggermont, JJ, 1994. Temporal modulation transfer functions for AM and FM stimuli in cat auditory cortex. Effects of carrier type, modulating waveform and intensity. Hear Res, 74, 51-66.

Friston, KJ, Ashburner, J, Kiebel, SJ, Nichols, TE, Penny, WD (Eds.), 2007. Statistical parametric mapping: The analysis of functional brain images. Academic Press, Boston.

Gerrits, RJ, Raczynski, C, Greene, AS, Stein, EA, 2000. Regional cerebral blood flow responses to variable frequency whisker stimulation: an autoradiographic analysis. Brain Res, 864, 205-212.

Hall, DA, Haggard, MP, Akeroyd, MA, Palmer, AR, Summerfield, AQ, Elliott, MR, Gurney, EM, Bowtell, RW, 1999. "Sparse" temporal sampling in auditory fMRI. Hum Brain Mapp, 7, 213-223.

Harrison, RV, Harel, N, Panesar, J, Mount, RJ, 2002. Blood capillary distribution correlates with hemodynamic-based functional imaging in cerebral cortex. Cereb Cortex, 12, 225-233.

Hu, XP, Kim, SG, 1994. Reduction of signal fluctuation in functional MRI using navigator echoes. Magn Reson Med, 31, 495-503.

Imig, TJ, Reale, RA, 1980. Pattern of cortico-cortical connections related to tonotopic maps in cat auditory-cortex. J Comp Neurol, 192, 293-332.

Inan, S, Mitchell, T, Song, A, Bizzell, J, Belger, A, 2004. Hemodynamic correlates of stimulus repetition in the visual and auditory cortices: an fMRI study. Neuroimage, 21, 886-893.

Klassen, LM, Menon, RS, 2004. Robust automated shimming technique using arbitrary mapping acquisition parameters (RASTAMAP). Magn Reson Med, 51, 881-887.

Langers, DRM, Backes, WH, van Dijk, P, 2007. Representation of lateralization and tonotopy in primary versus secondary human auditory cortex. Neuroimage, 34, 264-273.

Malmierca, MS, Hackett, TA, 2010. Structural organization of the ascending auditory pathway. In: Moore, DR (Ed.), The oxford handbook of auditory science: The auditory brain. Oxford University Press, Oxford, pp. 9-42.

Moelker, A, Pattynama, PMT, 2003. Acoustic noise concerns in functional magnetic resonance imaging. Hum Brain Mapp, 20, 123-141.

Olfert, ED, Cross, BM, McWilliam, AA, 1993. Guide to the care and use of experimental animals. Canadian Council on Animal Care.

Peelle, JE, Eason, RJ, Schmitter, S, Schwarzbauer, C, Davis, MH, 2010. Evaluating an acoustically quiet EPI sequence for use in fMRI studies of speech and auditory processing. Neuroimage, 52, 1410-1419.

Petkov, CI, Kayser, C, Augath, M, Logothetis, NK, 2009. Optimizing the imaging of the monkey auditory cortex: sparse vs. continuous fMRI. Magn Reson Imaging, 27, 1065-1073.

Price, DL, De Wilde, JP, Papadaki, AM, Curran, JS, Kitney, RI, 2001. Investigation of acoustic noise on 15 MRI scanners from 0.2 T to 3 T. J Magn Reson Imaging, 13, 288-293.

Ravicz, ME, Melcher, JR, Kiang, NYS, 2000. Acoustic noise during functional magnetic resonance imaging. J Acoust Soc Am, 108, 1683-1696.

Reale, RA, Imig, TJ, 1980. Tonotopic organization in auditory cortex of the cat. J Comp Neurol, 192, 265-291.

Scarff, CJ, Reynolds, A, Goodyear, BG, Ponton, CW, Dort, JC, Eggermont, JJ, 2004. Simultaneous 3-T fMRI and high-density recording of human auditory evoked potentials. Neuroimage, 23, 1129-1142.

Schmidt, CF, Zaehle, T, Meyer, M, Geiser, E, Boesiger, P, Jancke, L, 2008. Silent and continuous fMRI scanning differentially modulate activation in an auditory language comprehension task. Hum Brain Mapp, 29, 46-56.

Schreiner, CE, Langner, G, 1997. Laminar fine structure of frequency organization in auditory midbrain. Nature, 388, 383-386.

Song, Y, Mellott, JG, Winer, JA, 2011. Microvascular organization of the cat inferior colliculus. Hear Res, 274, 5-12.

Talavage, TM, Edmister, WB, Ledden, PJ, Weisskoff, RM, 1999. Quantitative assessment of auditory cortex responses induced by imager acoustic noise. Hum Brain Mapp, 7, 79-88.

Talavage, TM, Ledden, PJ, Benson, RR, Rosen, BR, Melcher, JR, 2000. Frequency-dependent responses exhibited by multiple regions in human auditory cortex. Hear Res, 150, 225-244.

van den Noort, M, Specht, K, Rimol, LM, Ersland, L, Hugdahl, K, 2008. A new verbal reports fMRI dichotic listening paradigm for studies of hemispheric asymmetry. Neuroimage, 40, 902-911.

Van Sluyters, RC, Ballinger, M, Bayne, K, Cunningham, C, Degryse, A-D, Dubner, R, Evans, H, Gdowski, MJ, Knight, R, Mench, J, Nelson, RJ, Parks, C, Stein, B, Toth, L, Zola, S, 2003. Guidelines for the care and use of mammals in neuroscience and behavioral research. National Research Council, Washington D.C.

Vannest, JJ, Karunanayaka, PR, Altaye, M, Schmithorst, VJ, Plante, EM, Eaton, KJ, Rasmussen, JM, Holland, SK, 2009. Comparison of fMRI Data From Passive Listening and Active-Response Story Processing Tasks in Children. J Magn Reson Imaging, 29, 971-976.

Wessinger, CM, Buonocore, MH, Kussmaul, CL, Mangun, GR, 1997. Tonotopy in human auditory cortex examined with functional magnetic resonance imaging. Hum Brain Mapp, 5, 18-25.

Woods, DL, Stecker, GC, Rinne, T, Herron, TJ, Cate, AD, Yund, EW, Liao, I, Kang, XJ, 2009. Functional maps of human auditory cortex: effects of acoustic features and attention. PLoS One, 4, e5183.

Zaehle, T, Wustenberg, T, Meyer, M, Jancke, L, 2004. Evidence for rapid auditory perception as the foundation of speech processing: a sparse temporal sampling fMRI study. Eur J Neurosci, 20, 2447-2456.

.

Chapter 3 – High-field fMRI Reveals Tonotopically Organized And Core Auditory Cortex In The Cat.[2]

3.1 Abstract

As frequency is one of the most basic elements of sound, it is not surprising that the earliest stages of auditory cortical processing are tonotopically organized. In cats, there are four known tonotopically organized cortical areas: the anterior (AAF), posterior (PAF), and ventral posterior (VPAF) auditory fields and primary auditory cortex (A1). Electrophysiological and anatomical evidence have suggested that AAF and A1 form core auditory cortex. The purpose of this investigation was to determine if high-field functional magnetic resonance imaging (fMRI) could be used to define the borders of all four tonotopically organized areas, identify core auditory cortex, and demonstrate tonotopy similar to that found using more invasive techniques. Five adult cats were examined. Eight different pure tones or one broad-band noise (BBN) stimuli were presented in a block paradigm during continuous fMRI scanning. Analysis was performed on each animal individually using conservative familywise error thresholds. Group analysis was performed by extracting data from fMRI analysis software and performing a battery of statistical tests. In auditory cortex, a reversal of the tonotopic gradient is known to occur at the borders between tonotopically organized areas. Therefore, high and low tones were used to delineate these borders. Activations in response to BBN as opposed to tonal stimulation demonstrated that core auditory cortex consists of both A1 and AAF. Finally, tonotopy was identified in each of the four known tonotopically organized areas. Therefore, we conclude that fMRI is effective at defining all four tonotopically organized cortical areas and delineating core auditory cortex.

Keywords: fMRI, Cat, Auditory Cortex, Core, Tonotopy

---

[2] A version of this chapter is published as:

Hall, AJ, and, Lomber, SG, 2015. High-field fMRI reveals tonotopically organized and core auditory cortex in the cat. *Hearing Research*, 325, 1-11.

3.2 Introduction

One striking feature of auditory cortex is its frequency-based organization, known as tonotopy. Functional magnetic resonance imaging (fMRI) is a non-invasive technique that has recently been used to identify tonotopy and areal organization within human auditory cortex. While there is debate as to specific details, current literature agrees that there is a tonotopic core, consisting of at least two subdivisions, residing within Heschel's gyrus in the temporal lobe of human cortex (Langers and van Dijk, 2012; Moerel et al., 2014, 2012; Saenz and Langers, 2014; Schönwiesner et al., 2014). Belt areas, surrounding the core, can be difficult to distinguish based purely on tonotopy (Humphries et al., 2010; Langers et al., 2014). However, using sensitivity to other acoustic characteristics, the belt region can be delineated (Woods et al., 2010). The organization within non-human primate (NHP) auditory cortex is understood in much more detail and is often used to make inferences about the organization within human auditory cortex.

The NHP auditory cortex is broadly organized into core, belt, and parabelt regions, each of which consists of multiple cortical areas (Hackett, 2008; Kaas and Hackett, 1998, 2000; Rauschecker, 1998; Rauschecker et al., 1997). The core, containing primary auditory cortex (AI), the rostral field (R), and rostrotemporal field (RT), represents the initial level of processing in auditory cortex and is known to be tonotopic (Kaas and Hackett, 1998; Kaas et al., 1999; Merzenich and Brugge, 1973). While tonotopy is considered to be a characteristic of lower level processing it is not constrained to primary auditory cortices. However, while it is more difficult to evoke activity in areas outside of core auditory cortex using pure tone stimuli (Rauschecker et al., 1995) tonotopic organization has also been identified in subdivisions of the belt (Kaas and Hackett, 1998; Merzenich and Brugge, 1973; Petkov et al., 2006). Functionally, belt areas differ from core areas in that they show a preference for more complex stimuli (Petkov et al., 2006; Rauschecker and Tian, 2004).

In the cat, anatomical (Hackett, 2011; Lee and Winer, 2011; Rouiller et al., 1991) and electrophysiological (Carrasco and Lomber, 2009a) studies suggest that primary auditory cortex (A1) and the anterior auditory field (AAF) together form a primary "core" that is tontopically organized (Carrasco and Lomber, 2009a; Reale and Imig,

1980). Similar to NHPs, however, A1 and AAF are not the only tonotopic cortical areas; the posterior auditory field (PAF) and ventral posterior auditory field (VPAF) are also tonotopically organized (Phillips and Orman, 1984; Reale and Imig, 1980). Previous investigations have found significant differences in neuronal responses such as latency, bandwidth, characteristic frequencies, stimulus location, and stimulus intensity (Carrasco and Lomber, 2009b; Harrington et al., 2008), behavior (Lomber and Malhotra, 2008; Malhotra et al., 2004), and anatomy (Lee and Winer, 2011) between core areas and PAF. While VPAF has not been studied extensively, one study has shown that the response properties of VPAF also differ significantly from core areas (Schreiner and Urbas, 1988). Taken together, these studies suggest that PAF and VPAF operate at a higher functional level within the hierarchy of auditory processing (Hackett, 2011; Lee and Winer, 2011; Rouiller et al., 1991).

All four tonotopic areas form a continuous swath in cat auditory cortex. A reversal in tonotopic gradients from one area to the next provides a means for a functional delineation of areal borders. At the border between A1 and AAF there is a reversal at high frequencies; A1 and PAF is a reversal at low frequencies; and finally, PAF and VPAF is a reversal at high frequencies (Imig et al., 1982; Reale and Imig, 1980). Using fMRI, similar borders in the monkey have been demonstrated using high- and low-frequency pure tone stimuli (Baumann et al., 2010; Petkov et al., 2006). The purpose of the present investigation was to demonstrate that fMRI can be used to define core versus non-core areas, delineate boarders between tonotopically organized areas, and demonstrate tonotopy in each of the areas of the cat.

The results of the current investigation demonstrate a non-invasive technique for identifying four tonotopically organized cortical areas in the cat. It also confirms electrophysiological and anatomical evidence of a core auditory cortex consisting of A1 and AAF, and supports the theory of a hierarchical organization within auditory cortex.

3.3 Methods

Five adult (>6 months) domestic shorthair cats, different from the first study, were selected for this project. All animals were obtained from a commercial laboratory animal breeding facility (Liberty Labs, Waverly, NY) and housed as a clowder. All procedures

were approved by the University of Western Ontario's Animal Use Subcommittee of the University Council on Animal Care and were in accordance with the National Research Council's *Guidelines for the Care and Use of Mammals in Neuroscience and Behavioral Research* (Van Sluyters et al., 2003) and the Canadian Council on Animal Care's *Guide to the Care and Use of Experimental Animals* (Olfert et al., 1993).

3.3.1 Anesthesia and recovery

The anesthesia protocol used in this study has been previously described in detail (Brown et al., 2014; Brown et al., 2013; Hall et al., 2014). Briefly, animals were pre-medicated using a mixture of atropine (0.02 mg/kg) and acepromizine (0.02 mg/kg, i.m.) and anesthesia was induced (4 mg/kg ketamine and 0.025 mg/kg dexdomitor, i.m.). Once anesthetized, each animal was intubated and an indwelling feline catheter was inserted in the saphenous vein for the purposes of anesthesia maintenance. Body temperature was maintained with heating discs and vital signs were continually monitored. Each cat was placed in a custom made Plexiglas apparatus in a sternal (sphinx-like) position. The animal's head was inserted into a custom built RF coil and MRI compatible ear inserts, which contained sound attenuating buds and a tube to direct the auditory stimulus close to the tympanic membrane, were placed in each ear. Both sides of the head were stabilized with sound dampening foam padding. The cat and apparatus were then placed inside the bore of the magnet. Anesthesia was maintained through continuous administration of ketamine (0.6-0.75 mg/kg/hr, i.v.) and spontaneous inhalation of isofluorane (0.4-0.5%). On average, sessions lasted 2 hours.

Following each scanning session, anesthesia was discontinued and the cat was monitored closely until fully recovered from the effects of anesthesia, at which time it was returned to the clowder. Generally, animals exhibited normal behavior within 1h of anesthesia cessation.

The choice of anesthetic regime used in the current investigation was based on a prior, unpublished, pilot study. Briefly, we qualitatively assessed four different common anesthetics: isofluorane, ketamine, propofol, and pentobarbital. Anesthetic levels of propofol (5-6 mg/kg induction, 0.3 mg/kg/h maintenance) and isoflurane (2-4%) had to be reduced beyond those capable of maintaining sedation for fMRI purposes. Regardless

of the dosage, pentobarbital (25 mg/kg induction, 4-5 mg/kg as needed for maintenance) resulted in no identifiable activations. The best results, using a single anesthetic, was with Ketamine (4-5 mg/kg induction, 0.05 mg/kg/h maintenance), but was also unable to maintain an acceptable level of sedation for fMRI purposes. The combination of ketamine and isoflurane allowed levels of each to be reduced, beyond those required when using either separately, and still maintain an acceptable level of sedation. The combination also resulted in maximal BOLD responses. This anesthetic regime has been applied in multiple investigations using fMRI in the cat model (Brown et al., 2014; Brown et al., 2013; Hall et al., 2014).

3.3.2 Image Acquisition

All data were acquired on an actively shielded 68 cm human head 7-Tesla horizontal bore scanner with a DirectDrive console (Agilent, Santa Clara, California) equipped with a Siemens AC84 gradient subsystem (Erlangen, Germany) operating at a slew rate of 200 mT/m/s. An in-house designed and manufactured conformal 3-channel transceive cat head RF coil was used for all experiments. Magnetic field optimization (B0 shimming) was performed using an automated 3D mapping procedure (Klassen and Menon, 2004) over the specific imaging volume of interest.

For each cat, functional volumes were collected using a segmented interleaved EPI acquisition (TR = 1000 ms; TE = 15 ms; 3 segments/plane; slices = 21 x 1 mm; matrix = 96 x 96; FOV = 72 x 72 mm; acquisition voxel size = 0.75 mm x 0.75 mm x 1.0 mm; acquisition time (TA) = 3 sec/volume). Images were corrected for physiological fluctuations using navigator echo correction (Hu and Kim, 1994). A high-resolution PD-weighted anatomical reference volume was acquired along the same orientation and field-of-view as the functional images using a FLASH imaging sequence (TR = 750 ms; TE = 8 ms; matrix = 256 x 256; acquisition voxel size = 281 μm x 281 μm x 1.0 mm). Functional imaging data sets were acquired for a continuous (130 continuous volumes) scanning paradigm during every session.

3.3.3 Stimulus presentation

Stimuli included a broadband white noise (BBN) and eight pure tones (1, 5, 10, 13, 16, 17, 20, and 30 kHz). Tones were originally selected at 5 kHz intervals. However, initial

scanning resulted in no activity using 15 kHz tones. Therefore, tones surrounding this were selected which did elicit activity. Each tone was presented in bursts of 400ms with a 100ms gap for the entire (30s) block. Stimuli were generated using MatLab (MathWorks) and presented using custom C+ program (Microsoft visual studio) on a Dell laptop through an external Roland Corporation soundcard (24-bit/96kHz ; Model UA-25EX), a PylePro power amplifier (Model PCAU11) and Sensimetrics MRI-compatible ear inserts (Model S14). Sound card and amplifier output levels were the same for all stimuli. All stimuli were calibrated to 85dB SPL, and output frequency confirmed, using an ear simulator (Bruel & Kjaer, model # 4157), an ear plug simulator (model # DP 0370) and microphone (model # 4134) all mounted on a sound level meter (model #2250).

The continuous scanning method was used during completion of this project as it has been shown to be superior for auditory cortical activations within the cat (Hall et al., 2014). All scanning was completed using a block design (Fig 3.1A) in which a block of 10 volumes (TR and TA=3s; Fig 3.1B) was collected every 30s. Blocks of auditory stimulus presentation were interleaved with baseline blocks of equal length, during which no stimulus was present. A total of 13 blocks (6 stimulus blocks and 7 baseline) were collected in each run. Two stimuli were included during each run for a total of 3 blocks (30 volumes) of each stimulus during each run.

A structural MRI was collected at the beginning of each session after which a minimum of two shortened runs, including 7 blocks, were collected using BBN only. This facilitated confirmation of cortical activity using online analysis. Once acoustically-evoked activity was confirmed, runs commenced using tonal stimuli. Each session included a minimum of 6 runs per session and two sessions per animal were conducted.

3.3.4 Data analysis

Regions of Interest - The structural image from each session was used to generate hand-drawn (MRIcron, McCausland Center, Columbia, SC) region of interest (ROI) masks, based on anatomical structures, for use during analysis. Two ROI's were generated for each session: 1) an ROI encompassing the entire cerebrum (excluding the cerebellum) that was used in normalization during pre-processing, and 2) an ROI encompassing the

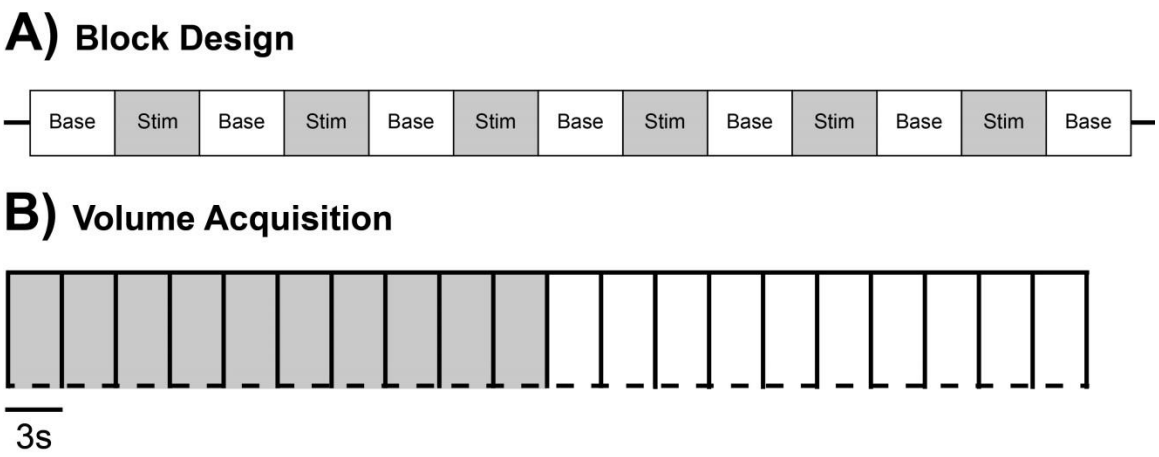

Figure 3.1 Acquisition design.

A) Schematic of the block design. Stimuli were presented in blocks of ten volumes (Stim) interleaved by similarly sized blocks of relative silence (Base). **B)** Schematic of volume acquisition relative to stimulus presentation. Two blocks, a stimulus presentation (shaded) and baseline (white), are diagramed. Stimuli were presented during acquisition allowing ten volumes of data to be collected every 30 seconds.

auditory cortex. The suprasylvian (ss) sulcus was used to delineate the borders of auditory cortex. All thirteen acoustically-responsive areas of auditory cortex in a hearing animal (Fig 3.2) can be found within these bounds (Mellott et al., 2010). This latter ROI was used during data analysis as a mask to isolate activations within auditory cortex. Following border delineation of the tonotopic areas using activations, individual ROI's for AAF, A1, PAF, and VPAF were also generated for use during the assessment of tonotopy.

Pre-Processing - Data from each animal were processed and analyzed separately using SPM8 (Wellcome Trust Centre for Neuroimaging, UCL, London, UK) and MatLab (MathWorks) software. All images were reoriented, corrected for motion (movements in all 6 directions were <0.5mm) and co-registered to the structural image acquired at the beginning of each session. Data were then normalized to a single structural image of the animal and smoothed using a 2mm Gaussian full width at half maximum (FWHM) kernel.

Data Analysis - Data were analyzed independently for each animal and session with motion parameters included as regressors. A single run for each stimulus, which included 30 volumes, was used to build statistical models in order to make the comparison between stimuli equal. Models were built using a restricted maximum likelihood (ReML) estimation and a correlational AR(1) model with high pass filter of 128 s. Following model estimation, separate t-contrasts were generated for each of the stimuli (tones and BBN) as well as one that included all tones. A voxelwise threshold of $p<0.01$ was applied initially, and further analysis was performed only on clusters which also passed a familywise error (FWE) threshold of $p<0.05$. Clusters passing FWE thresholds were identified in all cats for all stimuli presented with the exception of 30kHz.

BBN vs tones - Peak voxels within each cluster of activity related to the BBN stimulus and to the activity across all pure tones were evaluated using anatomical landmarks, for their location in one of thirteen areas within auditory cortex. Timecourses for all peak voxels within a 1 mm spherical radius were extracted from each animal's data and analyzed using custom MatLab programming. A mean percent signal change (PSC) from baseline was calculated from raw data for each volume within a stimulus

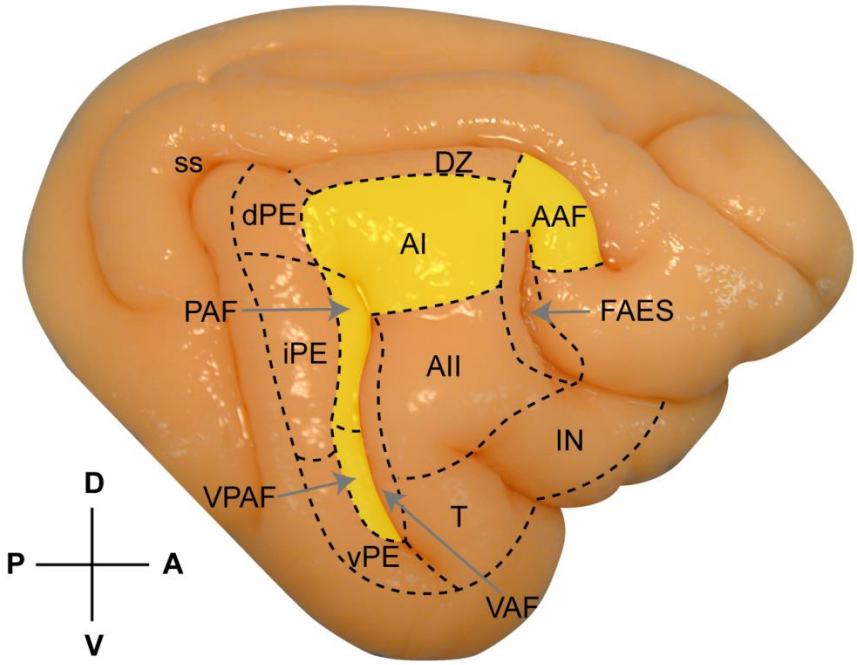

Figure 3.2 Thirteen auditory cortex areas and areas of interest.

Lateral view of the cat cortical surface with the thirteen acoustically responsive areas outlined as defined by electrophysiological and anatomical investigations. The four areas known to be tonotopically organized are highlighted in yellow. Cortical areas and sulci are abbreviated: anterior auditory field, AAF; auditory field of the anterior ectosylvian sulcus, FAES; dorsal zone of the auditory cortex, DZ; insular region, IN; posterior auditory field, PAF; primary auditory cortex, A1; second auditory cortex, A2; temporal region, T; ventral auditory field, VAF; ventral posterior auditory field, VPAF; dorsal posterior ectosylvian gyrus, dPE; intermediate posterior ectosylvian gyrus, iPE; ventral posterior ectosylvian gyrus, vPE; and the supersylvian sulcus, ss. Anatomical terms of direction are abbreviated: anterior, A; dorsal, D; posterior, P; ventral, V.

block across all animals for peaks within a given cortical area as assessed by functional borders defined by tone or BBN stimulation. One-way analysis of variance (ANOVA) and Tukey's honestly significant difference criteria were used to identify statistically significant differences between volumes in a stimulus block and baseline levels. A two sample t-test was then used to determine significant differences between similar volumes of different stimuli. To demonstrate voxel specificity for tones or BBN, the timecourse for the most significantly active voxel to each stimulus type was analyzed using the same methods already described.

Defining borders of tonotopic areas – Borders between tonotopic areas are determined in electrophysiological investigations by a reversal in the tonotopic gradient. Therefore, analyses of the 1kHz tone and 20kHz tones were performed to demonstrate borders between tonotopically organized areas. Each cluster generated by the two stimuli was evaluated by location in relation to anatomical structures, as well as voxelwise specificity for either stimulus. Methods used for generation of PSC values and statistical testing applied for the comparisons of peak voxels generated by these two stimuli were the same as the BBN and tone comparisons.

Tonotopy – While the 1 kHz and 20 kHz tones both produced peaks and clusters passing FWE thresholds within every session, intermediate tones (those between 1 kHz and 20 kHz in frequency) were not as reliable. Therefore, the intermediate tone that produced the strongest activations for each cat was used to demonstrate tonotopy within auditory cortex. Methods used for generation of PSC values and statistical testing applied for the comparisons of the timeline and between the three stimuli were the same as the previously detailed. When peak activations for the low, mid, or high tones were within a 1mm radius of each other, analysis of voxel stimulus specificity was performed on a voxel that fell within the cluster of activity elicited by that particular stimulus, but which was not included in the cluster of activity in response to any other stimulus. Activations within AAF were not strong enough to pass the FWE threshold of $p<0.05$. Therefore, for purposes of defining the area, thresholds were lowered, with the lowest having a FWE value of $p<0.1$, until clear clusters of activations could be visualized.

3.4 Results

The purpose of this investigation was to determine if high-field fMRI could be used in the cat to demonstrate the following: 1) a core region of acoustically responsive areas similar to that found in non-human primate (NHP) auditory cortex can be disassociated from the rest of auditory cortex; 2) borders between individual cortical areas can be delineated using the reversal of tonotopic organization; 3) and tonotopy can be imaged in each of the four tonotopically-organized cortical areas.

3.4.1 Core Auditory Cortex

In NHPs, auditory cortex consists of multiple areas, each belonging to either the core, belt, or parabelt region (Kaas and Hackett, 1998, 2000). Areas within the core represent the initial stages of acoustic processing. These core areas are defined functionally by their specificity for pure tone stimuli over more complex stimuli. Recent electrophysiological and anatomical investigations of cat auditory cortex have revealed that a similar core may exist within the auditory cortex of the cat, consisting of A1 and AAF (Carrasco and Lomber, 2009a; Lee and Winer, 2008a, b). Therefore, using fMRI, the delineation of a core region within auditory cortex consisting of A1 and AAF should be possible by contrasting the patterns of activation produced by pure tone and BBN stimulation.

Time courses for peak voxels within A1, AAF, PAF, and VPAF exhibited very similar patterns in response to tone stimuli (Fig 3.3A). Peaks within all four areas were significantly above baseline levels by volume 2 and maintained this level throughout the remainder of the block. In contrast, during BBN stimuli, PAF and VPAF reach a significant difference from baseline in early volumes, maintain this level throughout the block, and are only significantly different from one another in two volumes (Fig 3.3B). A1 and AAF are much more variable throughout the block but reach a reliable significant difference from baseline much later in the block. This finding supports previous studies which suggest A1 and AAF function as a core separate from PAF and VPAF. The results from the present study also support previous investigations, which have provided evidence that PAF and VPAF function at similar levels within a hierarchy (Lee and Winer, 2011).

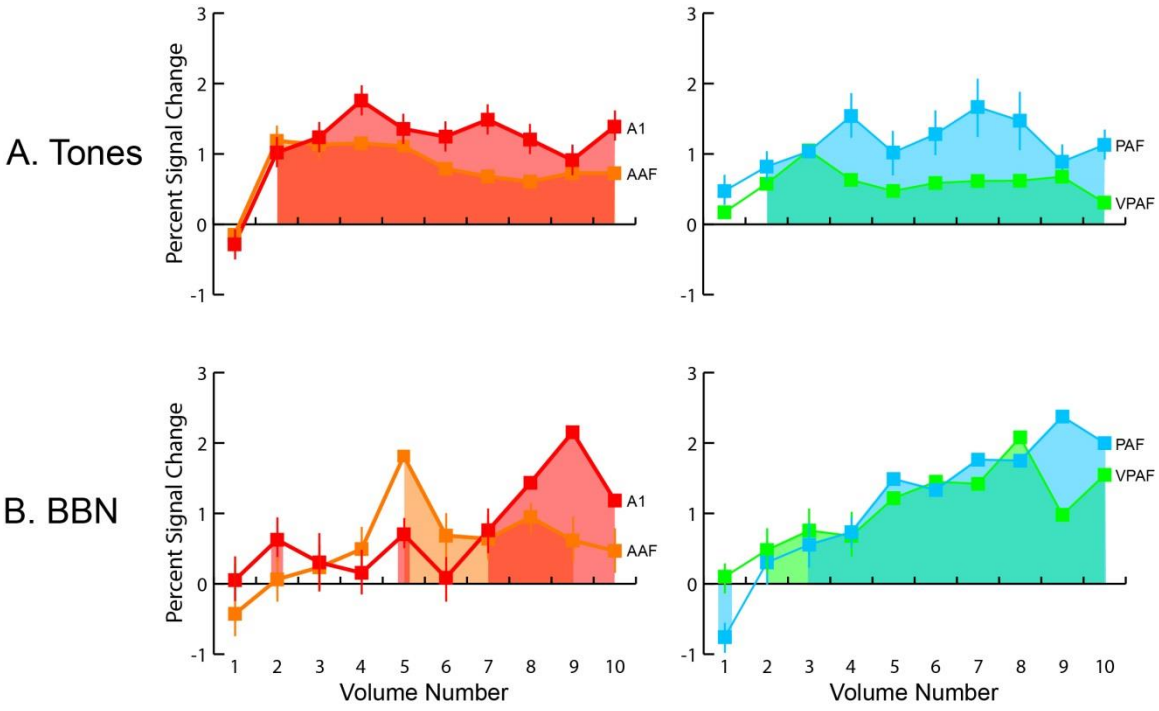

Figure 3.3 PSC timecourses for the four tonotopic areas.

Mean PSC for each volume within stimulus blocks for peak voxels in response to tones (A) or BBN (B) stimuli within A1 (red), AAF (orange), PAF (blue), and VPAF (green) across all animals. Shading in respective colors indicates significant difference from baseline levels as indicated by ANOVA. Error bars are 95% confidence intervals.

Peak voxels within each cluster of activation in response to either pure tones or BBN were assessed for their location within the 13 auditory cortex areas (Fig 3.2). When a pure tone was presented, over 70% of the peak voxels appeared within an area previously known to be tonotopically organized (AAF, A1, PAF and VPAF; Fig 3.4, left). Approximately half of the peaks which appeared within tonotopic areas were localized to the posterior bank of the posterior ectosylvian sulcus (PES), namely in PAF or VPAF (Fig 3.2). The remaining peaks which appeared within tonotopic areas were localized to A1 or AAF. However, when a BBN was presented, 75% of all peaks appeared along the PES, within PAF or VPAF, with only 8.3% appearing within A1 or AAF (Fig 3.4, center). Wong et al. (2014) reported that the four tonotopic areas comprise 44% of all of auditory cortex (Fig 3.4, right). This is interesting given the activations observed in the present study; the four tonotopically organized areas together contained 83.3% of the peak voxels in response to pure tones despite comprising only 44% of the total auditory cortex volume. Also, although they comprise only 8.3% of all of auditory cortex volume, PAF and VPAF contained 75% of the response to BBN.

Activations resulting from either pure tones or BBN stimuli usually favored one hemisphere, and were present along the full depth of cortex (Fig 3.5A,E). By collapsing across all animals tested, a preference for pure tone stimuli can be illustrated in A1 and AAF by comparing mean PSC within each volume of a block across all peaks occurring within these regions (Fig 3.5B). Activations in response to pure tones within these areas are significantly different from baseline levels by volume two, whereas a significant difference is not seen in response to BBN until volume 5. Although the two stimuli start at approximately the same value in the first volume, the pure tone stimulus remains at a significantly higher PSC, than that of the BBN, until volume 5. A similar preference for pure tone stimuli can be seen in PAF and VPAF, with pure tone stimuli evoking a significantly stronger PSC for the majority of the stimulus block (Fig 3.5C). However, the response to the BBN becomes significant from baseline values by the third volume and continues to get stronger throughout the block. Interestingly, non-tonotopic areas also show a preference for tone stimulation, with BBN stimuli only reaching significance at volume 5, and pure tone stimuli evoking a significantly stronger PSC before that (Fig 3.5D).

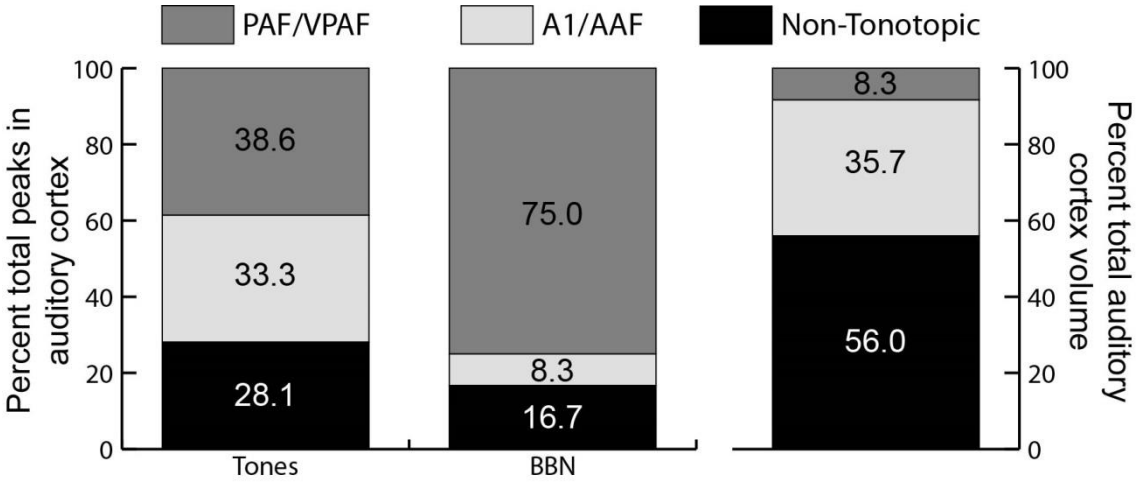

Figure 3.4 Percent representations within auditory cortex.

Left) Percentage of total peaks found responding to tone stimuli in PAF and VPAF (dark grey), A1 and AAF (light grey), or all other non-tonotopic areas (black). **Center)** Percentage of total peaks found responding to BBN stimuli. **Right)** Percentage of total auditory cortex volume occupied by the same three divisions as reported by Wong et al (2014).

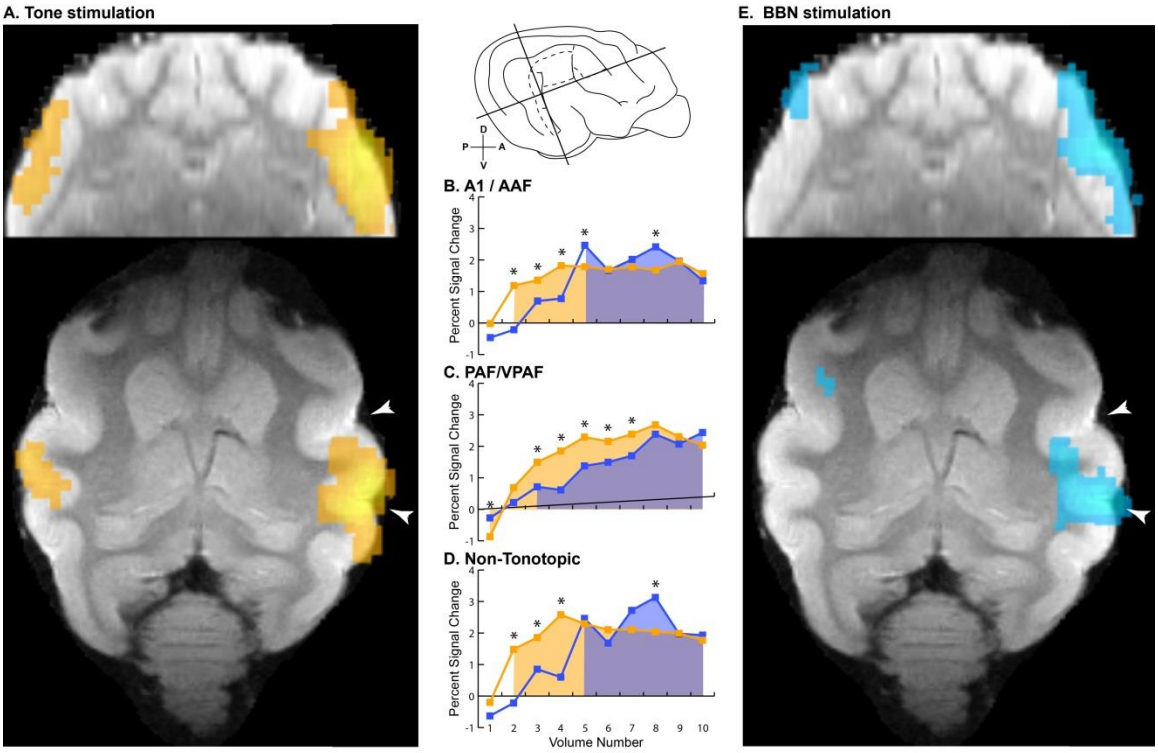

Figure 3.5 BBN v. tones.

A, E) Cortical activations in response to tones or BBN for an individual animal. Anterior and posterior white arrowheads indicate AES and PES sulci, respectively. Top, coronal; bottom, horizontal take at levels indicated by the line drawing in the center. **B, C, D)** Mean PSC for each volume within stimulus blocks for tone (orange) or BBN (blue) stimuli within A1 and AAF (B), PAF and VPAF (C), or all other non-tonotopic (D) areas across all animals. Orange and blue shading indicate significant ($p<0.05$) difference from baseline, as indicated by ANOVA, for similarly colored data. Asterisks indicate significant (t-test, $p<0.05$) difference between tone and BBN stimulus activation.

The localization of BBN activation along the PES can be better visualized when the corresponding activations are overlaid on those from pure tones (Fig 3.6A,C). A clear difference can be seen between areas situated on the middle ectosylvian gyrus, such as A1, and those along the PES. To better illustrate these differences, the peak voxels for each were analyzed separately for individual animals to demonstrate voxel specificity (Fig 3.6B,D). Peak voxels appearing in A1 or AAF demonstrate a clear preference for pure tone stimulation (Fig 3.6B); the PSC differed significantly from baseline activity early in the block and maintained this difference throughout. In contrast, the BBN stimulus failed to exceed baseline level throughout the block. Thus, with very few exceptions, activity in response to pure tone stimulation was significantly greater ($p<0.05$) in each volume from that of activity in response to BBN stimulation.

Peak voxels appearing in PAF or VPAF did not exhibit clear specificity (Fig 3.6D). Activity in response to pure tone stimulation exceeded baseline activity early in the block, but failed to maintain this level throughout. Conversely, activity in response to BBN stimulation was not significantly greater than baseline until later in the block. When a significant difference between the two stimuli did occur, it was most often when BBN activation exceeded that of pure tones.

Therefore, a core region can be delineated from surrounding cortical areas of the cat, including those which are also tonotopically organized, using fMRI.

3.4.2 Borders between tonotopic areas

Borders between tonotopically organized areas of auditory cortex are classically defined by a reversal in the tonotopic gradient (Carrasco and Lomber, 2009a; Carrasco and Lomber, 2009b; Imig and Reale, 1980; Reale and Imig, 1980). The borders between A1 and AAF, and between PAF and VPAF, are defined by a reversal at high frequencies. In contrast, the border between A1 and PAF is defined by a reversal at low frequencies. Therefore, borders between the four tonotopically organized areas can be revealed by analyzing the activations in response to 20 kHz (high) and 1 kHz (low) pure tones.

The bounds of A1 generally span, on the anterior-posterior axis, from the posterior bank of the anterior ectosylvian sulcus (AES) to the anterior bank of the PES (Fig 3.7C-E). The border between A1 and AAF should have a high frequency

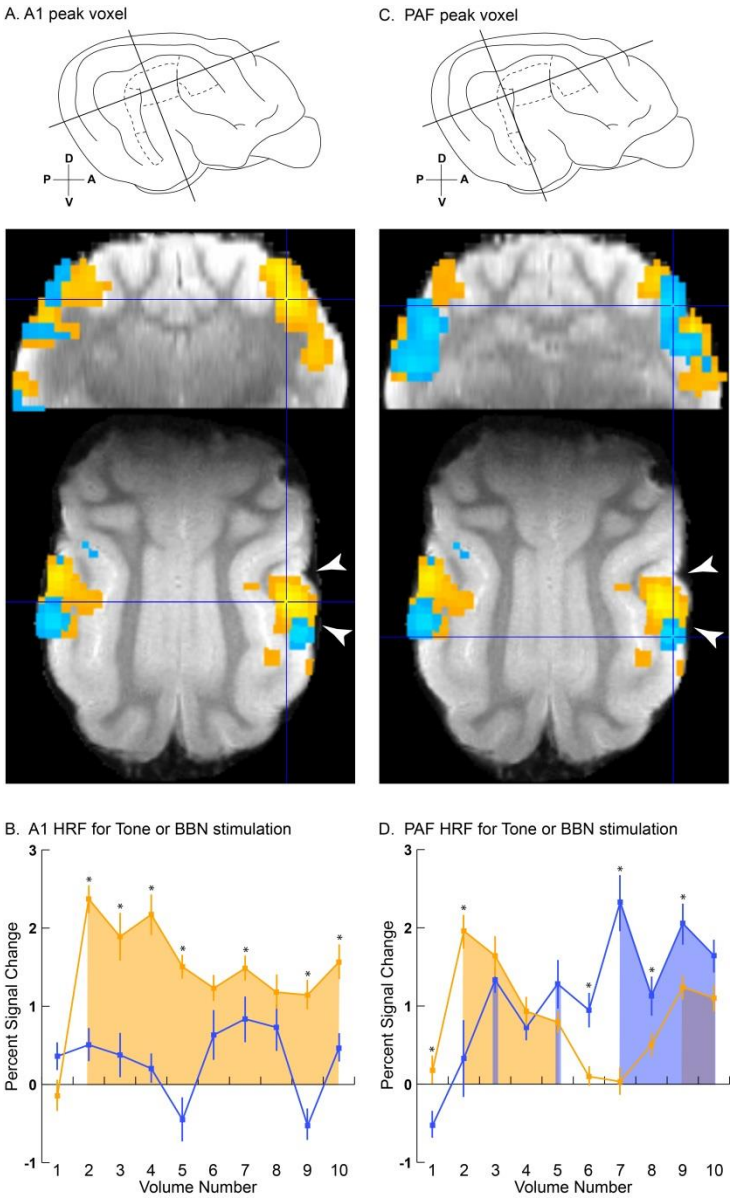

Figure 3.6 Voxel specificity.

A, C) Activations within a representative animal by tones (orange) or BBN (blue) overlaid onto the corresponding anatomical image. Dark blue crosshatches indicate location of voxel used for analysis in plots directly below each. Line drawing insets indicate the location of coronal and horizontal slices show below. Anterior and posterior white arrowheads indicate AES and PES sulci, respectively. **B, D)** Mean PSC for each volume within blocks of tone or BBN stimuli for a representative voxel in A1 or PAF respectively. Error Bars indicate s.e.m. Conventions the same as in Fig 3.5.

representation, and in the current investigation, is demonstrated by activity in response to a 20 kHz tone dorsal to the AES (Fig 3.7A,B). At the posterior border of A1 there is a tonotopic reversal at low frequencies, dorsal to the PES which delineates the A1 and PAF border (Fig 3.7B,C). The ventral border of A1 can also be functionally differentiated by a lack of tonotopic organization (Fig 3.7F).

Selectivity for high or low tones can also be demonstrated by analyzing the timecourses for individual peak voxels. At the A1/AAF border, peak voxels (Fig 3.7G) were significantly greater ($p<0.01$) than baseline by the second volume in a block in response to both high- and low-frequency tones. However, only high-frequency tones were able to maintain a level significantly above baseline. A significant difference ($p<0.01$) between the two occurred most commonly with high-frequency tone activation exceeding that of low-frequency tones. At the A1/PAF border, peak voxels (Fig 3.7H) most commonly exceeded baseline values in response to low-frequency tones, and activations in response to these tones often significantly exceeded responses to high-frequency tones.

PAF and VPAF were also visualized along the PES (Fig 3.8A). Low frequencies activated the most dorsal part of PAF and ventral part of VPAF, and the border between the two was delineated by high-frequency tone activations. In the most dorsal activations, individual voxels showed a preference for low-frequency tones, significantly exceeding baseline values early in the block while high-frequency tones rarely did so (Fig 3.8B). Although not as clear, individual voxels at the border of PAF and VPAF showed a preference for high tones (Fig 3.8C). Activations at the ventral border of VPAF by low-frequency tones were visualized (Fig 3.8A) but individual voxels did not show a clear preference for these stimuli.

Therefore, borders between tonotopically organized cortical areas of the cat can be defined using fMRI.

3.4.3 Tonotopy

In previous electrophysiological investigations of cat auditory cortex, AAF, A1, PAF, and VPAF have all been identified as tonotopically organized (Carrasco and Lomber, 2009a; Carrasco and Lomber, 2009b; Imig and Reale, 1980; Reale and Imig, 1980).

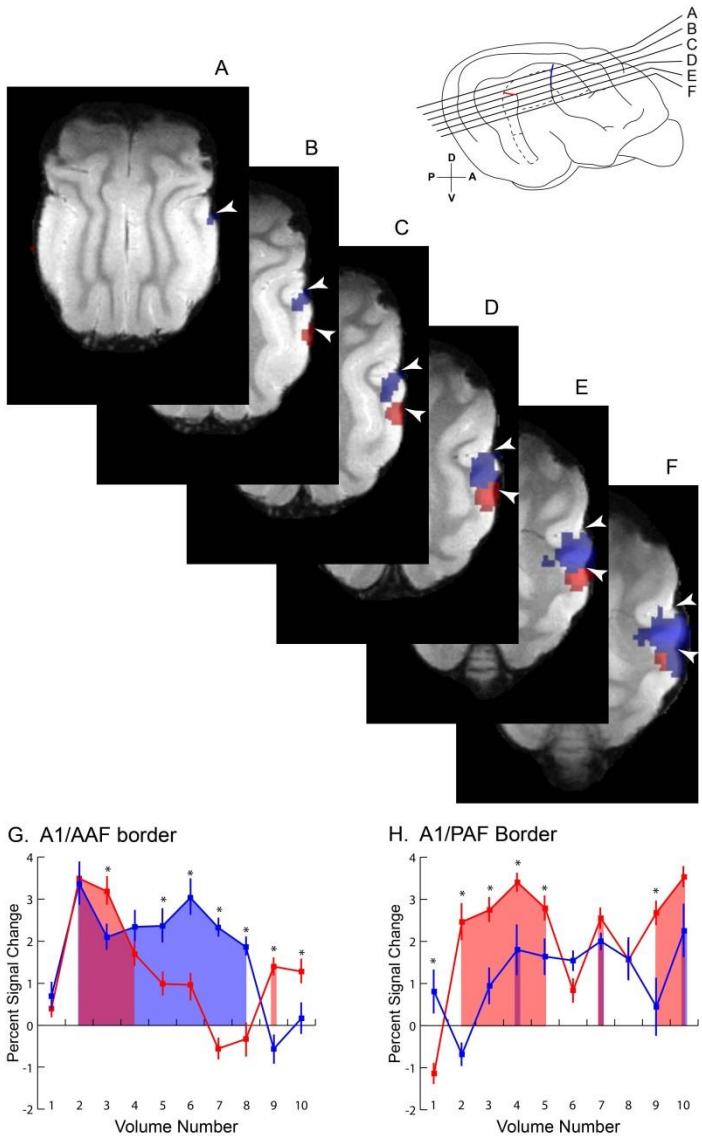

Figure 3.7 A1 Borders.

A-F) Activations within a representative animal in response to 1kHz (red) and 20kHz (blue) tones overlaid onto the corresponding anatomical images. The location of each horizontal section is indicated by the correspondingly labeled lines traversing the inset rendering of the lateral view of the cat cortex. Anterior and posterior white arrowheads indicate AES and PES sulci, respectively. **G, H)** Mean PSC for each volume within blocks of 1kHz (red) or 20kHz (blue) stimulation for a representative voxel at the anterior border of A1 (G) or posterior border of A1 (H). Error Bars indicate s.e.m. Conventions the same as in Fig 3.5.

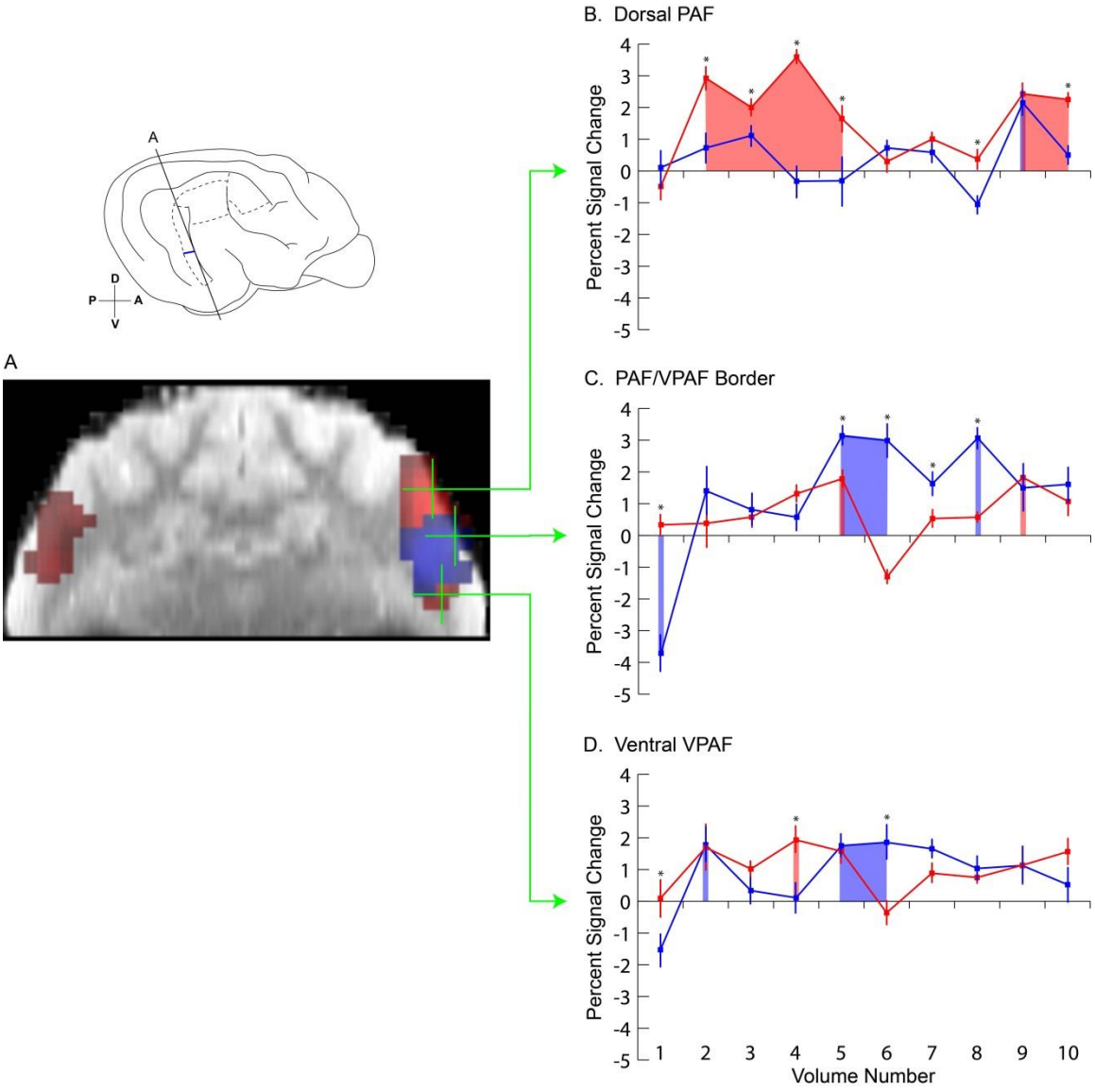

Figure 3.8 Border between PAF and VPAF.

A) Activations within a representative animal in response to 1kHz (red) and 20kHz (blue) overlaid onto the corresponding anatomical image. The location of the coronal section is indicated by the correspondingly labeled line traversing the inset rendering of the lateral view of the cat cortex. **B, C, D)** Mean PSC for each volume within blocks of 1kHz (red) or 20kHz (blue) stimulation for a voxel at the dorsal border of PAF (B), the PAF and VPAF border (C) or ventral border of VPAF (D). Error Bars indicate s.e.m. Conventions the same as in Fig 3.5.

Once the borders of these areas were identified using fMRI, tonotopic organization within these bounds could then be demonstrated.

Activations in AAF did not pass FWE thresholds and therefore are not shown. Activations in A1 that passed FWE thresholds in response to low-, mid-, or high-frequency tones exhibited tonotopic organization when overlaid on each other (Fig 3.9A-E). Low-frequency tones resulted in activation in the posterior portion of A1 while mid- and high-frequency tones resulted in progressively more anterior activations. This is consistent with electrophysiological recordings within A1 in the cat (Carrasco and Lomber, 2009a; Carrasco and Lomber, 2009b; Reale and Imig, 1980). The cessation of tonotopic organization can also be identified at the border between A1 and second auditory cortex (A2; Fig 3.9F).

Reversal of the tonotopic gradient between A1 and PAF can be seen at the dorsal tip of pes going from an anterior-posterior axis in A1 (Fig 3.9B) to a dorsal-ventral axis (Fig 3.10). Visualization of tonotopy within PAF was also possible starting at low-frequency tones dorsally and progressing through mid-frequency tones and finally high-frequency tones at the VPAF border (Fig 3.10). Within VPAF, a less defined tonotopy can be visualized progressing down from high-frequency tones at the PAF border, through intermediate tones and with a small representation of low-frequency tones ventrally (Fig 3.10).

Therefore, tonotopy can be visualized in cat auditory cortex using fMRI.

3.5 Discussion

In summary, the four tonotopically organized areas (AAF, A1, PAF, and VPAF) of cat auditory cortex can be functionally delineated using high-field fMRI. These areas appear to be preferentially sensitive to tonal stimuli, and tonotopy can be visualized within each area. The borders between areas can be identified at the point of reversal of the tonotopic gradients. Finally, core auditory cortex, consisting of A1 and AAF, can also be identified using a comparison of pure tone and BBN activations.

3.5.1 Ability to transfer knowledge to human organization

One of the benefits of using fMRI, is the potential for a more direct comparison and application of the wealth of more invasive techniques to human fMRI data. Comparisons

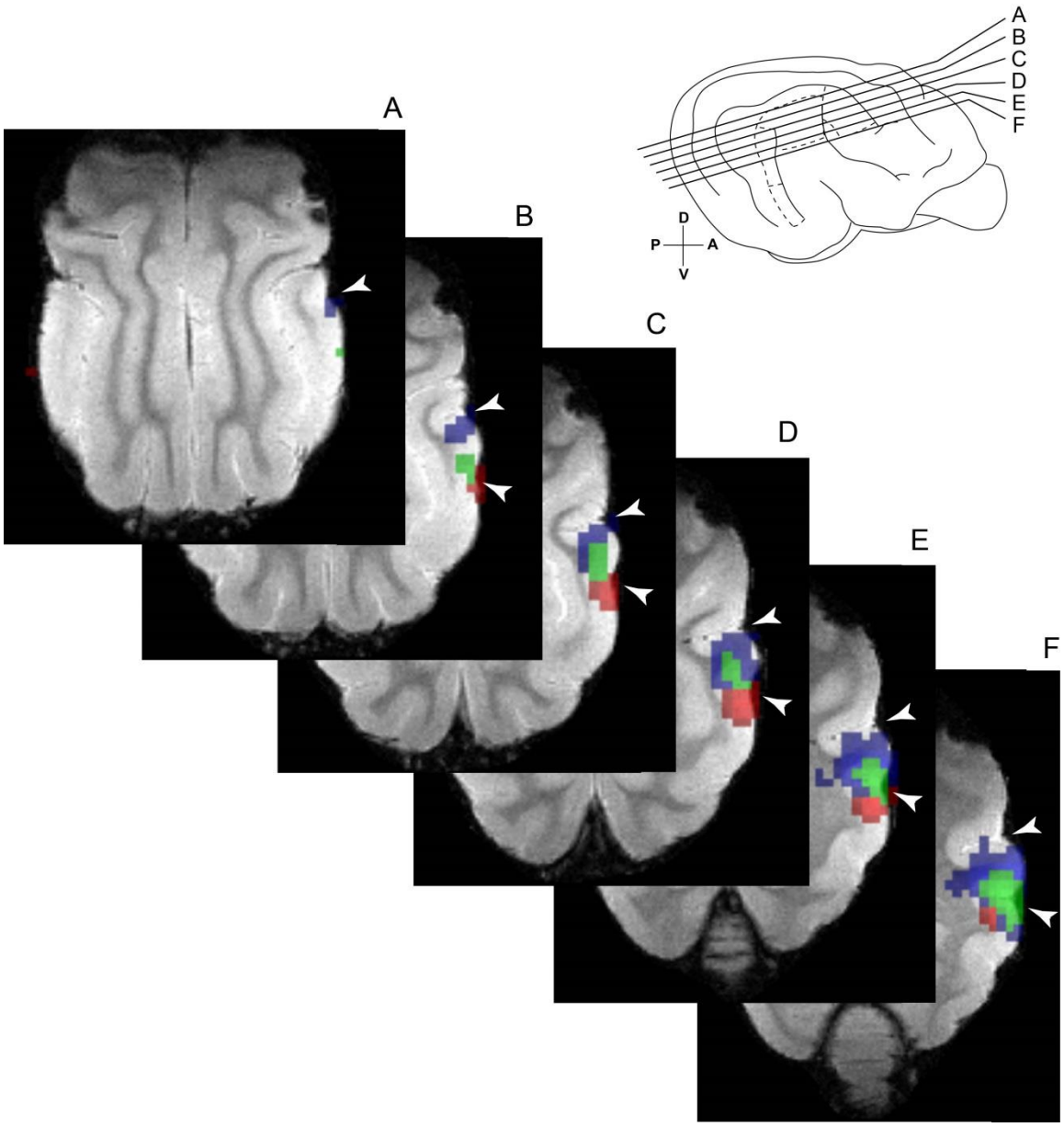

Figure 3.9 A1 Tonotopy.

A-F) Horizontal sections 1mm apart with resulting clusters for high (blue), mid (green), and low (red) tone stimuli in a single animal. The location of the horizontal section is indicated by the correspondingly labeled line traversing the inset rendering of the lateral view of the cat cortex. Anterior and posterior white arrowheads indicate AES and PES sulci, respectively.

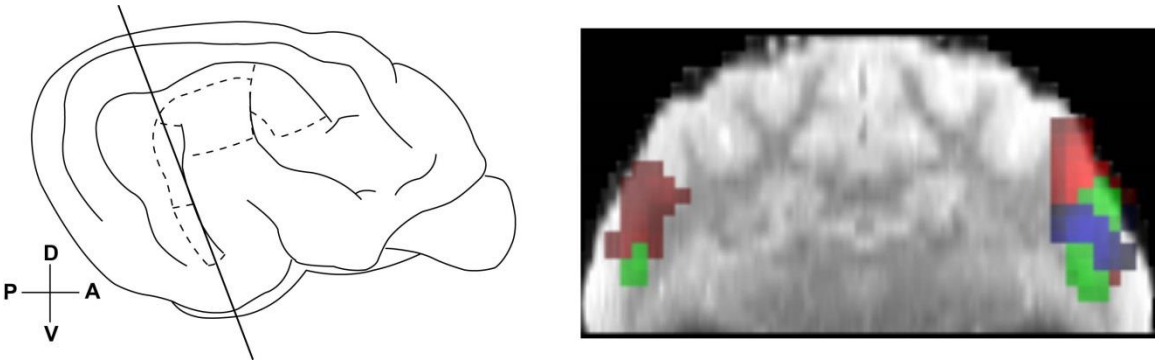

Figure 3.10 PAF and VPAF Tonotopy.

Coronal section aligned with the posterior bank of the PES sulcus with resulting clusters for high (blue), mid (green), and low (red) tone stimuli overlaid on the corresponding anatomical in a single animal. The location of the coronal section is indicated by the corresponding line traversing the rendering of the lateral view of the cat cortex.

are already being made between the functional organization of human and monkey auditory cortex (Schönwiesner et al., 2014; Woods et al., 2010) The present investigation provides foundational evidence for the potential of comparisons between human and primate fMRI studies to the wealth of electophysiological and anatomical investigations of cat auditory cortex. The core and belt organization of auditory cortex has been demonstrated in both human (Chevillet et al., 2011; Wessinger et al., 1997; Wessinger et al., 2001; Woods et al., 2009) and monkey (Petkov et al., 2006; Tanji et al., 2010) subjects using fMRI. In fact, the core and belt areas have been subdivided into multiple cortical fields using fMRI. In the present investigation a similar organizational principal has been demonstrated also using fMRI, where a core auditory cortex, consisting of A1 and AAF, has been localized. The presence of a strong tonotopic organization within cortical areas of the core has also been demonstrated in human, primate, and now cat core areas. This provides some confidence that the well documented principles found within auditory cortex of the cat could be more directly compared to that of the human using fMRI.

3.5.2 Benefits of using fMRI

Classically, tonotopic maps are derived using electrophysiology which produce a grainy map that reflects local heterogeneity despite more large scale organization. The local heterogeneity reflected in electrophysiological investigations is the product of individual neurons, or small local networks, with characteristic frequencies that differ significantly from that of surrounding neurons (Carrasco and Lomber, 2009a; Carrasco and Lomber, 2009b, 2010). Methods that employ a more macroscopic view can produce results that allow a more gestalt view revealing a more defined tonotopic map (Rothschild et al., 2010). While unable to resolve microscopic heterogeneities using present methods, the use of fMRI in this investigation revealed large scale cortical organizational principles without the discontinuity that is commonly observed using electrophysiology.

3.5.3 Sound intensity

The tonotopy reported in the present investigation is coarser and activations in response to a single tone spread further across the cortical surface than would be expected using electrophysiology. Previous investigations of tonotopy using electrophysiology employ

sparsely presented tone pips at, or just above, threshold levels. The intensity of the sound produced while using continuous scanning methods necessitate more intense stimuli and therefore could account, in part, for the tonotopic discrepancy.

Stimulus intensity affects psychoacoustical testing by broadening the responsiveness with increasing intensity (Moore, 2012). Electrophysiological investigations show a similar effect of intensity on tuning curves of individual neurons (Pienkowski and Eggermont, 2011). As the intensity is increased the base of the tuning curve, for an individual neuron, broadens and the best frequency can shift or even become bi-peaked. However, by using a more spectrotemporally rich presentation, individual units become more intensity tolerant (Pienkowski and Eggermont, 2011). Based on this information, two potential alternatives for observing a more refined tonotopic map using fMRI would be 1) To employ sparse scanning methods. The use of sparse scanning methods would enable presentation of stimuli closer to threshold levels during a relatively silent period between aquisitions. However, sparse scanning also extends the time needed to collect the same amount of data which is not ideal with an anesthetized preparation (Hall et al., 2014). Or, 2) A temporally jittered stimulus presentation that would enable a more spectrotemporally rich stimulus presentation. According to Pienkowski and Eggermont (2011), this may alleviate or negate the effects of an increased intensity on the tuning curve. The study by Pienkowski and Eggermont (2011) however only addressed tones up to 65dB which may not be sufficient, with the ambient noise during continuous scanning, to observe tonotopy.

The effects of intensity on the observed tonotopic map may affect core auditory areas more than other areas. The effects of increasing stimulus intensity on activations within core auditory cortex in both human (Woods et al., 2010) and monkey (Tanji et al., 2010) using fMRI are exaggerated in core auditory cortex. Tanji et al. (2010) noted that tones <70dB were unable to drive activations outside of core auditory cortex using fMRI. They also noted that above this level tonotopy could be observed in belt areas surrounding the core. Therefore, stimuli >70dB may be necessary to observe tonotopy in cortical areas such as PAF and VPAF in the cat. The difference in activation between core and belt areas could also provide another avenue for differentiating core from surrounding areas in future investigations.

3.6 Acknowledgements

The authors would like to acknowledge the contributions of Dr. Ewan MacPherson, who assisted in calibrating stimuli, Joe Gati and Trevor Szekeres, who designed and implemented scanning protocols, Kyle Gilbert, who designed the custom RF coil, and Kevin Barker, who designed the apparatus supporting the animals. This work was supported by the Canadian Institutes of Health Research (CIHR), Natural Sciences and Engineering Research Council of Canada (NSERC), and Canada Foundation for Innovation (CFI).

3.7 References

Baumann, S, Griffiths, TD, Rees, A, Hunter, D, Sun, L, Thiele, A, 2010. Characterisation of the BOLD response time course at different levels of the auditory pathway in non-human primates. Neuroimage, 50, 1099-1108.

Brown, TA, Gati, JS, Hughes, SM, Nixon, PL, Menon, RS, Lomber, SG, 2014. Functional imaging of auditory cortex in adult cats using high-field fMRI. Journal of Visualized Experiments, e50872.

Brown, TA, Joanisse, MF, Gati, JS, Hughes, SM, Nixon, PL, Menon, RS, Lomber, SG, 2013. Characterisation of the BOLD response in cat auditory cortex. Neuroimage, 64, 458-465.

Carrasco, A, Lomber, SG, 2009a. Differential modulatory influences between primary auditory cortex and the anterior auditory field. J Neurosci, 29, 8350-8362.

Carrasco, A, Lomber, SG, 2009b. Evidence for Hierarchical Processing in Cat Auditory Cortex: Nonreciprocal Influence of Primary Auditory Cortex on the Posterior Auditory Field. J Neurosci, 29, 14323-14333.

Carrasco, A, Lomber, SG, 2010. Reciprocal modulatory influences between tonotopic and nontonotopic cortical fields in the cat. J Neurosci, 30, 1476-1487.

Chevillet, M, Riesenhuber, M, Rauschecker, JP, 2011. Functional correlates of the anterolateral processing hierarchy in human auditory cortex. J Neurosci, 31, 9345-9352.

Hackett, TA, 2008. Anatomical organization of the auditory cortex. Journal of the American Academy of Audiology, 19, 774-779.

Hackett, TA, 2011. Information flow in the auditory cortical network. Hear Res, 271, 133-146.

Hall, AJ, Brown, TA, Grahn, JA, Gati, JS, Nixon, PL, Hughes, SM, Menon, RS, Lomber, SG, 2014. There's more than one way to scan a cat: Imaging cat auditory cortex with high-field fMRI using continuous or sparse sampling. J Neurosci Methods, 224, 96-106.

Harrington, IA, Stecker, GC, Macpherson, EA, Middlebrooks, JC, 2008. Spatial sensitivity of neurons in the anterior, posterior, and primary fields of cat auditory cortex. Hear Res, 240, 22-41.

Hu, XP, Kim, SG, 1994. Reduction of signal fluctuation in functional MRI using navigator echoes. Magn Reson Med, 31, 495-503.

Humphries, C, Liebenthal, E, Binder, JR, 2010. Tonotopic organization of human auditory cortex. Neuroimage, 50, 1202-1211.

Imig, TJ, Reale, RA, 1980. Pattern of cortico-cortical connections related to tonotopic maps in cat auditory-cortex. J Comp Neurol, 192, 293-332.

Imig, TJ, Reale, RA, Brugge, JF, 1982. The auditory cortex: Patterns of corticocortical projections related to physiological maps in the cat. In: Woolsey, CN (Ed.), Cortical sensory organization: Multiple auditory areas. Humana Press, Clifton, NJ.

Kaas, JH, Hackett, TA, 1998. Subdivisions of auditory cortex and levels of processing in primates. Audiol Neurootol, 3, 73-85.

Kaas, JH, Hackett, TA, 2000. Subdivisions of auditory cortex and processing streams in primates. Proc Natl Acad Sci USA, 97, 11793-11799.

Kaas, JH, Hackett, TA, Tramo, MJ, 1999. Auditory processing in primate cerebral cortex. Curr Opin Neurobiol, 9, 164-170.

Klassen, LM, Menon, RS, 2004. Robust automated shimming technique using arbitrary mapping acquisition parameters (RASTAMAP). Magn Reson Med, 51, 881-887.

Langers, DRM, Krumbholz, K, Bowtell, RW, Hall, DA, 2014. Neuroimaging paradigms for tonotopic mapping (I): The influence of sound stimulus type. Neuroimage, 100, 650-662.

Langers, DRM, van Dijk, P, 2012. Mapping the Tonotopic Organization in Human Auditory Cortex with Minimally Salient Acoustic Stimulation. Cereb Cortex, 22, 2024-2038.

Lee, CC, Winer, JA, 2008a. Connections of cat auditory cortex: I. Thalamocortical system. J Comp Neurol, 507, 1879-1900.

Lee, CC, Winer, JA, 2008b. Connections of cat auditory cortex: III. Corticocortical system. J Comp Neurol, 507, 1920-1943.

Lee, CC, Winer, JA, 2011. Convergence of thalamic and cortical pathways in cat auditory cortex. Hear Res, 274, 85-94.

Lomber, SG, Malhotra, S, 2008. Double dissociation of 'what' and 'where' processing in auditory cortex. Nat Neurosci, 11, 609-616.

Malhotra, S, Hall, AJ, Lomber, SG, 2004. Cortical control of sound localization in the cat: Unilateral cooling deactivation of 19 cerebral areas. J Neurophysiol, 92, 1625-1643.

Mellott, JG, Van der Gucht, E, Lee, CC, Carrasco, A, Winer, JA, Lomber, SG, 2010. Areas of cat auditory cortex as defined by neurofilament proteins expressing SMI-32. Hear Res, 267, 119-136.

Merzenich, MM, Brugge, JF, 1973. Representation of the cochlear partition on the superior temporal plane of the macaque monkey. Brain Res, 50, 275-296.

Moerel, M, De Martino, F, Formisano, E, 2012. Processing of Natural Sounds in Human Auditory Cortex: Tonotopy, Spectral Tuning, and Relation to Voice Sensitivity. J Neurosci, 32, 14205-14216.

Moerel, M, De Martino, F, Formisano, E, 2014. An anatomical and functional topography of human auditory cortical areas. Frontiers in neuroscience, 8.

Moore, BC, 2012. An introduction to the psychology of hearing, 6 ed. Emerald Group Publishing Ltd., Bingley, UK.

Olfert, ED, Cross, BM, McWilliam, AA, 1993. Guide to the care and use of experimental animals. Canadian Council on Animal Care.

Petkov, CI, Kayser, C, Augath, M, Logothetis, NK, 2006. Functional imaging reveals numerous fields in the monkey auditory cortex. PLoS Biol, 4, 1213-1226.

Phillips, DP, Orman, SS, 1984. Responses of single neurons in posterior field of cat auditory cortex to tonal stimulation. J Neurophysiol, 51, 147-163.

Pienkowski, M, Eggermont, JJ, 2011. Sound frequency representation in primary auditory cortex is level tolerant for moderately loud, complex sounds. J Neurophysiol, 106, 1016-1027.

Rauschecker, JP, 1998. Parallel processing in the auditory cortex of primates. Audiol Neurootol, 3, 86-103.

Rauschecker, JP, Tian, B, 2004. Processing of band-passed noise in the lateral auditory belt cortex of the rhesus monkey. J Neurophysiol, 91, 2578-2589.

Rauschecker, JP, Tian, B, Hauser, M, 1995. Processing of complex sounds in the macaque nonprimary auditory cortex. Science, 268, 111-114.

Rauschecker, JP, Tian, B, Pons, T, Mishkin, M, 1997. Serial and parallel processing in rhesus monkey auditory cortex. J Comp Neurol, 382, 89-103.

Reale, RA, Imig, TJ, 1980. Tonotopic organization in auditory cortex of the cat. J Comp Neurol, 192, 265-291.

Rothschild, G, Nelken, I, Mizrahi, A, 2010. Functional organization and population dynamics in the mouse primary auditory cortex. Nat Neurosci, 13, 353-U321.

Rouiller, EM, Simm, GM, Villa, AEP, Deribaupierre, Y, Deribaupierre, F, 1991. Auditory corticocortical interconnections in the cat - evidence for parallel and hierarchical arrangement of the auditory cortical areas. Exp Brain Res, 86, 483-505.

Saenz, M, Langers, DRM, 2014. Tonotopic mapping of human auditory cortex. Hear Res, 307, 42-52.

Schönwiesner, M, Dechent, P, Voit, D, Petkov, CI, Krumbholz, K, 2014. Parcellation of human and monkey core auditory cortex with fMRI pattern classification and objective detection of tonotopic gradient reversals. Cereb Cortex.

Schreiner, CE, Urbas, JV, 1988. Representation of amplitude modulation in the auditory cortex of the cat. II. Comparison between cortical fields. Hear Res, 32, 49-64.

Tanji, K, Leopold, DA, Ye, FQ, Zhu, C, Malloy, M, Saunders, RC, Mishkin, M, 2010. Effect of sound intensity on tonotopic fMRI maps in the unanesthetized monkey. Neuroimage, 49, 150-157.

Van Sluyters, RC, Ballinger, M, Bayne, K, Cunningham, C, Degryse, A-D, Dubner, R, Evans, H, Gdowski, MJ, Knight, R, Mench, J, Nelson, RJ, Parks, C, Stein, B, Toth, L, Zola, S, 2003. Guidelines for the care and use of mammals in neuroscience and behavioral research. National Research Council, Washington D.C.

Wessinger, CM, Buonocore, MH, Kussmaul, CL, Mangun, GR, 1997. Tonotopy in human auditory cortex examined with functional magnetic resonance imaging. Hum Brain Mapp, 5, 18-25.

Wessinger, CM, VanMeter, J, Tian, B, Van Lare, J, Pekar, J, Rauschecker, JP, 2001. Hierarchical organization of the human auditory cortex revealed by functional magnetic resonance imaging. J Cogn Neurosci, 13, 1-7.

Wong, C, Chabot, N, Kok, MA, Lomber, SG, 2014. Modified areal cartography in auditory cortex following early and late onset deafness. Cereb Cortex, 24, 1778-1792.

Woods, DL, Herron, TJ, Cate, AD, Yund, EW, Stecker, GC, Rinne, T, Kang, X, 2010. Functional properties of human auditory cortical fields. Front Syst Neurosci, 4, 155.

Woods, DL, Stecker, GC, Rinne, T, Herron, TJ, Cate, AD, Yund, EW, Liao, I, Kang, XJ, 2009. Functional maps of human auditory cortex: effects of acoustic features and attention. PLoS One, 4, e5183.

Chapter 4 – The Cat's Meow: A High-Field fMRI Assessment of Cortical Activity in Response to Vocalizations and Complex Auditory Stimuli

4.1 Abstract

Sensory systems are typically constructed in a hierarchical fashion such that lower level subcortical and cortical areas process basic stimulus features, while higher level areas reassemble these features into object-level representations. A number of anatomical pathway tracing studies have suggested that the auditory cortical hierarchy of the cat extends from a core region, consisting of the primary auditory cortex (A1) and the anterior auditory field (AAF), to higher level, auditory fields that are located ventrally. Unfortunately, limitations on electrophysiological examination of these higher level fields have resulted in an incomplete understanding of the functional organization of the auditory cortex. Thus, the current study uses functional MRI in conjunction with a variety of simple and complex auditory stimuli to provide the first comprehensive examination of function across the entire cortical hierarchy. Auditory cortex function is shown to be largely lateralized to the left hemisphere, and is concentrated bilaterally in fields surrounding the posterior ectosylvian sulcus. The use of narrowband noise stimuli enables the visualization of tonotopic gradients in the posterior auditory field (PAF) and ventral posterior auditory field (VPAF) that have previously been unverifiable using fMRI and pure tones. Furthermore, auditory fields that are inaccessible to more invasive techniques, such as the insular (IN) and temporal (T) cortices, are shown to be selectively responsive to vocalizations. Collectively, these data provide a much needed functional correlate for anatomical examinations of the hierarchy of cortical structures within the cat auditory cortex.

Key Words: fMRI, cat, auditory cortex, complex sounds, functional hierarchy

4.2 Introduction

Sensory systems are typically arranged in a processing hierarchy that begins with the coding of basic stimulus features at the sensory epithelium and leads to full-scale object representation in secondary and associative cortical areas. At each level of this ascending pathway, more complex features are represented. For example, in the visual system, neurons in primary visual cortex (V1) are most responsive to simple stimuli like spots or bars of light (Drager, 1975; Hubel and Wiesel, 1959, 1968; Singer et al., 1975). Ascending from V1, more complex stimuli are required for best activation eventually leading to two parallel streams processing spatial location ("where") dorsally or identification ("what") ventrally (Haxby et al., 1991; Ungerleider and Mishkin, 1982). These streams are comprised of individual areas specialized for specific stimuli such as visually-guided reaching (Karnath and Perenin, 2005; Singhal et al., 2013) in the dorsal stream or faces (Collins and Olson, 2014; Kanwisher et al., 1997; Liu et al., 2010) in the ventral stream. Auditory cortex is not understood in the same level of detail as the visual cortex. However, Chevillet and colleagues (2011) demonstrated that the core, belt, and parabelt regions within human auditory cortex can be delineated using pure tones, band-passed noise bursts, or vocalizations, respectively. Thus, an understanding of the way in which hierarchies of cortical fields are arranged has significant consequences for our interpretation of how stimuli in the world around us are encoded and reconstructed in the brain.

Rouiller and colleagues (1991) first proposed a hierarchical organization within auditory cortex of the cat that was based on anatomical connections (Fig 4.1 A,B). This study focused on the second auditory cortex (A2) and the four areas of the auditory cortex known to be organized by frequency (i.e. those with tonotopic organization); primary auditory cortex (A1), the anterior auditory field (AAF), the posterior auditory field (PAF), and the ventral posterior auditory field (VPAF). Based on anatomical connectivity, Rouiller and colleagues placed A1 and AAF at the base of the hierarchy, with A2, VPAF, and PAF at increasingly higher levels. More recent anatomical investigations have confirmed the separation between core (A1 and AAF) and higher-level (A2, VPAF, PAF) cortical areas (Fig 4.1C; for a review see (Lee and Winer, 2011).

In addition, anatomical evidence suggests there are parallel processing streams in auditory cortex (Lee et al., 2004; Lee and Winer, 2011) that may be analogous to the separate ventral and dorsal streams of visual cortex (Ungerleider and Mishkin, 1982). While these studies have been critical to establishing a proposed hierarchy within auditory cortex of the cat, complementary functional data are necessary to provide a complete understanding of perception within the auditory system.

Electrophysiological (Carrasco et al., 2013; Carrasco and Lomber, 2009a, 2011) and functional imaging (Hall and Lomber, 2015) studies have confirmed that A1 and AAF are at similar levels of cortical processing, comprising the core auditory cortex of the cat (Fig 4.1). Collectively, A1 and AAF are considered to be analogous to the auditory core of old world monkeys (Fig 4.1D,E; Carrasco et al., 2013; Carrasco et al., 2015; Hackett, 2011, 2015; Hall and Lomber, 2015; Ma et al., 2013; Petkov et al., 2006; Schönwiesner et al., 2014), which also consists of multiple areas. Beyond core areas, it has been proposed that information flow within auditory cortex of the cat proceeds postero-ventrally (Carrasco and Lomber, 2011; Hackett, 2011). Latencies within individual areas are increasingly longer moving ventrally with AAF and A1 having similar, shorter latencies and A2 and PAF having longer latencies (Carrasco and Lomber, 2011). Also, there is some electrophysiological evidence to support parallel processing streams within auditory cortex of the cat (Carrasco and Lomber, 2009a, b) while behavioural studies have identified areas that are selective for localization but not for discrimination, and vice versa (Lomber and Malhotra, 2008; Malhotra et al., 2004; Malhotra and Lomber, 2007). Indeed, functional evidence for dual-stream processing in auditory cortex has also been observed in humans (DeWitt and Rauschecker, 2012, 2013; Rauschecker, 1997), and monkeys (Rauschecker, 1997; Rauschecker and Tian, 2004; Rauschecker et al., 1995; Rauschecker et al., 1997). However, functional investigations of cortical processing in the cat have provided only a limited glimpse of the hierarchy of cortical processing due to three major limitations: 1) electrophysiological studies often focus on only one or two cortical areas per animal, 2) the position of the external auditory meatus typically limits investigations to the more dorsal fields of auditory cortex, and 3) these studies have traditionally relied on simple acoustic stimuli which may not be well-suited to evoking activity in higher-level cortical areas.

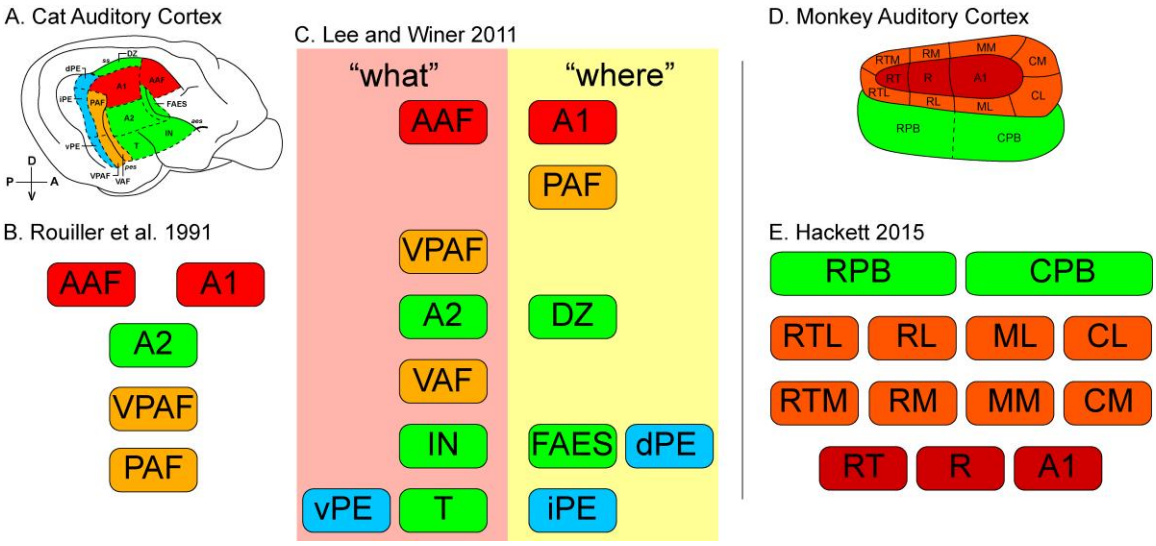

Figure 4.1 Hierarchy of auditory cortex

A) Lateral view of the cat cortical surface with the thirteen acoustically responsive areas outlined as defined by electrophysiological and anatomical investigations. Core (red), tonotopic non-core (orange), non-tonotopic (green) and multisensory (blue) areas are also indicated. **B)** Hierarchy of cat auditory cortex as originally proposed by Rouiller et al. (1991) including only 5 of the 13 cortical areas. **C)** More recent hierarchy of cat auditory cortex as proposed by Lee and Winer (2011) included all 13 areas. **D)** Auditory cortex of the old world monkey with core (red), tonotopically organized belt (orange), and non-tonotopic para-belt (green) areas indicated. **E)** Most recent hierarchy within old world monkey auditory cortex as proposed by Hackett (2015).

While electrophysiological methods may be limited to dorsal auditory cortex, functional magnetic resonance imaging (fMRI), which has been used extensively with human and non-human primate (NHP) subjects, provides the ability to observe activity throughout cortex. Recently, fMRI has also been used to demonstrate activity in the cat, along the auditory pathway (Hall et al., 2014). Moreover, fMRI signals in auditory cortex have been shown to correlate well with electrophysiological measures; for example, using fMRI, A1 and AAF have been shown to have core properties, while the borders of AAF, A1, PAF and VPAF can be visualized though tonotopy (Hall and Lomber, 2015). Thus, fMRI is well suited to investigate the function of ventral auditory cortex in the cat, including the ventral auditory field (VAF), insular cortex (IN) and temporal cortex (T). In addition, the present investigation employs a variety of more complex stimuli including conspecific vocalizations, narrow band noise (NBN), frequency modulated (FM) sweeps, harmonics, and broadband noise (BBN) that are better suited to elicit activity from higher-level auditory cortical areas. We hypothesize that these complex stimuli will most effectively activate areas outside of core auditory cortex. Also, static stimuli will be presented with no location information, such that the functional stream dedicated to discrimination or identification, will be preferentially activated.

4.3 Methods

Ten adult (>6 month) domestic shorthair cats, different from the previous experiments, were selected for this project. All animals were housed as a clowder and obtained from a commercial breeding facility (Liberty Labs, Waverly, NY). The University of Western Ontario's Animal Use Subcommittee approved all procedures. All procedures were also in accordance with the National Research Council's *Guidelines for the Care and Use of Mammals in Neuroscience and Behavioral Research* (Van Sluyters et al., 2003) and the Canadian Council on Animal Care's *Guide to the Care and Use of Experimental Animals* (Olfert et al., 1993).

4.3.1 Anesthesia and Recovery

Anesthetic and recovery procedures have been reported in detail previously (Brown et al., 2014; Brown et al., 2013; Hall et al., 2014). Briefly, each animal was pre-medicated with an intramuscular injection of atropine (0.02 mg/kg) and acepromizine (0.02 mg/kg), then anesthesia was induced by intramuscular injection of a mixture of ketamine (4mg/kg) and dexdomitor (0.025 mg/kg). Once anesthetized, the animal was intubated and an indwelling feline catheter was placed in the cephalic vein for the maintenance of anesthesia. Body temperature and vital signs were continuously monitored. Each cat was then placed, in a sternal position, inside a custom made plexiglass apparatus with the head in a custom-built RF coil (Fig 4.2). MRI-compatible ear inserts were placed in each ear and the head was stabilized with sound-attenuating foam padding. The animal and apparatus were then inserted into the bore of the magnet. Anesthesia was maintained through continuous administration of ketamine (0.6-0.75 mg/kg/hr, i.v.) and spontaneous inhalation of isofluorane (0.4-0.5%). Each session lasted approximately 2 hours.

Following each session, anesthesia was terminated and the animal was monitored closely until fully recovered. The cat was then returned to the clowder. Generally, animals exhibited normal behavior within 1h of anesthesia cessation.

4.3.2 Image Acquisition

All data were acquired on an actively shielded 68 cm 7-Tesla horizontal bore scanner with a DirectDrive console (Agilent, Santa Clara, California) equipped with a Siemens AC84 gradient subsystem (Erlangen, Germany) operating at a slew rate of 300 mT/m/s. An in-house designed and manufactured 10 cm cylindrical 8-channel transceive RF coil was used for all experiments. Magnetic field optimization (B0 shimming) was performed using an automated 3D mapping procedure (Klassen and Menon, 2004) over the specific imaging volume of interest.

For each cat, functional volumes were collected using a single-shot EPI acquisition with grappa acceleration (R=3) and the following scanning parameters: TR = 2000 ms; TE = 19 ms; flip = 70 degrees; slices = 26 x 1mm; matrix = 96 x 96; FOV = 84 x 84 mm; acquisition voxel size = 0.88 mm x 0.88 mm x 1.0 mm; acquisition time (TA) =

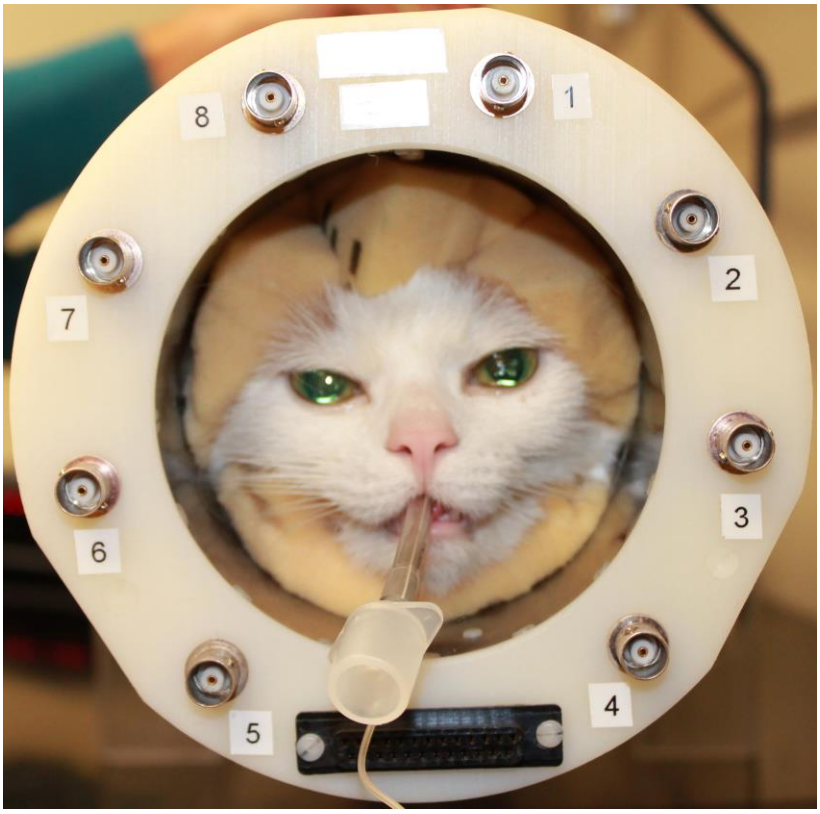

Figure 4.2 Photograph of the eight channel RF coil.

The anesthetized animal's head, enveloped in foam to minimize movement and attenuate scanner noise, is inserted inside an eight channel RF transceiver. The animal is intubated (plastic tube ventral to nose) to permit administration of isofluorane anesthesia.

2 sec/volume; BW = 3719 Hz/px. Images were corrected for physiological fluctuations using navigator echo correction. A high-resolution PD-weighted anatomical reference volume was acquired along the same orientation and field-of-view as the functional images using a FLASH imaging sequence (TR = 750 ms; TE = 8 ms; matrix = 256 x 256; acquisition voxel size = 281 μm x 281 μm x 1.0 mm).

4.3.3 Stimulus presentation

Eleven stimuli were generated including: four, quarter octave narrow band noises (NBN; Fig 4.3A) centered at 1 kHz, 10 kHz, 17 kHz, or 20 kHz; one broad band white noise (BBN; Fig 4.3F); two frequency-modulated (FM) sweeps (Fig 4.3B), one swept from 1 kHz to 25 kHz (upsweep) and the other from 25 kHz to 1 kHz (downsweep); two conspecific vocalizations of similar duration (Fig 4.3 C,D) recorded in a sound attenuating chamber from two separate animals who were not participants in the present experiment; and two harmonic stimuli (Fig 4.3E), generated using the fundamental frequency from each of the vocalizations (0.75 kHz and 1 kHz) and three additional harmonics. All stimuli, with the exception of vocalizations and harmonics, were presented in 400 ms bursts with a 100 ms gap for the entire (30 s) block. Vocalizations were 750 and 850 ms long which necessitated a slower presentation rate (1 Hz) for the entire (30 s) block. Harmonics were duration-matched to the vocalizations and were also presented at a rate of 1 Hz.

With the exception of the vocalizations, all stimuli were generated using MatLab (MathWorks). All stimuli were presented using custom programming in C+ (Microsoft visual studio) on a Dell laptop through an external Roland Corporation soundcard (24-bit/96 kHz ; Model UA-25EX), a PylePro power amplifier (Model PCAU11) and Sensimetrics MRI-compatible ear inserts (Model S14). Sound card and amplifier output levels were the same for all stimuli. All stimuli were calibrated to 85dB SPL using an ear simulator (Bruel & Kjaer, model # 4157), an ear plug simulator (model # DP 0370), and microphone (model # 4134) all mounted on a sound level meter (model #2250).

All scanning was done using the continuous method which has been evaluated as optimal for fMRI of the cat auditory cortex (Hall et al., 2014). A block design (Fig 4.4A)

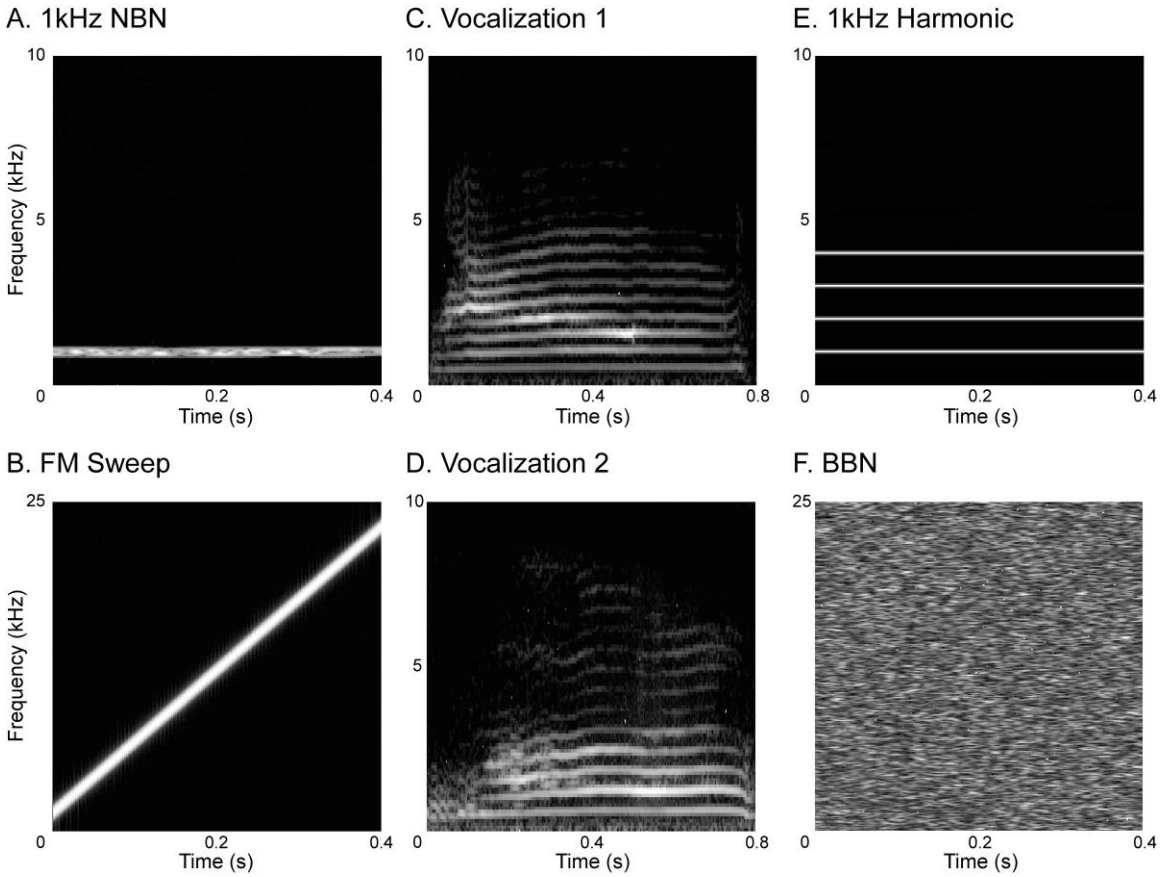

Figure 4.3 Stimulus spectrograms.

Spectrograms for the 1 kHz NBN (A), upward FM sweep (B), each of the vocalizations (C,D), 1kHz Harmonic (E), and BBN (F) stimuli.

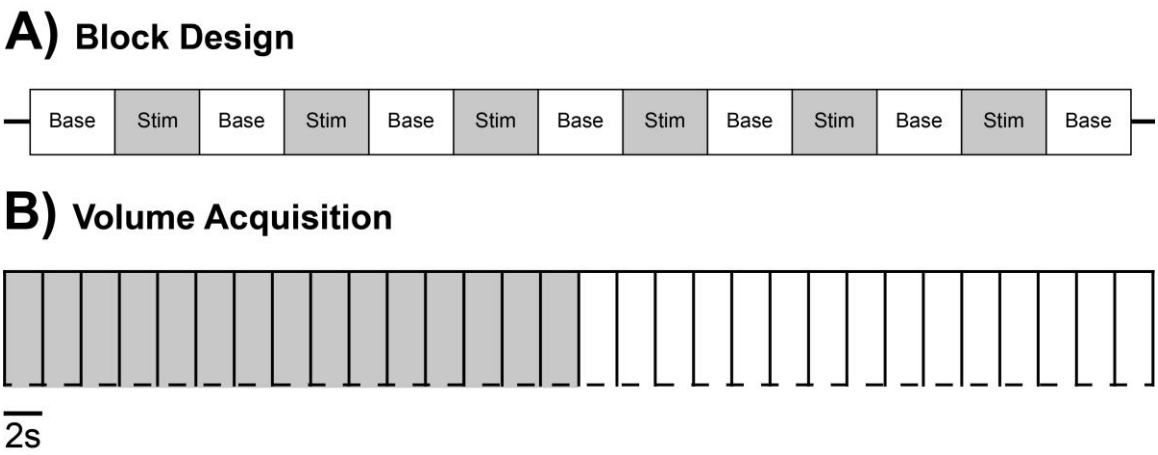

Figure 4.4 Acquisition design.

A) Schematic of the block design. Stimuli were presented in blocks (Stim) interleaved by blocks during which no stimulus was presented (Base). **B)** Schematic of volume acquisition relative to stimulus presentation. Two blocks, a stimulus presentation (shaded) and baseline (white), are diagrammed. Stimuli were presented during acquisition allowing fifteen volumes of data to be collected every 30 seconds.

was used for all runs using blocks of 15 volumes (Fig 4.4B; TR and TA=2s) collected every 30s. Each block of auditory stimulation was interleaved with equal duration blocks during which no stimulus was presented. Thirteen blocks (6 stimulus and 7 baseline; 195 volumes) were collected every run (Fig 4.4A). Two stimuli were presented alternately during each run for a total of 3 blocks (45 volumes) of each stimulus per run.

At the beginning of every session a structural MRI was collected followed by two runs using only the BBN stimulus. This enabled online analysis to confirm that the anaesthetic depth permitted cortical activity before continuing. Following this, regular runs commenced. Each session included a minimum of 6 runs per session and 3 sessions were conducted for each animal.

4.3.4 Data Analysis

Pre-Processing – Data from each animal were processed and analyzed using SPM8 (Wellcome Trust Centre for Neuroimaging, UCL, London, UK) and MatLab (MathWorks) software. All images were reoriented, corrected for motion (movements in all 6 directions were <0.5mm) and co-registered to the structural image acquired at the beginning of each session. Data were then normalized to an anatomical template image and smoothed using a 2mm Gaussian full width at half maximum (FWHM) kernel.

Anatomical Template – All data were normalized to an anatomical template generated in-house. A manuscript detailing the specifics of this template is in preparation. In short, 12 feline anatomical scans collected on a 7T high-field MRI scanner were preprocessed using SPM8 (Wellcome Trust Centre for Neuroimaging, UCL, London) and MatLab (Mathworks) software to align them to a common coordinate system. In a two-phase process, these reoriented images were then normalized and averaged, first to a reference scan chosen from the group, then to the average generated by the first pass processing. Finally, this second pass average was smoothed and provided for group analysis. After normalization to this template, data from individual animals were inspected to confirm accurate alignment of sculci to the template.

Regions of Interest – Hand drawn (MRIcron, McCausland Center, Columbia, SC) region of interest (ROI) masks, based on anatomy, were generated to be used during pre-processing and analysis. One ROI mask which encompassed the cerebrum and excluded the skull, soft tissues and cerebellum was generated using the anatomical scan from each animal and scanning session, and for the template to be used for normalization during pre-processing. A hand-drawn ROI was also generated using the anatomical template which encompassed all of auditory cortex in both hemispheres. The suprasylvian (*ss*) sulcus was used to delineate auditory cortex as all thirteen acoustically responsive areas can be found within these bounds (Mellott et al., 2010). This ROI was used during data analysis as a mask to isolate activations within auditory cortex. The template was also used to generate a ROI for each of the thirteen auditory areas. These masks were used during analysis to examine blood-oxygen level-dependent (BOLD) activity within and between different areas.

Data Analysis – Data were initially analyzed independently for each animal with motion parameters included in each model as regressors. Models were built using a restricted maximum likelihood (ReML) estimation and a correlational AR(1) model with high pass filter of 128 s. Following model estimation, contrasts were generated for each of the stimuli in individual runs. A cluster forming threshold of $p<0.01$ uncorrected was applied initially. Inclusion of an individual animal in further analysis depended on two criteria: 1) at least a single run which produced a cluster of activation passing a familywise error (FWE) threshold of $p<0.05$ for each of the BBN, harmonics, vocalization, and sweep stimuli and, 2) at least a single run which produced clusters of activation passing a FWE threshold of $p<0.05$ for three of the four NBN stimuli.

In order to make fair comparisons between activations, a single run containing 45 volumes was identified for each animal for each NBN stimulus, to be included in further analysis. For the remaining stimulus categories, individual stimuli did not consistently result in clusters of activity which satisfied the FWE threshold. However, if pairs of stimuli of the same category were grouped together (e.g. harmonics, sweeps, or vocalizations) there were robust clusters of activity which passed the FWE threshold. Therefore, individual runs for each of the remaining stimulus categories (BBN, sweeps,

vocalizations and harmonics) contained 90 volumes of stimulus-evoked data (45 upsweeps + 45 downsweeps, 45 vocalization #1 + 45 vocalization #2, etc.). These runs were then incorporated into a model with all animals for group analysis.

Average Timecourses – Timecourses for all voxels within clusters passing the FWE ($p<0.05$) threshold were extracted. A mean percent signal change (PSC) from baseline was calculated for every volume within a block collapsed across animals and hemispheres. A one-way analysis of variance (ANOVA) and Tukey's honestly significant difference criteria were used to evaluate significant differences from baseline values. This evaluation was performed for every stimulus separately.

Average PSC – The average PSC for each animal, cortical area, and stimulus type, was extracted using the MarsBaR (Brett et al., 2002) region of interest toolbox and the individual mask for each cortical area. These numbers were then averaged across animals, a 95% confidence interval was calculated, and a paired t-test was performed to determine significant differences between stimuli within each area. Using the same cortical masks, timecourses for only active voxels across all animals were extracted and average PSC values and block timecourses were calculated.

4.4 Results

Clusters of BOLD activity in response to NBN, FM sweeps, harmonics, BBN, and vocalizations were analyzed for their strength and location within auditory cortex. It was hypothesized that: 1) areas outside of core auditory cortex (A1 and AAF) would be preferentially activated; 2) areas that are specialized for auditory identification (presumptive "what" pathway areas) would be preferentially activated; 3) vocalizations would preferentially activate areas ventral to A2.

Individual animals that did not demonstrate clusters of activity which satisfied the FWE ($p<0.05$) threshold for at least three of the four NBN stimuli were excluded from further analysis. This standard resulted in four animals being excluded while the remaining six were analyzed further for lateralization of activity, the location of peak

activity within the thirteen areas of auditory cortex (Fig 4.1A), and the strength of activation within each of those areas.

4.4.1 Lateralization

Lateralization of auditory function, specifically for the processing of speech, has been well documented in human subjects (Hickok and Poeppel, 2015). Previously, lateralization of function in the cat has been technically difficult to analyze because of the inability to assess activity throughout cortex. However, in the present study, analysis of lateralization was made possible as fMRI enables analysis of the whole of auditory cortex, and the addition of a cortical template enables the normalization and analysis of group data.

A contrast for each stimulus was created across all animals against baseline levels. For each stimulus type, this resulted in a single cluster of activity in each of the left and right hemispheres, with the exception of the 1 kHz NBN stimulus which elicited a unilateral cluster of activity in the right hemisphere (Table 4.1). Most stimuli resulted in a cluster consisting of a larger number of voxels in the left hemisphere. The two exceptions were the 1 kHz NBN stimulus, which elicited a unilateral cluster of activity in the right hemisphere, and the FM sweeps stimulus which elicited a greater number of active voxels in the right hemisphere. The statistical strength at the peak voxels within these clusters echoes the results of the cluster size with all but the 1 kHz NBN and FM sweep stimuli having a left hemisphere bias.

In summary, most cortical activity was lateralized, both in size and statistical strength, to the left hemisphere with the exception of 1 kHz NBN and FM sweeps.

4.4.2 Cortical Activity

One of the many advantages of fMRI is the ability to observe activation throughout auditory cortex. Previous electrophysiological investigations of auditory cortex in the cat have largely focused on dorsal areas including A1, AAF, PAF, the dorsal zone (DZ), and the auditory field of the anterior ectosylvian sulcus (FAES). The use of fMRI affords the capability to investigate neural function within all cortical areas.

		Narrow Band Noise				Sweep	Vocal	Harmonic	BBN
		1 kHz	10 kHz	17 kHz	20 kHz				
Number of Voxels	L		596	531	485	183	676	404	397
	R	65	66	385	183	502	112	113	56
Peak T-statistic*	L		9.15	10.89	7.54	8.85	7.05	7.03	7.92
	R	3.77 (0.269)	5.03 (0.001)	7.75	4.72 (0.004)	9.5	5.18	5.25	3.99

Table 4.1 Lateralization of activations.

Number of voxels (top) in clusters found in either the left (L) or right (R) hemispheres. Also, T-statistic values (bottom) for the peak voxel in the left or right hemispheres. Blue shading indicates a larger number of voxels or statistically stronger activation in the left hemisphere. Red shading indicates a larger number of voxels or statistically stronger activation in the right hemisphere.

Across animals, BOLD activity in response to NBN stimuli is observed in both hemispheres except to the 1 kHz NBN stimulus (Fig 4.5A). NBN stimuli centered at 1 kHz are only observed in the right hemisphere in AAF (Fig 4.5A). NBN stimuli centered at 10, 17, and 20 kHz elicit bilateral activity with peak activations observed in A1 and along the posterior ectosylvian sulcus (*pes*) in areas such as PAF and the VPAF. Significantly active voxels can be observed in all cortical areas with the exception of the insular (IN) and dorsal posterior ectosylvian (dPE) areas. In addition, a tonotopic progression along the *pes* can be observed (Fig 4.5A). Response to the 10 kHz NBN is represented at the dorsal extent of *pes*, with higher frequencies represented toward the midpoint, at which point the gradient is reversed toward the ventral extent of *pes*. This pattern of reversing tonotopic gradients is well documented for abutting cortical fields, and is well-reproduced here using fMRI.

In response to the 1 kHz NBN, average timecourses for all significantly active voxels, across animals are highly variable and are only intermittently greater than baseline activity levels (Fig 4.5B). In response to the remaining NBN stimuli, average timecourses for significantly active voxels show a typical hemodynamic response and are significantly different from baseline ($p<0.05$) throughout the block (Fig 4.5C-E).

BOLD responses to FM sweeps, across animals, are robust and bilateral (Fig 4.6A). Active voxels are observed in all cortical areas except the most ventral areas: temporal cortex (T), IN, VPAF, or the ventral posterior ectosylvian (vPE) area. Peaks of activity are located on the posterior bank of *pes* in the left hemisphere, and anterior bank of the right hemisphere. The average timecourse for active voxels in response to FM sweeps (Fig 4.6B), although at lower percent signal change (PSC) levels than those resulting from NBN stimuli, is significantly different from baseline throughout the block.

Activity in response to vocalizations, across animals, is also bilateral (Fig 4.7A). Active voxels are observed in all cortical areas, with no exceptions. Peak activations occur within the *pes* in the left hemisphere and on the lateral bank of the suprasylvian sulcus (*ss*) in the right hemisphere. The average timecourse for active voxels in response

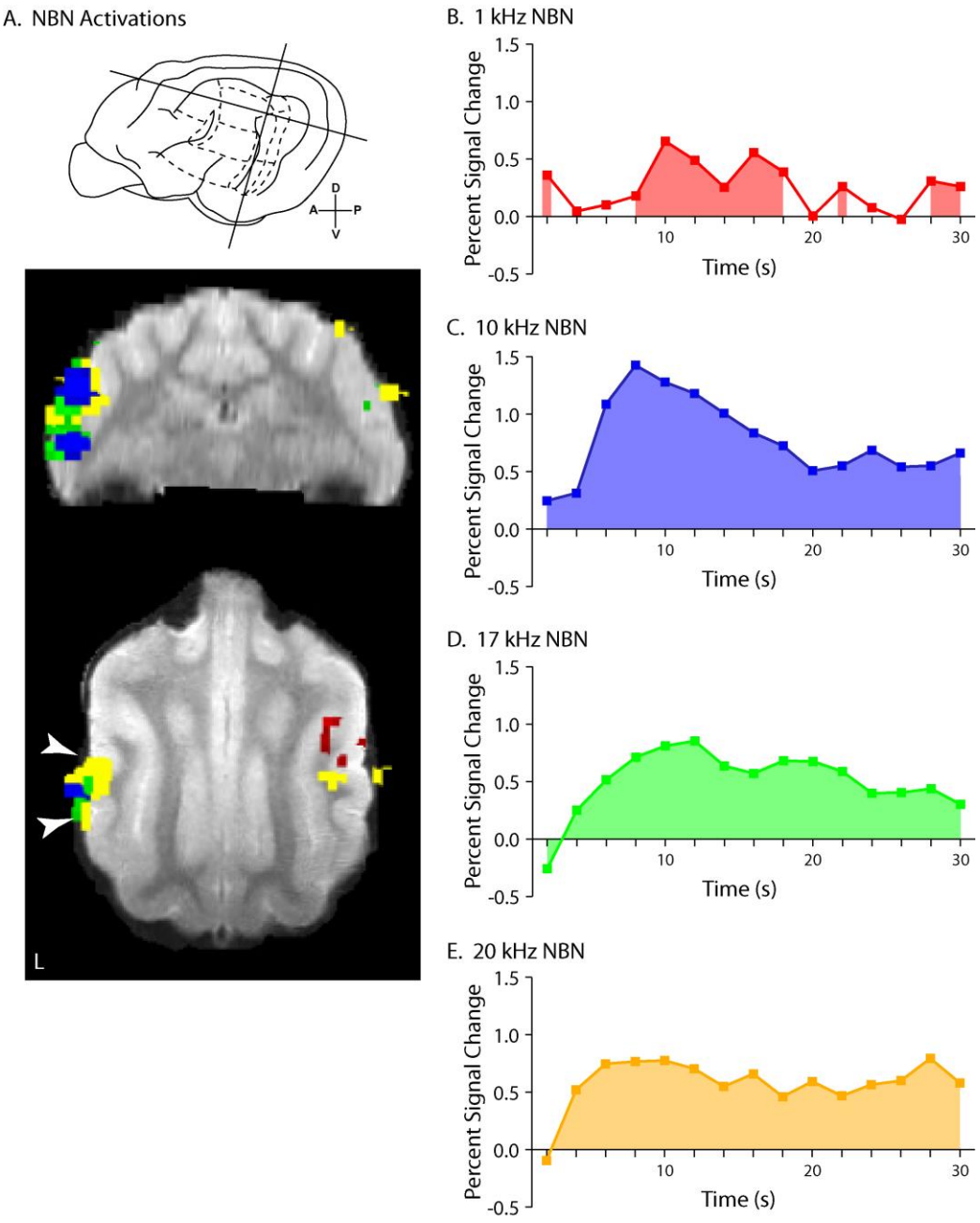

Figure 4.5 Narrow band noise (NBN) activations

A) 1 kHz (red), 10 kHz (blue), 17 kHz (green), and 20 kHz (yellow) NBN stimuli contrasts across animals. The coronal and axial sections correspond to those indicated in the inset above. White arrowheads indicate the anterior ectosylvian sulcus and posterior ectosylvian sulcus. **B-E)** Average percent signal change for blocks of each NBN stimulus. Shading indicates significant difference ($p>0.05$) from baseline as indicated by ANOVA.

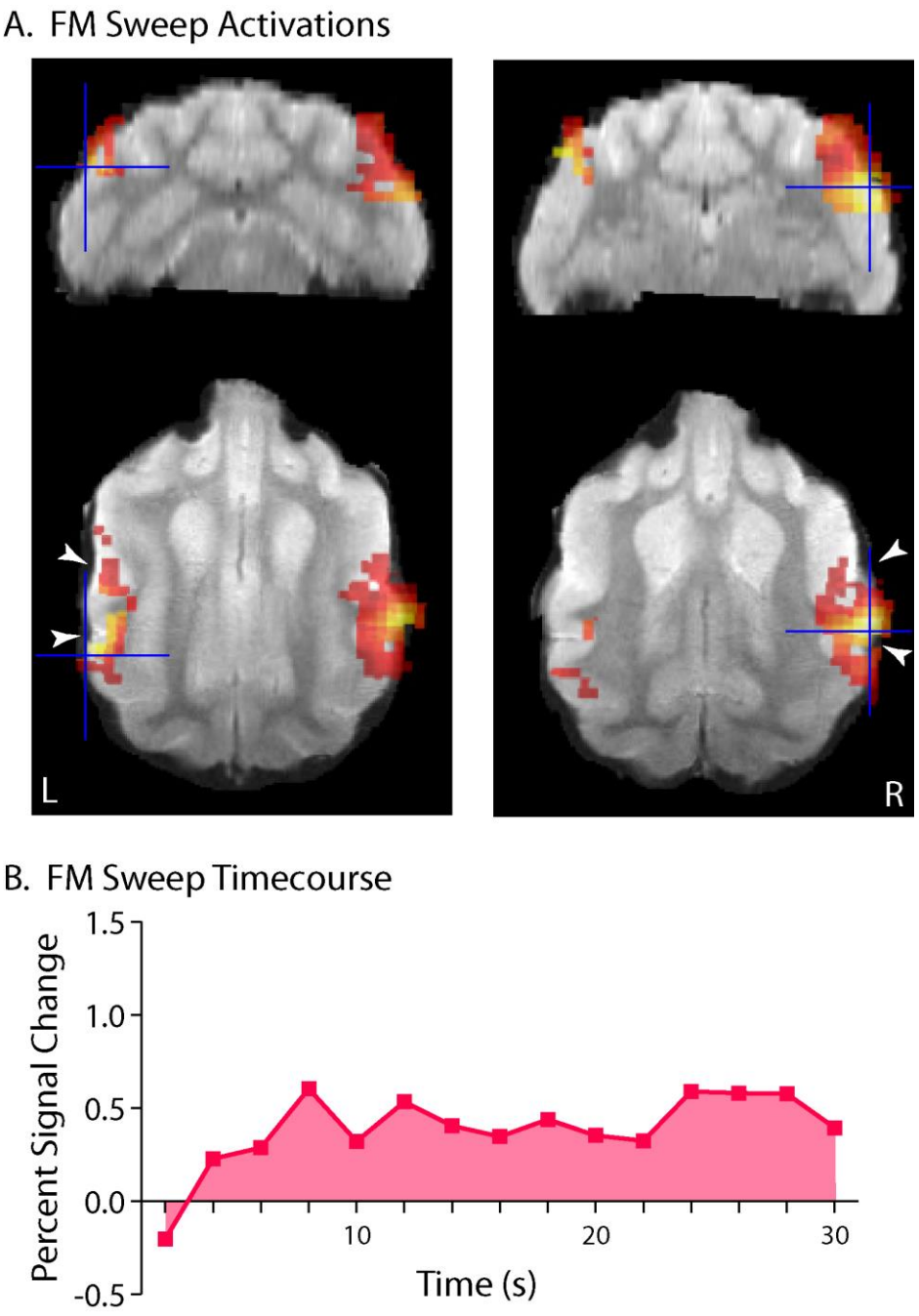

Figure 4.6 Frequency modulated (FM) sweeps activations.

A) Contrast for FM sweep stimuli across all animals. Statistically strongest peak for each cluster is indicated by blue crosshairs for either the left (L) or right (R) hemisphere. **B)** Average percent signal change for blocks of the FM sweep stimuli. Shading indicates significant difference ($p<0.05$) from baseline as indicated by ANOVA.

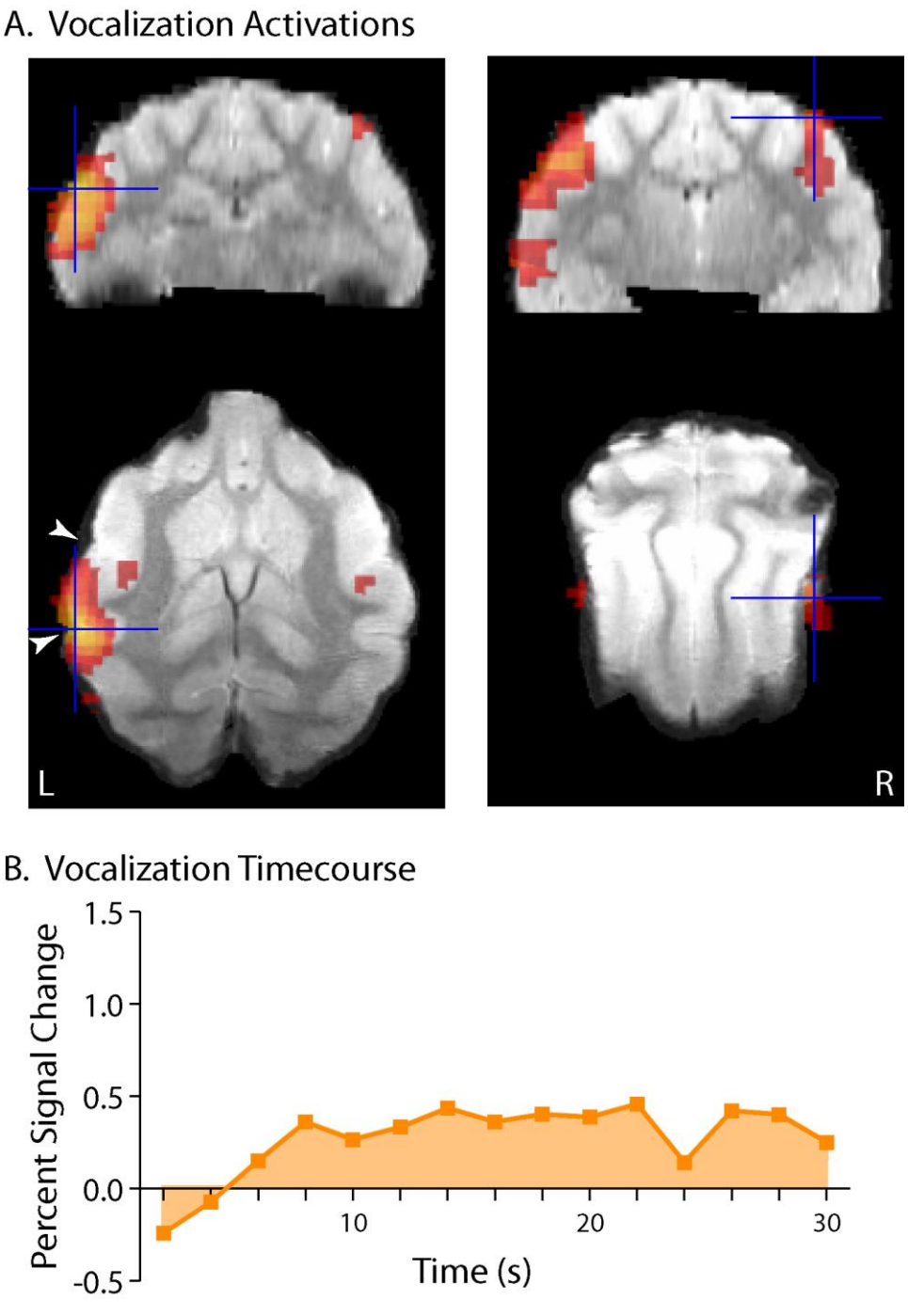

Figure 4.7 Conspecific vocalizations activation.

A) Contrast for vocalization stimuli across all animals. Statistically strongest peak for each cluster is indicated by blue crosshairs for either the left (L) or right (R) hemisphere. **B)** Average percent signal change for blocks of the vocalization stimuli. Shading indicates significant difference ($p<0.05$) from baseline as indicated by ANOVA.

to vocalizations (Fig 4.7B) shows low PSC levels but maintains a significant difference from baseline throughout the block.

Activity in response to harmonics, across animals, is bilateral (Fig 4.8A). Active voxels are observed in all cortical areas except T and IN. Peaks of activity are observed in the *pes* in the left hemisphere and on the middle ectosylvian gyrus in the right hemisphere. The average timecourse for active voxels in response to harmonics (Fig 4.8B) shows low PSC levels, starts significantly below baseline level, and takes 6s to rise significantly above baseline, maintaining this level to the end of the block.

Activity in response to BBN, across animals, is bilateral (Fig 4.9A). Active voxels are observed in all cortical areas except IN and the intermediate posterior ectosylvian (iPE) areas. The average timecourse for active voxels in response to BBN (Fig 4.9B) is only significantly greater than baseline after 6s but maintains this level to the end of the block.

Average PSC levels across all voxels within each cortical area were calculated for the NBN stimuli. The 1 kHz NBN stimulus is only significantly above baseline levels in AAF (Fig 4.10A). The 10, 17 and 20 kHz NBN stimuli are most effective at eliciting activity from A1 and areas along the *pes*, namely PAF, VPAF, and the ventral auditory field (VAF). There are very few significant differences between NBN stimuli within each area. Where significant differences ($p<0.05$) do exist within an area, they involve the 1 kHz stimulus.

Average PSC levels across all voxels in each area were also calculated for the more complex stimuli. FM sweeps result in the largest average PSC in every area except IN (Fig 4.10B), and these changes are significantly greater than those elicited by vocalizations, harmonics, or BBN stimuli in A1, PAF, VPAF, VAF, and vPE. Vocalizations elicit a significant BOLD response in A1, AAF, PAF, VPAF, A2, and FAES. The harmonic and BBN stimuli fail to elicit a signal that is significantly greater than baseline activity in any area.

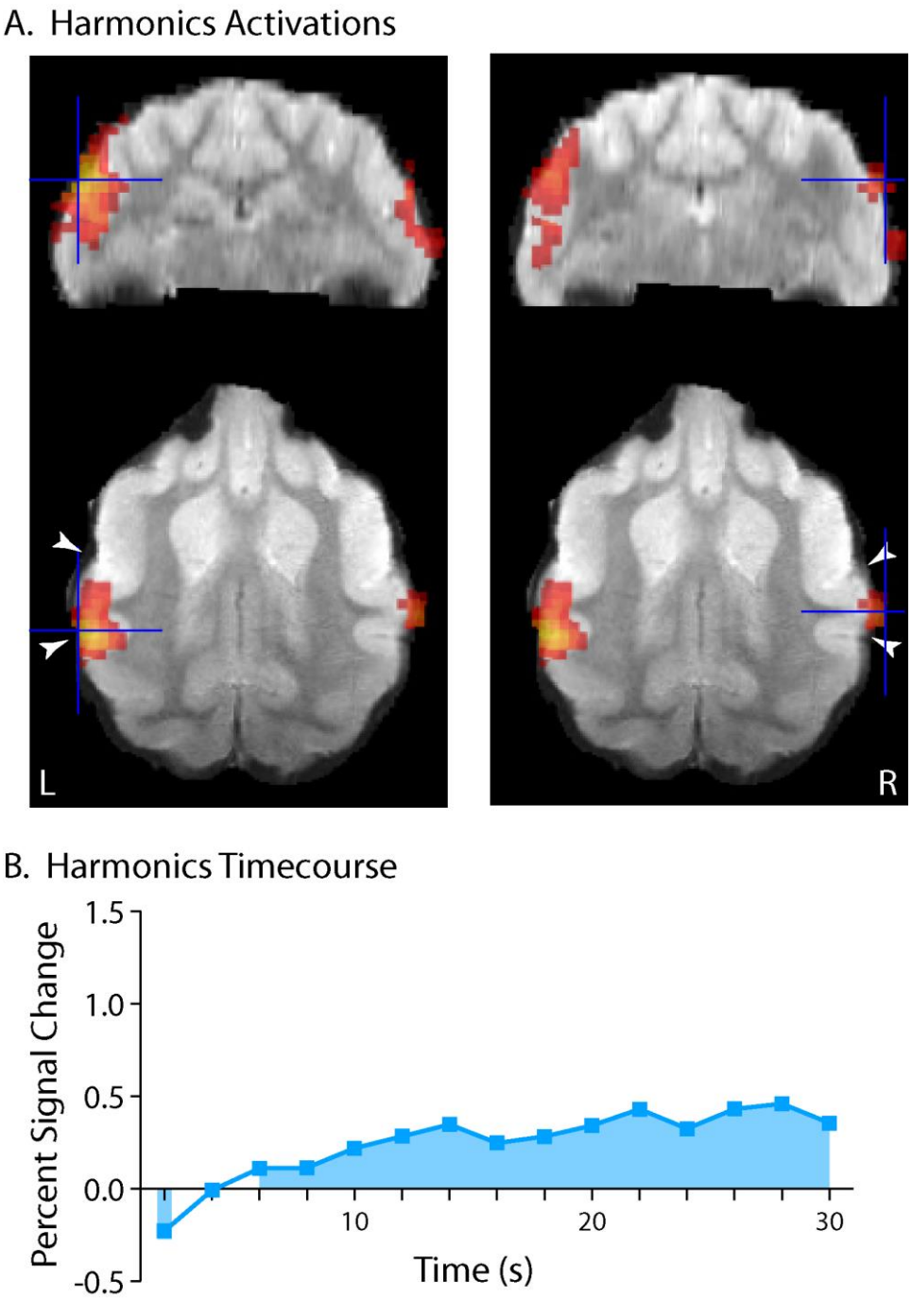

Figure 4.8 Harmonics Activations.

A) Contrast for harmonic stimuli across all animals. Statistically strongest peak for each cluster is indicated by blue crosshairs for either the left (L) or right (R) hemisphere. **B)** Average percent signal change for blocks of the harmonic stimuli. Shading indicates significant difference ($p<0.05$) from baseline as indicated by ANOVA.

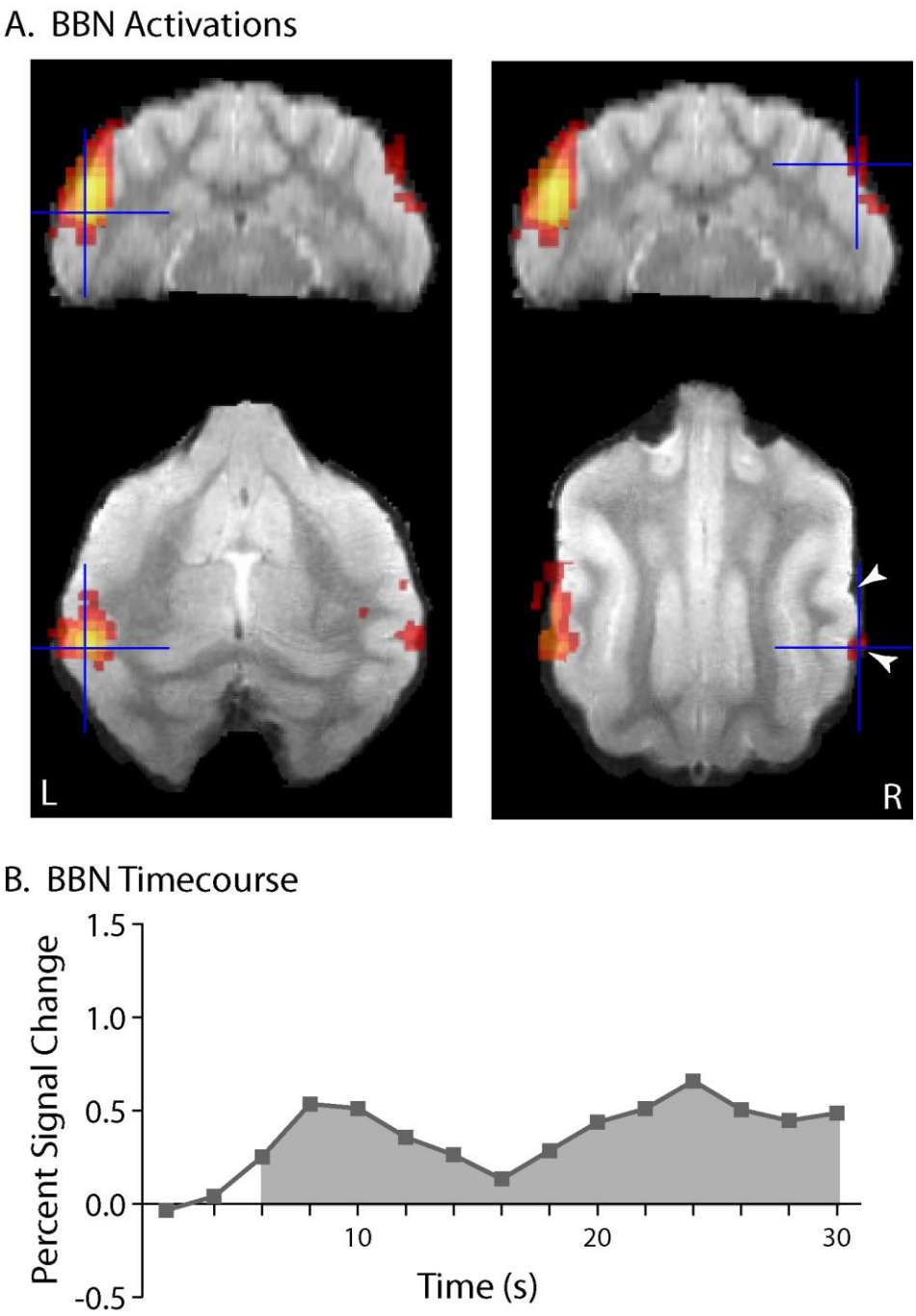

Figure 4.9 Broadband noise (BBN) activations.

A) Contrast for the BBN stimulus across all animals. Statistically strongest peak for each cluster is indicated by blue crosshairs for either the left (L) or right (R) hemisphere. **B)** Average percent signal change for blocks of the BBN stimulus. Shading indicates significant difference ($p<0.05$) from baseline as indicated by ANOVA.

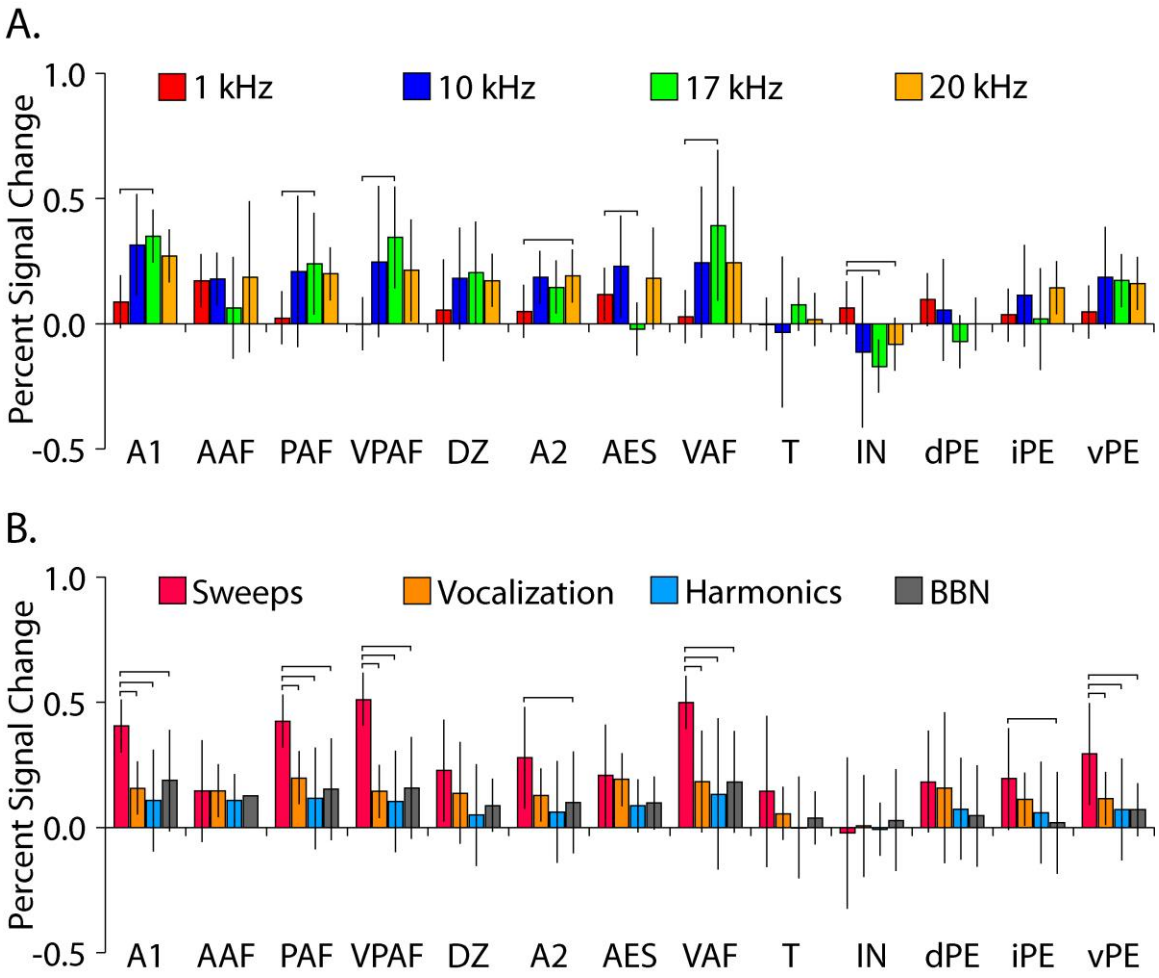

Figure 4.10 Average percent signal change.

A) Average percent signal change across all voxels in an individual area for each of the NBN stimuli. **B)** Average percent signal change across all voxels in an individual area for remaining stimuli. Error bars are 95% confidence intervals. Horizontal bars indicate where a significant difference (t-test, $p<0.05$) exists between two stimuli within an individual area.

4.4.3 Vocalization Specific Activation

Within the visual cortex of multiple species, cortical areas have been discovered that appear to be specialized for the identification of faces (Taylor and Downing, 2011). Similarly, cortical fields which process language have been identified in the auditory cortex of humans, and this network appears to be largely lateralized (Hickok and Poeppel, 2015). A homologue of these areas in the cat has yet to be identified and was the focus of the next set of analyses.

In the present study, it was noted that no active voxels are observed in IN except to vocalization stimuli. Area T appears less functionally specialized, showing significantly active voxels in response to all stimuli except the 1 kHz NBN and FM sweep stimuli. However, average time courses within area T reveal that vocalizations are the only stimuli for which the BOLD signal remains significantly ($p<0.05$) above baseline levels for the majority of the stimulus block (data not shown). The average timecourse in area IN is much more variable than that of T in response to vocalizations (Fig 4.11) such that area T is more consistently responsive to vocalizations than IN.

The harmonic stimuli used in the current study were designed to have similar spectral qualities as the vocalizations, but without temporal variance. Therefore a contrast between blocks of vocalization stimuli and those of harmonic stimuli was performed to elucidate potential cortical areas specific to vocalizations. Harmonic stimuli were designed to have the same fundamental frequencies as the vocalizations and multiple harmonics comperable to vocalizations. This contrast results in a cluster ($p<0.05$ FWE) of 59 voxels in the left hemisphere, at the ventral end of *pes*, which includes VPAF and VAF, that spreads anteriorly across the gyrus corresponding to area T (Fig 4.12).

4.5 Discussion

This current investigation represents the first comprehensive fMRI study to examine responses of auditory cortical areas in the cat to a variety of auditory stimuli ranging from simple noise stimuli to complex conspecific vocalizations. fMRI provides the unique opportunity to gain access to cortical areas that are inaccessible to electrophysiological

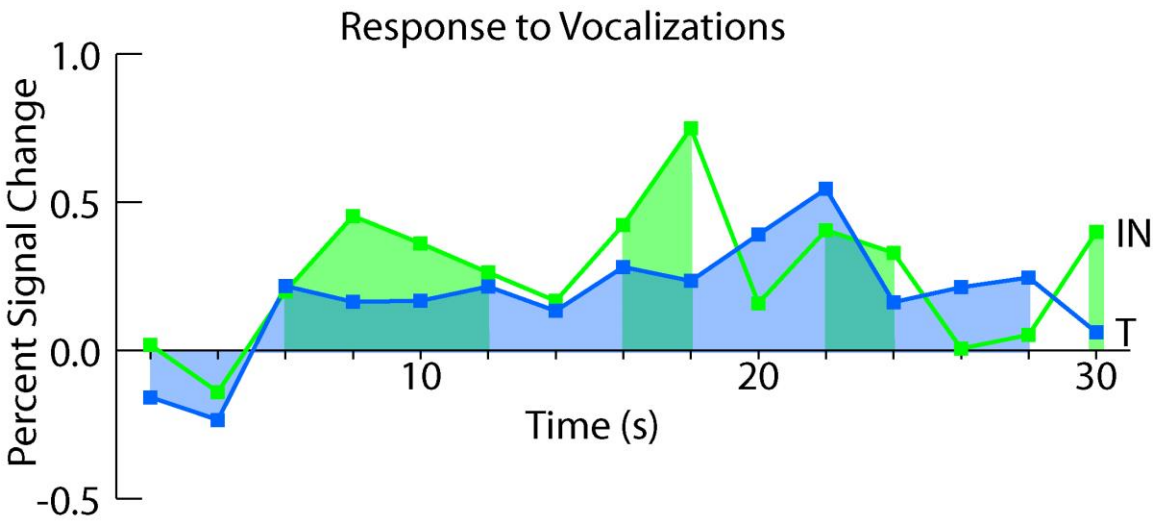

Figure 4.11 Vocalization timecourses in IN and T.

Average percent signal change of active voxels within IN (green) or T (blue) for blocks of vocalization stimuli . Shading in corresponding colors indicates significant difference ($p<0.05$) from baseline as indicated by ANOVA.

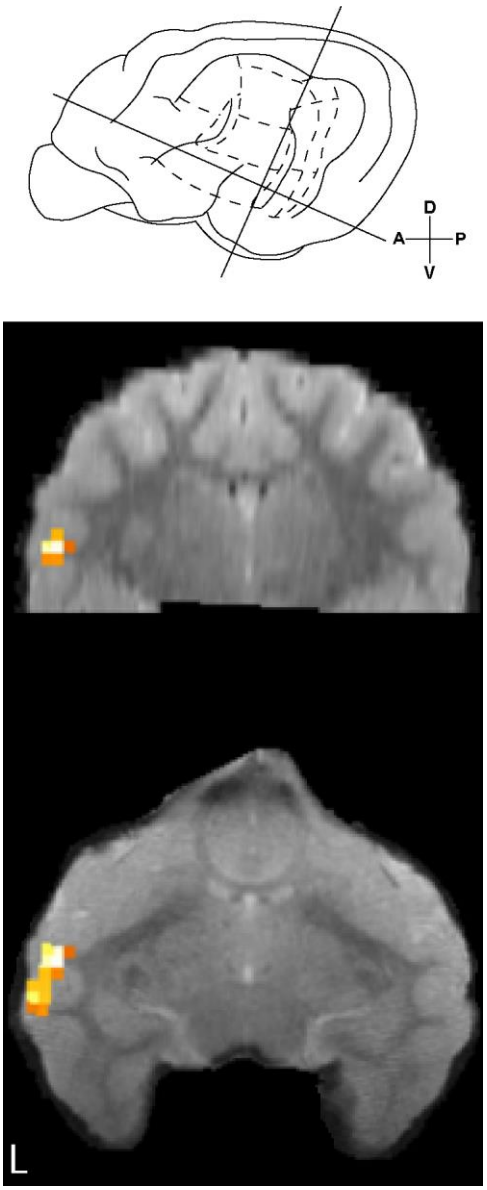

Figure 4.12 Vocalization and harmonics contrast.

Contrast of the vocalization stimuli against the harmonic stimuli. Coronal and axial sections reflect those indicated in the line drawing.

examination, and the current study extends the functional hierarchy to include the more ventral, higher-level cortical fields. With few exceptions, analyses reveal a general left hemisphere lateralization. While responses to more complex stimuli were also observed, FM sweeps were most effective across auditory cortex. Finally, using a contrast against frequency-matched harmonic complexes, vocalizations were found to be selectively processed in area T.

4.5.1 Cortical Lateralization

Within human auditory cortices, lateralization of function, especially with respect to language, is a commonly accepted principle (Hickok and Poeppel, 2015; Kolb and Whishaw, 1996). This lateralization has been attributed to differences in temporal or spectral change (for a review see Scott and McGettigan, 2013), or attention and sensorimotor interactions (Mottonen et al., 2014), and can be enhanced for self-generated sounds, relative to externally generated stimuli (Reznik et al., 2014). Investigations of lateralization of auditory cortex processing in non-human species are limited. Joly and colleagues (2012) noted that activations in response to intact conspecific vocalizations were lateralized to the right hemisphere. Specifically, lateral belt and parabelt areas of the right hemisphere. Conversely, scrambled vocalizations were lateralized to auditory cortex in the left hemisphere.

In the present investigation, a cerebral template was used which enabled group analysis across animals as well as analysis of hemispheric lateralization which was not previously possible. Lateralization of function, both in size and strength, was observed for all stimuli in the auditory cortices of the cat. Visual inspection of data from individual animals confirmed accurate alignment of sulci within auditory cortex. The observed lateralization cannot, therefore, be a product of misalignment of ROIs used to analyze data. BOLD signals were larger and stronger in the left-hemisphere for all stimuli with the exception of 1 kHz NBN, which elicited unilateral activity in the right hemisphere, and FM sweeps which elicited a larger, stronger signal in the right hemisphere.

Stimuli in the current study can be grossly divided into those that change in frequency over time, and those that remain static. For example, the vocalizations employed are comprised of multiple harmonics over several segments including rising and falling phases, similar to formant transitions in human speech, and a plateau (Fig 4.3 C,D). Additionally, FM sweeps were included which rise or fall in frequency at a fast rate, across a large frequency spectrum (Fig 4.3B). Conversely, all NBN (Fig 4.3A), BBN (Fig 4.3F)), and harmonic (Fig 4.3E) stimuli used were of constant frequency across their duration. The fact that BOLD activity for FM sweeps was right-lateralized while vocalization-evoked activity showed left-lateralization similar to the static stimuli begs the question – how are FM sweeps unique? While the vocalizations used here do have sweep-like phases, they did not occur at the same rate and do not span the same frequency range as the FM sweep stimuli. Interestingly, sweep rate and frequency range have been shown to effect lateralization in humans (for a review see (Scott and McGettigan, 2013). Thus, it is possible that these factors are also driving the difference in hemispheric lateralization for FM sweeps observed in the present study. Future investigations of lateralization using a variety of rates and frequency ranges, particularly those more closely matched to what is commonly found in vocalizations, would enable a more precise understanding of the contributory mechanisms.

The orientation with respect to the brain that images were acquired could potentially affect laterality as a result of sampling order. However, in the present investigation images were acquired in the transverse plain resulting in both left and right hemispheres being sampled simultaneously. Therefore, this was not a factor affecting the observed lateralization of function.

The unilateral, right-hemisphere activity elicited by 1 kHz NBN is not easily interpreted. This stimulus is the same as other NBN stimuli, except that it is centered at 1 kHz. The frequency difference could conceivably result in a variance in lateralization since, unlike the other NBN stimuli, it is within normal vocalization frequency ranges. However, it cannot account for the unilateral nature of the activation.

4.5.2 Tonotopy Using Narrow Band Noise

Using pure tones, Hall and Lomber (2015) demonstrated tonotopy within core auditory cortex of the cat, namely areas A1 and AAF, and a weaker tonotopic progression along the *pes* in areas PAF and VPAF. However, it was noted that more complex stimuli were particularly effective at eliciting activation along the *pes*. In the present study, NBN stimuli selectively activated regions along the *pes* enabling tonotopy to be better visualized within PAF and VPAF. In contrast, tonotopy was not visualized in core areas using NBN stimuli. In combination, these findings echo those from rhesus monkey and human studies that found core areas to be more frequency selective and belt areas more responsive to complex, or behaviourally relevant, acoustic stimuli (Kusmierek and Rauschecker, 2009; Petkov et al., 2006, 2009; Schönwiesner et al., 2014; Woods et al., 2010). Thus, the current study further supports the claim that areas A1 and AAF form a core auditory cortex similar to that observed in non-human primates. In addition, the tonotopic organization and preference for complex stimuli observed in PAF and VPAF warrant comparison with auditory belt areas in the NHP (Kusmierek and Rauschecker, 2009; Petkov et al., 2006).

4.5.3 Vocalization Representation in Auditory Cortex

Cats have a wide variety of vocalizations, used for communication between animals (Boudreau and Tsuchitani, 1973). Similar to human speech, cat vocalizations have components such as sweeps and harmonic stacks (Fig 4.3 C, D; (Gehr et al., 2000). Distinct vocalization differences from individual cats also allow for discrimination between animals. The importance of vocalization in identification and communication between individual cats suggests that there would be a subdivision of auditory cortex dedicated to the processing of these stimuli.

In the current study, vocalizations elicited a BOLD response that included much of the bilateral auditory cortices. In both hemispheres, active voxels were found on the middle ectosylvian gyrus including A1, A2, IN, and T, and along the *pes* including PAF, VPAF, and VAF. However, a contrast designed to identify areas that respond preferentially to vocalizations rather than more generally to stimuli with harmonically-

related frequency components demonstrated a focus of activity in area T. Petkov and colleagues (2008) found similar results using conspecific vocalization stimuli with monkeys, noting activity within auditory cortex corresponding to both core and belt areas as well as activity outside of auditory cortex, in the posterior-parietal cortex of conscious behaving subjects. Unlike in the present study, excitation in the NHP extended to anterior auditory cortex (Petkov et al., 2008); however, they did note that these anterior areas were silenced when animals were anesthetized.

It has been suggested that conclusions regarding the existence of a single vocalization-specific area of auditory cortex should be made with caution as evidence suggests multiple areas working in concert (Bizley and Walker, 2009; Gaucher et al., 2013; Petkov et al., 2008). For example Petkov and colleagues (2008) demonstrated that areas outside of auditory cortex become active in response to vocalizations in the NHP, indicating more integrative processing. Thus, it is possible that areas within auditory cortex that respond preferentially to vocalizations are, in fact, processing features of more complex acoustic stimuli rather than being specifically tuned to vocal stimuli per se. Consequently, it should be noted that area T, which is selectively activated by vocalization stimuli in the current study, may be processing features present in vocal stimuli rather than the vocalization as a whole.

While fMRI has the ability to examine the entirety of auditory cortex, area IN, located just anterior to T, was difficult to activate using the present methods. While we were able to demonstrate cortical activity across the remainder of auditory cortex using these stimuli, it may be that a particular feature for which IN is tuned was not included. It is also possible that the effects of anesthesia in the current study may be precluding significant activity in IN. It may be that future investigations using an un-anesthetized preparation may be more successful in recording activity in areas like IN that will be more comparable to that observed in the NHP (Petkov et al., 2008).

4.5.4 Hierarchical Organization

Electrophysiological and anatomical evidence has indicated that A1 and AAF in cat auditory cortex function at the same level (Fig 4.1 B, C), similar to core auditory cortex

of the monkey (Carrasco and Lomber, 2009a, 2011; Hackett, 2011, 2015; Lee and Winer, 2011; Petkov et al., 2006, 2009). This has also been confirmed recently using fMRI, where activity in response to pure tones was isolated largely within these two areas (Hall et al., 2014; Hall and Lomber, 2015) while BBN-elicited activity was concentrated along the *pes* (Hall et al., 2014; Hall and Lomber, 2015).

Recent anatomical investigations have placed PAF just above core areas of the auditory processing hierarchy (Lee and Winer, 2011) with principal inputs originating from A1, VAF, and VPAF (Lee and Winer, 2008). Electrophysiological studies have demonstrated that PAF neurons have longer latencies than those of A1 and AAF (Carrasco and Lomber, 2009a, b) also suggesting that it is at a higher level of cortical processing. Results from behavioural investigations using reversible deactivation have indicated that A1 and PAF are functionally tuned for auditory localization (Lomber and Malhotra, 2008; Malhotra et al., 2004; Malhotra and Lomber, 2007). However, the stimuli in the current study contained no localization cues, but elicited robust responses in PAF, suggesting a role for PAF beyond auditory object localization. Anatomical evidence for a connection from AAF to PAF has been noted (Lee and Winer, 2008), and Carrasco and Lomber (2011) have confirmed this possibility based on electrophysiological latencies. Thus it appears that PAF may be in receipt of information critical both to stimulus identification and localization. Indeed, a recent investigation presenting conspecific vocalizations to un-anesthetized cats suggested that it would be premature to exclude PAF from theories of auditory identification processing (Ma et al., 2013). Taken together, the results of Ma and colleagues and the current study suggest that if parallel processing of identification ("what") and location ("where") does exist within auditory cortex, it may not begin until after PAF.

The processing of conspecific vocalizations, specifically for identification, has been compared to facial recognition in the visual cortex (Gauthier et al., 2000; Petkov et al., 2008). Cortical areas involved in face perceptions are at the highest level of the hierarchy within the "what" stream. In the present investigation, T was selectively responsive to conspecific vocalizations. This agrees with the proposed flow of

information within auditory cortex of the cat (Carrasco and Lomber, 2011; Hackett, 2011) and confirms the hierarchy proposed by the anatomy (Lee and Winer, 2011).

4.6 Conclusion

The current study uses non-invasive imaging techniques to examine the functional hierarchy of processing in a well-studied model of auditory perception. Using a variety of simple and complex stimuli, we were able to image activity in areas of cortex that respond poorly to the simple pure tone stimuli employed in a large proportion of the existing literature. Through the presentation of narrow band noises centred on different frequencies, we demonstrate tonotopic activity in cortical areas along the posterior ectosylvian sulcus. Moreover, we provide functional evidence of specialized processing of vocalization in temporal cortex, and suggest a reinterpretation of the role of the posterior auditory field in dorsal/ventral stream processing. Collectively, these data provide the first comprehensive view of the functional hierarchy of auditory processing in the cat, bolstering a body of work that has, to date, been limited to anatomical evidence.

4.7 Acknowledgements

The authors would like to acknowledge the contributions of Joe Gati and Trevor Szekeres who designed and implemented scanning protocols; Kyle Gilbert, who designed the custom RF coil; Kevin Barker, who designed the apparatus supporting the animals; and Pam Nixon, the veterinary technician assisting with animal care.

4.8 References

Bizley, JK, Walker, KMM, 2009. Distributed sensitivity to conspecific vocalizations and implications for the auditory dual stream hypothesis. J Neurosci, 29, 3011-3013.

Boudreau, JC, Tsuchitani, C, 1973. Sensory Neurophysiology. Van Nostrand Reinhold, New York, NY.

Brett, M, JAnton, J-L, Valabregue, R, Poline, J-B, 2002. Region of interest analysis using an SPM toolbox. International Conference on Functional Mapping of the Human Brain, Sendai, Japan.

Brown, TA, Gati, JS, Hughes, SM, Nixon, PL, Menon, RS, Lomber, SG, 2014. Functional imaging of auditory cortex in adult cats using high-field fMRI. Journal of Visualized Experiments, e50872.

Brown, TA, Joanisse, MF, Gati, JS, Hughes, SM, Nixon, PL, Menon, RS, Lomber, SG, 2013. Characterisation of the BOLD response in cat auditory cortex. Neuroimage, 64, 458-465.

Carrasco, A, Brown, TA, Kok, MA, Chabot, N, Kral, A, Lomber, SG, 2013. Influence of core auditory cortical areas on acoustically evoked activity in contralateral primary auditory cortex. J Neurosci, 33, 776-789.

Carrasco, A, Kok, MA, Lomber, SG, 2015. Effects of core auditory cortex deactivation on neuronal response to simple and complex acoustic signals in the contralateral anterior auditory field. Cereb Cortex, 25, 84-96.

Carrasco, A, Lomber, SG, 2009a. Differential modulatory influences between primary auditory cortex and the anterior auditory field. J Neurosci, 29, 8350-8362.

Carrasco, A, Lomber, SG, 2009b. Evidence for Hierarchical Processing in Cat Auditory Cortex: Nonreciprocal Influence of Primary Auditory Cortex on the Posterior Auditory Field. J Neurosci, 29, 14323-14333.

Carrasco, A, Lomber, SG, 2011. Neuronal activation times to simple, complex, and natural sounds in cat primary and nonprimary auditory cortex. J Neurophysiol, 106, 1166-1178.

Chevillet, M, Riesenhuber, M, Rauschecker, JP, 2011. Functional correlates of the anterolateral processing hierarchy in human auditory cortex. J Neurosci, 31, 9345-9352.

Collins, JA, Olson, IR, 2014. Beyond the FFA: The role of the ventral anterior temporal lobes in face processing. Neuropsychologia, 61, 65-79.

DeWitt, I, Rauschecker, JP, 2012. Phoneme and word recognition in the auditory ventral stream. Proc Natl Acad Sci USA, 109, E505-E514.

DeWitt, I, Rauschecker, JP, 2013. Wernicke's area revisited: Parallel streams and word processing. Brain and Language, 127, 181-191.

Drager, UC, 1975. Receptive fields of single cells and topography in mouse visual cortex. J Comp Neurol, 160, 269-290.

Gaucher, Q, Huetz, C, Gourevitch, B, Laudanski, J, Occelli, F, Edeline, JM, 2013. How do auditory cortex neurons represent communication sounds? Hear Res, 305, 102-112.

Gauthier, I, Tarr, MJ, Moylan, J, Skudlarski, P, Gore, JC, Anderson, AW, 2000. The fusiform "face area" is part of a network that processes faces at the individual level. J Cogn Neurosci, 12, 495-504.

Gehr, DD, Komiya, H, Eggermont, JJ, 2000. Neuronal responses in cat primary auditory cortex to natural and altered species-specific calls. Hear Res, 150, 27-42.

Hackett, TA, 2011. Information flow in the auditory cortical network. Hear Res, 271, 133-146.

Hackett, TA, 2015. Anatomic organization of the auditory cortex. Handb Clin Neurol, 129, 27-53.

Hall, AJ, Brown, TA, Grahn, JA, Gati, JS, Nixon, PL, Hughes, SM, Menon, RS, Lomber, SG, 2014. There's more than one way to scan a cat: Imaging cat auditory cortex with high-field fMRI using continuous or sparse sampling. J Neurosci Methods, 224, 96-106.

Hall, AJ, Lomber, SG, 2015. High-field fMRI reveals tonotopically-organized and core auditory cortex in the cat. Hear Res.

Haxby, JV, Grady, CL, Horwitz, B, Ungerleider, LG, Mishkin, M, Carson, RE, Herscovitch, P, Schapiro, MB, Rapoport, SI, 1991. Dissociation of object and spatial visual processing pathways in human extrastriate cortex. Proc Natl Acad Sci U S A, 88, 1621-1625.

Hickok, G, Poeppel, D, 2015. Neural basis of speech perception. Handb Clin Neurol, 129, 149-160.

Hubel, DH, Wiesel, TN, 1959. Receptive fields of single neurones in the cats striate cortex. Journal of Physiology-London, 148, 574-591.

Hubel, DH, Wiesel, TN, 1968. Receptive fields and functional architecture of monkey striate cortex. J Physiol, 195, 215-243.

Joly, O, Ramus, F, Pressnitzer, D, Vanduffel, W, Orban, GA, 2012. Interhemispheric differences in auditory processing revealed by fMRI in awake rhesus monkeys. Cereb Cortex, 22, 838-853.

Kanwisher, N, McDermott, J, Chun, MM, 1997. The fusiform face area: A module in human extrastriate cortex specialized for face perception. J Neurosci, 17, 4302-4311.

Karnath, HO, Perenin, MT, 2005. Cortical control of visually guided reaching: evidence from patients with optic ataxia. Cereb Cortex, 15, 1561-1569.

Klassen, LM, Menon, RS, 2004. Robust automated shimming technique using arbitrary mapping acquisition parameters (RASTAMAP). Magn Reson Med, 51, 881-887.

Kolb, B, Whishaw, IQ, 1996. Fundamentals of human neuropsychology, 4 ed. W.H. Freeman, New York, NY.

Kusmierek, P, Rauschecker, JP, 2009. Functional specialization of medial auditory belt cortex in the alert rhesus monkey. J Neurophysiol, 102, 1606-1622.

Lee, CC, Imaizumi, K, Schreiner, CE, Winer, JA, 2004. Concurrent tonotopic processing streams in auditory cortex. Cereb Cortex, 14, 441-451.

Lee, CC, Winer, JA, 2008. Connections of cat auditory cortex: III. Corticocortical system. J Comp Neurol, 507, 1920-1943.

Lee, CC, Winer, JA, 2011. Convergence of thalamic and cortical pathways in cat auditory cortex. Hear Res, 274, 85-94.

Liu, J, Harris, A, Kanwisher, N, 2010. Perception of face parts and face configurations: an FMRI study. J Cogn Neurosci, 22, 203-211.

Lomber, SG, Malhotra, S, 2008. Double dissociation of 'what' and 'where' processing in auditory cortex. Nat Neurosci, 11, 609-616.

Ma, H, Qin, L, Dong, C, Zhong, R, Sato, Y, 2013. Comparison of neural responses to cat meows and human vowels in the anterior and posterior auditory field of awake cats. PLoS One, 8.

Malhotra, S, Hall, AJ, Lomber, SG, 2004. Cortical control of sound localization in the cat: Unilateral cooling deactivation of 19 cerebral areas. J Neurophysiol, 92, 1625-1643.

Malhotra, S, Lomber, SG, 2007. Sound localization during homotopic and heterotopic bilateral cooling deactivation of primary and nonprimary auditory cortical areas in the cat. J Neurophysiol, 97, 26-43.

Mellott, JG, Van der Gucht, E, Lee, CC, Carrasco, A, Winer, JA, Lomber, SG, 2010. Areas of cat auditory cortex as defined by neurofilament proteins expressing SMI-32. Hear Res, 267, 119-136.

Mottonen, R, van de Ven, GM, Watkins, KE, 2014. Attention fine-tunes auditory-motor processing of speech sounds. J Neurosci, 34, 4064-4069.

Olfert, ED, Cross, BM, McWilliam, AA, 1993. Guide to the care and use of experimental animals. Canadian Council on Animal Care.

Petkov, CI, Kayser, C, Augath, M, Logothetis, NK, 2006. Functional imaging reveals numerous fields in the monkey auditory cortex. PLoS Biol, 4, 1213-1226.

Petkov, CI, Kayser, C, Augath, M, Logothetis, NK, 2009. Optimizing the imaging of the monkey auditory cortex: sparse vs. continuous fMRI. Magn Reson Imaging, 27, 1065-1073.

Petkov, CI, Kayser, C, Steudel, T, Whittingstall, K, Augath, M, Logothetis, NK, 2008. A voice region in the monkey brain. Nat Neurosci, 11, 367-374.

Rauschecker, JP, 1997. Processing of complex sounds in the auditory cortex of cat, monkey, and man. Acta oto-laryngologica Supplementum, 532, 34-38.

Rauschecker, JP, Tian, B, 2004. Processing of band-passed noise in the lateral auditory belt cortex of the rhesus monkey. J Neurophysiol, 91, 2578-2589.

Rauschecker, JP, Tian, B, Hauser, M, 1995. Processing of complex sounds in the macaque nonprimary auditory cortex. Science, 268, 111-114.

Rauschecker, JP, Tian, B, Pons, T, Mishkin, M, 1997. Serial and parallel processing in rhesus monkey auditory cortex. J Comp Neurol, 382, 89-103.

Reznik, D, Henkin, Y, Schadel, N, Mukamel, R, 2014. Lateralized enhancement of auditory cortex activity and increased sensitivity to self-generated sounds. Nat Commun, 5, 4059.

Rouiller, EM, Simm, GM, Villa, AEP, Deribaupierre, Y, Deribaupierre, F, 1991. Auditory corticocortical interconnections in the cat - evidence for parallel and hierarchical arrangement of the auditory cortical areas. Exp Brain Res, 86, 483-505.

Schönwiesner, M, Dechent, P, Voit, D, Petkov, CI, Krumbholz, K, 2014. Parcellation of human and monkey core auditory cortex with fMRI pattern classification and objective detection of tonotopic gradient reversals. Cereb Cortex.

Scott, SK, McGettigan, C, 2013. Do temporal processes underlie left hemisphere dominance in speech perception? Brain and Language, 127, 36-45.

Singer, W, Tretter, F, Cynader, M, 1975. Organization of cat striate cortex: a correlation of receptive-field properties with afferent and efferent connections. J Neurophysiol, 38, 1080-1098.

Singhal, A, Monaco, S, Kaufman, LD, Culham, JC, 2013. Human fMRI reveals that delayed action re-recruits visual perception. PLoS One, 8, e73629.

Taylor, JC, Downing, PE, 2011. Division of labor between lateral and ventral extrastriate representations of faces, bodies, and objects. J Cogn Neurosci, 23, 4122-4137.

Ungerleider, LG, Mishkin, M, 1982. Two cortical visual systems. In: Ingle, DJ, Goodale, MA, Mansfield, RJW (Eds.), Analysis of visual behavior. MIT Press, Cambridge, MA, pp. 549-586.

Van Sluyters, RC, Ballinger, M, Bayne, K, Cunningham, C, Degryse, A-D, Dubner, R, Evans, H, Gdowski, MJ, Knight, R, Mench, J, Nelson, RJ, Parks, C, Stein, B, Toth, L, Zola, S, 2003. Guidelines for the care and use of mammals in neuroscience and behavioral research. National Research Council, Washington D.C.

Woods, DL, Herron, TJ, Cate, AD, Yund, EW, Stecker, GC, Rinne, T, Kang, X, 2010. Functional properties of human auditory cortical fields. Front Syst Neurosci, 4, 155.

Chapter 5 – Conclusions

The investigations within this work were designed to provide functional evidence of a hierarchy in auditory cortex of the cat. Chapter 2 optimized the fMRI method to be used. Chapter 3 demonstrated that tonotopic and core areas can be identified in auditory cortex of the cat using fMRI. Chapter 4 used complex stimuli to investigate ventral areas of auditory cortex of the cat. The current chapter will summarize the results and conclusions drawn from each of the individual investigations. Then, the impact of the whole body of results on current knowledge and future directions will be discussed.

5.1 Individual Investigations

Each investigation included in this work targeted specific lines of enquiry. The following subsections will include; a summary of results from each study and a brief discussion of the significance of the results.

5.1.1 There's more than one way to scan a cat: Imaging cat auditory cortex with high-field fMRI using continuous or sparse sampling.

This investigation compared sparse and continuous sampling techniques using fMRI. As a result, similar statistical strengths were found for both methods in both the auditory cortex and midbrain. Significant differences between the two methods occurred in extent of activation with larger activations occurring while using the continuous method. Also, the location of activation varied with stimulus type. Pure tone stimuli resulted in activations largely located in known tonotopic areas while broadband noise (BBN) stimuli resulted in activations located along the pes.

Contrary to studies in humans (Hall et al., 1999; Peelle et al., 2010; Schmidt et al., 2008; Woods et al., 2009) and monkeys (Petkov et al., 2009), the present comparison indicated no difference in statistical strength of activations, significant difference in extent of activation using continuous sampling, and better demonstration of functional organization using continuous sampling. Some of these differences could be attributed to variations in acquisition (Petkov et al., 2009), volume sampling (Hall et al., 1999), or stimulus presentation timing (Schmidt et al., 2008).

Therefore, general conclusions drawn for this investigation were that, during passive stimulation in an anesthetized animal, continuous scanning is the preferred method for investigations of auditory cortex in the cat using fMRI.

5.1.2 High-field fMRI reveals tonotopically organized and core auditory cortex in the cat.

This investigation was designed to demonstrate that known principles of auditory cortex of the cat can be demonstrated using fMRI. Four tonotopically organized areas (AAF, A1, PAF, and VPAF) were delineated and tonotopy was also demonstrated. Also, core auditory cortex, consisting of A1 and AAF, was identified by comparing the location of activation in response to either pure tone or BBN stimuli.

Classical tonotopic methods, such as electrophysiology, reflect local heterogeneity which can obscure tonotopic mapping. fMRI employs a more macroscopic view which can allow for a more defined tonotopic map. This, combined with the non-invasive nature and ability to investigate all cortices, makes fMRI optimal for investigations of cat auditory cortex. The importance of these results extends beyond application to cat auditory cortex. It provides the foundation for application of known principles of cat auditory cortex to both monkey and human auditory cortex.

5.1.3 The cat's meow: A high-field fMRI assessment of cortical activity in response to vocalizations and complex auditory stimuli.

This study was designed to investigate areas of cat auditory cortex that have previously been elusive. Results indicate multiple areas of interest. First, auditory responses are largely lateralized to the left hemisphere. Also, tonotopy in PAF and VPAF can best be observed using narrowband noise (NBN). Additionally, vocalization stimuli result in a focus of activity in area T. Finally, activations in PAF indicate that it has a role in the "what" stream.

Lateralization of function in humans, especially with respect to speech, is widely accepted (Hickok and Poeppel, 2015; Kolb and Whishaw, 1996). In the cat, this had not previously been identified and was difficult to interpret. Future investigations using stimuli specifically designed to probe lateralization would shed light on the underlying mechanisms. Chapter 3 (Hall and Lomber, 2015) demonstrated that pure tones could be

used to identify tonotopy. In chapter 4 it was demonstrated that NBN, centered at different frequencies, effectively revealed tonotopy in PAF and VPAF with minimal effect in core areas. These results further supported conclustions from Chapter 3, that A1 and AAF function as a core similar to that of the monkey. Also, while PAF and VPAF are tonotopically organized, they are selective to more complex stimuli. Finally, all stimuli included in this study were devoid of location information and still resulted in activations in PAF. Previous studies have shown that PAF is necessary for sound localization (Lomber and Malhotra, 2008; Malhotra et al., 2004; Malhotra and Lomber, 2007), which has resulted in theories that it is solidly involved in the "where" pathway. Results from this study indicate that PAF also has a role in sound identification, which modifies current organizational theories pertaining to the parallel processing of auditory cortex of the cat.

5.2 General Conclusions

The overarching goal of this work was to investigate the hierarchical organization within auditory cortex of the cat using fMRI. It successfully demonstrated known elements of the hierarchy within auditory cortex of the cat. It also revealed elements of the hierarchy that was previously unknown. In this section the advances in understanding of the cortical organization as a result of this work will be discussed.

5.2.1 Core vs. Non-Core Cortex

Previous investigations, using more invasive techniques, have proposed that A1 and AAF function as a core auditory cortex similar to that of the monkey (Carrasco and Lomber, 2009a, b; Hackett, 2011, 2015; Lee and Sherman, 2011; Rauschecker and Tian, 2000). Core auditory cortex of the monkey has been successfully delineated from the belt by comparing activations in response to pure tones or broadband noise (BBN) using fMRI (Petkov et al., 2006, 2009). Activations in response to pure tones were present in both core and belt auditory cortex of the monkey. However, belt cortex was selectively responsive to BBN stimuli. A similar pattern of activation was observed in the present work. Response to pure tone stimuli, including a tonotopic progression, was observed in AAF, A1, PAF and VPAF. However, activations in response to BBN were concentrated

along the posterior ectosylvian sulcus (*pes*) corresponding to PAF and VPAF. This further supports the proposal of AAF and A1 forming a core auditory cortex similar to the monkey. It also strengthens comparisons of results between species.

5.2.2 Lateralization of function

Lateralization of function in human audition, particularly with respect to speech perception, is a commonly accepted principle (Dhanjal et al., 2008; Hickok and Poeppel, 2015; Kolb and Whishaw, 1996; Spitsyna et al., 2006). Binder and colleagues (2000) noted that a lateralization of activity didn't occur until stimuli took the form of words or pseudo-words with reversed words, tones and noises all resulting in equivalent bilateral activations. They also noted that left hemisphere levels of activation were not lowered between word, pseudo-word, or vocalization reversals. In fact, right hemisphere activations in response to pseudo-word or reversal stimuli were raised to match left hemisphere levels. This indicates that the asymmetry is not due to the left hemisphere being more responsive, but that the right hemisphere is less responsive to word stimuli. Interestingly, the initial processing of speech, on Heschl's gyrus (HG) and surrounding cortex, is symmetric bilaterally (Binder et al., 2000; Poeppel et al., 2004).

Investigations of functional lateralization within monkeys have not revealed a clear pattern. Early lesion studies in monkeys noted that unilateral left temporal lesions of the superior temporal gyrus, including auditory cortex, resulted in initial impairments in discrimination between vocalizations (Heffner and Heffner, 1984, 1986). However, similar right hemisphere lesions did not cause impairment. A more recent PET study also found an asymmetry, favoring the left temporal pole, restricted to conspecific vocalizations (Poremba et al., 2004). Interestingly, this same study found that severing the forebrain commissures eliminated the asymmetry and brought right hemisphere activity levels up to that of the left hemisphere. Other investigations using PET showed no lateralization of function (Gil-da-Costa et al., 2004; Gil-da-Costa et al., 2006). Using fMRI Petkov and colleagues (2008) found that activations in response to conspecific vocalizations appeared symmetric within auditory cortex of both hemispheres. However, they did note a region of activation within temporal cortex, anterior to auditory cortex, lateralized to the right hemisphere. In contrast, Joly and colleagues (2012) found that

activations in response to intact versus scrambled vocalizations were asymmetrical. In this study, belt and parabelt cortex in the left hemisphere selectively responded to intact human and monkey vocalization stimuli.

Asymmetries in lower animals have also been observed. Behavioral results indicate that mouse mothers cannot recognize pup calls when input to the right ear, or left auditory cortex, is obstructed (Ehret, 1987). In birds, while lateralization was noted in each individual case, the hemispheric focus of the asymmetry was not consistent across animals (George et al., 2002).

In the present investigation, all stimuli resulted in a larger and stronger activation in the left hemisphere, with the exception of 1kHz narrow band noise (NBN) and frequency modulated (FM) sweeps which were lateralized to the right hemisphere. The asymmetry in response to FM sweeps, opposite to that of vocalizations, has some precedence. Poeppel and colleagues (2004) noted a similar, less apparent, asymmetry favoring the right superior temporal gyrus. They suggested that the right hemisphere might be more responsive to slow rates of change or FM sweeps of longer durations. This is bolstered by results indicating that the left hemisphere is specialized for rapidly changing stimuli (Belin et al., 1998; Johnsrude et al., 1997). The present results largely support this theory, with asymmetrical activations in response to rapidly changing stimuli favoring the left hemisphere.

5.2.3 Cortical Subdivisions of interest.

Results from the present investigation highlight two specific subdivisions of auditory cortex. Robust activation, in response to all stimuli, was commonly found dorsally on the posterior lip of the posterior ectosylvian sulcus (pes) corresponding to PAF. Also, in chapter 4, the temporal (T) area were found to be selectively responsive to conspecific vocalizations.

5.2.3.1 PAF

Contrary to previous functional and behavioural investigations, the present results indicate that PAF may be more functionally diverse than previously thought. More than

35% of cortical input to PAF originates from A1 and VPAF which are also tonotopically organized (Lee and Winer, 2008b, 2011). Thalamic inputs to PAF are largely from dorsal nuclei which separates it from its cortical inputs: A1, which receives almost exclusively from ventral thalamic nuclei, and VPAF, which largely receives input from caudal thalamic nuclei (Lee and Winer, 2008a). Direct comparisons have been made of PAF and the caudomedial (CM) area in the monkey (Carrasco and Lomber, 2009b). Similar to PAF in the cat, area CM of the monkey receives the largest inputs from dorsal thalamic nuclei (de la Mothe et al., 2012), A1 of core cortex, and surrounding caudal belt areas (de la Mothe et al., 2006).

Adding to anatomical evidence of the position of PAF within the hierarchy, electrophysiological investigations of PAF have reported a significantly longer latency than A1 (Carrasco and Lomber, 2009b, 2011). This indicates that PAF is at a functionally higher level than A1 within a hierarchical model. Carrasco and Lomber (2009b) also found that reversible deactivation of A1 resulted in a significant decrease in response strength in PAF. This indicates a significant modulatory influence of A1 on PAF, and dependence of PAF on input from A1, also placing PAF at a higher functional level. Similar studies in the monkey have not noted significant differences between A1 and CM (Kajikawa et al., 2011).

The use of reversible deactivation also added to the understanding of the function of PAF. Multiple studies have shown that deactivation of PAF results in a deficit in the ability to localize auditory stimuli (Malhotra et al., 2004; Malhotra and Lomber, 2007). Using the same technique and behavioural testing, Lomber and Malhotra (2008) confirmed the function of PAF in auditory localization. This study also demonstrated that deactivation of PAF had no effect on auditory discrimination. Electrophysiological evidence has also indicated that PAF is well suited for guiding localization behaviour (Stecker et al., 2003). Together the electrophysiological and behavioural evidence have compelled theories that PAF may be the initial stages of a “where” stream, similar to that of the visual system. It has been proposed that a similar stream appears in auditory cortex of the monkey, with posterior belt and parabelt areas specialized for localization of sound sources (Recanzone and Cohen, 2010). Specific investigations have indicated that

neurons in CM of the monkey are spatially sensitive to auditory stimuli (Recanzone, 2001; Recanzone et al., 2000).

The present results confirm that PAF is at a hierarchically higher level than core auditory cortex. Activity in PAF was more robust in response to broadband noise (BBN) rather than pure tones and vice versa for core areas. This indicates that PAF is processing higher level stimuli. In the visual system, areas at higher levels within a stream process more complex stimuli culminating in specialization for things such as face perception (Collins and Olson, 2014; Kanwisher et al., 1997; Liu et al., 2010) or visually guided reaching (Karnath and Perenin, 2005; Singhal et al., 2013). Therefore, results of the present investigation confirm previous conclusions that PAF is operating at a higher level than core auditory cortex.

However, some results from this investigation contradict, or call into question, proposed theories that PAF functions exclusively in the "where" stream. All stimuli used in this work did not contain any interaural time or level differences which are often used to simulate spatial location. Therefore, stimuli did not include any spatial cues but resulted in highly significant levels of activation in PAF. Given the hierarchy based on anatomical connections (Lee and Winer, 2011) it was expected that areas along the "what" pathway, such as A2, would be selectively activated. Also, based on results from behavioural investigations (Lomber and Malhotra, 2008) it was expected that, using these stimuli, PAF would be minimally active as it attempted to process stimuli for location. Contrary to our predictions, PAF was often the center of activity for stimuli more complex than pure tones. This indicates that PAF may not be exclusively positioned in the localization "where" stream as previously thought.

5.2.3.2 Area T

Ventral subdivisions of auditory cortex of the cat such as the temporal (T) area are difficult to investigate using more invasive techniques. This is reflected in the paucity of literature addressing functional properties of these ventral-most areas. The use of fMRI in the present investigations facilitated functional observations within T and has revealed that it may be a center dedicated to processing vocalization stimuli. It has previously been proposed that a subdivision of auditory cortex exists which preferentially responds

to vocalizations. This is similar to subdivisions of visual cortex in both humans (Ghuman et al., 2014; Kanwisher et al., 1997; Kanwisher et al., 1999; Nasr and Tootell, 2012; Sergent et al., 1992) and monkeys (Ku et al., 2011; Ohayon et al., 2012; Sugase-Miyamoto et al., 2014; Tsao et al., 2006) which selectively respond to faces.

Voice selective areas in human auditory cortex have been identified along the bank of the superior temporal sulcus (STS (Altmann et al., 2007; Belin et al., 2002; Belin et al., 2000; Pernet et al., 2015). Contrasts comparing voice and non-voice stimuli also showed that cortex believed to be homologous to belt and parabelt in the monkey were more responsive to voice stimuli. However, clusters of activation were not attributed to any specific area.

In the monkey, several studies have indicated a species specific specialization along the superior temporal gyrus (STG) with varying reports of lateralization (Gil-da-Costa et al., 2004; Poremba et al., 2004). However, Petkov and colleagues (2008) identified two areas of auditory cortex that are voice selective. One area was located in posterior core and belt areas corresponding roughly to A1. The second area was anterior to classic belt areas in temporalis superior (Ts) 1 and 2. The anterior cluster of activation was present in awake and anesthetized preparations, and was sensitive to the identity of the caller. The posterior cluster, corresponding to posterior core and belt cortex, was not present in anesthetized preparations and did not show a sensitivity to caller identity.

It has been proposed that information flow within auditory cortex of the cat proceeds postero-ventrally (Carrasco and Lomber, 2011; Hackett, 2011) from core auditory cortex. Latencies within individual areas are increasingly longer moving ventrally with AAF and A1 having similar, shorter latencies and A2 and PAF having longer latencies (Carrasco and Lomber, 2011). Areas located higher within a functional stream in the visual system process successively more complex stimuli. With this in mind it was predicted, in these investigations, that more complex stimuli would result in activations in more ventral areas. Conspecific vocalizations were the most complex stimuli used and, as expected, resulted in a focus of activity in T, one of the ventral most areas of auditory cortex in the cat. This confirms theories of information flow and identifies cortical specialization for vocalization which had not previously been documented.

The activations in T were present in an anesthetized preparation similar to the anterior activations seen in the monkey (Petkov et al., 2008). Also, anatomical evidence places T at the top of the hierarchy (Lee and Winer, 2011), which agrees with the flow of information within auditory cortex that has been proposed (Carrasco and Lomber, 2011; Hackett, 2011). Ts1 and Ts2 of the monkey are also at the high levels of processing. Although only preliminary, this evidence suggests that area T of the cat and areas Ts1 and Ts2 of the monkey may be homologous.

5.3 Future Directions

Results from these investigations provide a foundation for a number of interesting future directions within the cat. For example, the present investigation did not include stimuli with location information highlighting the "where" stream of auditory cortex. A future investigation might include interaural time or level differences using the same stimuli. Inclusion of this information would enable analysis allowing a double dissociation of cortical areas included in both "what" and "where" streams in auditory cortex. Also, inclusion of stimuli with location information would shed further light on the role of PAF in the cortical hierarchy.

Also, further investigations using behavioural, electrophysiological, and fMRI techniques, into the functional properties of PAF are prompted by results of the present investigation. A more diverse set of stimuli or new behavioural paradigms may shed light on the conflict between the present results and previous investigations. For example, most stimuli in the present investigations included spectral change. Using different more targeted stimuli, may show that PAF is also sensitive to spectral changes of specific rates or within specific ranges.

The activations in response to conspecific vocalizations found in T also provide a previously inaccessible line of inquiry. For example, the present investigation used one kind of vocalization from two cats. Presenting different variations of vocalization stimuli would elucidate the specificity of these activations. For example: similar vocalizations from different cats that the current subject is or is not familiar with, different vocalization types (e.g., hissing, meowing, purring), reverse vocalizations, and vocalizations from different species would all provide interesting and relevant information. Petkov and

colleagues (2008) used these kinds of variations to more accurately define a vocalization specific region in monkey auditory cortex. Doing a similar analysis in the cat would further elucidate similarities between area T and Ts 1 and 2 in the monkey.

On a more technical note, the use of anesthesia affects our ability to assess perception of stimuli. Future investigations may consider training animals to lie in the MRI apparatus to facilitate assessment of the effects that this might be having on cortical activity. Also, the noise of the scanner required stimuli to be presented at 85 dB. This proved to be a potential confound, especially in determining tonotopy, since neuronal sensitivity to specific frequencies gets broader with higher intensities. While continuous scanning proved to be optimal for strength and size of activation in chapter 2, sparse scanning may be more beneficial in certain experimental designs. For example, the ability to use less intense pure tone stimuli may facilitate a more detailed tonotopy, especially in A1. It may also allow a better visualization of tonotopy within AAF which was difficult to interpret in the present investigations.

Results from the present investigations also indicate potential application in future studies of monkey auditory cortex and, by extension, human auditory cortex. The similarities in organization of cat and monkey auditory cortex indicate that principles discovered in the cat can be generally applied to the monkey. For example, PAF of the cat and CM of the monkey have been compared closely in past investigations. In fact, both have been noted to have auditory localization properties. Given the contradictions found with respect to PAF between this work and previous investigations, CM of the monkey should be probed similar to PAF in the cat for more specific functional properties.

5.4 References

Altmann, CF, Doehrmann, O, Kaiser, J, 2007. Selectivity for animal vocalizations in the human auditory cortex. Cereb Cortex, 17, 2601-2608.

Belin, P, Zatorre, RJ, Ahad, P, 2002. Human temporal-lobe response to vocal sounds. Brain Res Cogn Brain Res, 13, 17-26.

Belin, P, Zatorre, RJ, Lafaille, P, Ahad, P, Pike, B, 2000. Voice-selective areas in human auditory cortex. Nature, 403, 309-312.

Belin, P, Zilbovicius, M, Crozier, S, Thivard, L, Fontaine, A, Masure, MC, Samson, Y, 1998. Lateralization of speech and auditory temporal processing. J Cogn Neurosci, 10, 536-540.

Binder, JR, Frost, JA, Hammeke, TA, Bellgowan, PS, Springer, JA, Kaufman, JN, Possing, ET, 2000. Human temporal lobe activation by speech and nonspeech sounds. Cereb Cortex, 10, 512-528.

Carrasco, A, Lomber, SG, 2009a. Differential modulatory influences between primary auditory cortex and the anterior auditory field. J Neurosci, 29, 8350-8362.

Carrasco, A, Lomber, SG, 2009b. Evidence for Hierarchical Processing in Cat Auditory Cortex: Nonreciprocal Influence of Primary Auditory Cortex on the Posterior Auditory Field. J Neurosci, 29, 14323-14333.

Carrasco, A, Lomber, SG, 2011. Neuronal activation times to simple, complex, and natural sounds in cat primary and nonprimary auditory cortex. J Neurophysiol, 106, 1166-1178.

Collins, JA, Olson, IR, 2014. Beyond the FFA: The role of the ventral anterior temporal lobes in face processing. Neuropsychologia, 61, 65-79.

de la Mothe, LA, Blumell, S, Kajikawa, Y, Hackett, TA, 2006. Cortical connections of the auditory cortex in marmoset monkeys: core and medial belt regions. J Comp Neurol, 496, 27-71.

de la Mothe, LA, Blumell, S, Kajikawa, Y, Hackett, TA, 2012. Thalamic connections of auditory cortex in marmoset monkeys: lateral belt and parabelt regions. Anat Rec (Hoboken), 295, 822-836.

Dhanjal, NS, Handunnetthi, L, Patel, MC, Wise, RJ, 2008. Perceptual systems controlling speech production. J Neurosci, 28, 9969-9975.

Ehret, G, 1987. Left hemisphere advantage in the mouse brain for recognizing ultrasonic communication calls. Nature, 325, 249-251.

George, I, Cousillas, H, Richard, JP, Hausberger, M, 2002. Song perception in the European starling: hemispheric specialisation and individual variations. C R Biol, 325, 197-204.

Ghuman, AS, Brunet, NM, Li, Y, Konecky, RO, Pyles, JA, Walls, SA, Destefino, V, Wang, W, Richardson, RM, 2014. Dynamic encoding of face information in the human fusiform gyrus. Nat Commun, 5, 5672.

Gil-da-Costa, R, Braun, A, Lopes, M, Hauser, MD, Carson, RE, Herscovitch, P, Martin, A, 2004. Toward an evolutionary perspective on conceptual representation: species-specific calls activate visual and affective processing systems in the macaque. Proc Natl Acad Sci U S A, 101, 17516-17521.

Gil-da-Costa, R, Martin, A, Lopes, MA, Munoz, M, Fritz, JB, Braun, AR, 2006. Species-specific calls activate homologs of Broca's and Wernicke's areas in the macaque. Nat Neurosci, 9, 1064-1070.

Hackett, TA, 2011. Information flow in the auditory cortical network. Hear Res, 271, 133-146.

Hackett, TA, 2015. Anatomic organization of the auditory cortex. Handb Clin Neurol, 129, 27-53.

Hall, AJ, Lomber, SG, 2015. High-field fMRI reveals tonotopically-organized and core auditory cortex in the cat. Hear Res.

Hall, DA, Haggard, MP, Akeroyd, MA, Palmer, AR, Summerfield, AQ, Elliott, MR, Gurney, EM, Bowtell, RW, 1999. "Sparse" temporal sampling in auditory fMRI. Hum Brain Mapp, 7, 213-223.

Heffner, HE, Heffner, RS, 1984. Temporal lobe lesions and perception of species-specific vocalizations by macaques. Science, 226, 75-76.

Heffner, HE, Heffner, RS, 1986. Effect of unilateral and bilateral auditory cortex lesions on the discrimination of vocalizations by Japanese macaques. J Neurophysiol, 56, 683-701.

Hickok, G, Poeppel, D, 2015. Neural basis of speech perception. Handb Clin Neurol, 129, 149-160.

Johnsrude, IS, Zatorre, RJ, Milner, BA, Evans, AC, 1997. Left-hemisphere specialization for the processing of acoustic transients. Neuroreport, 8, 1761-1765.

Joly, O, Ramus, F, Pressnitzer, D, Vanduffel, W, Orban, GA, 2012. Interhemispheric differences in auditory processing revealed by fMRI in awake rhesus monkeys. Cereb Cortex, 22, 838-853.

Kajikawa, Y, Camalier, CR, de la Mothe, LA, D'Angelo, WR, Sterbing-D'Angelo, SJ, Hackett, TA, 2011. Auditory cortical tuning to band-pass noise in primate A1 and CM: a comparison to pure tones. Neurosci Res, 70, 401-407.

Kanwisher, N, McDermott, J, Chun, MM, 1997. The fusiform face area: A module in human extrastriate cortex specialized for face perception. J Neurosci, 17, 4302-4311.

Kanwisher, N, Stanley, D, Harris, A, 1999. The fusiform face area is selective for faces not animals. Neuroreport, 10, 183-187.

Karnath, HO, Perenin, MT, 2005. Cortical control of visually guided reaching: evidence from patients with optic ataxia. Cereb Cortex, 15, 1561-1569.

Kolb, B, Whishaw, IQ, 1996. Fundamentals of human neuropsychology, 4 ed. W.H. Freeman, New York, NY.

Ku, SP, Tolias, AS, Logothetis, NK, Goense, J, 2011. fMRI of the face-processing network in the ventral temporal lobe of awake and anesthetized macaques. Neuron, 70, 352-362.

Lee, CC, Sherman, SM, 2011. On the classification of pathways in the auditory midbrain, thalamus, and cortex. Hear Res, 276, 79-87.

Lee, CC, Winer, JA, 2008a. Connections of cat auditory cortex: I. Thalamocortical system. J Comp Neurol, 507, 1879-1900.

Lee, CC, Winer, JA, 2008b. Connections of cat auditory cortex: III. Corticocortical system. J Comp Neurol, 507, 1920-1943.

Lee, CC, Winer, JA, 2011. Convergence of thalamic and cortical pathways in cat auditory cortex. Hear Res, 274, 85-94.

Liu, J, Harris, A, Kanwisher, N, 2010. Perception of face parts and face configurations: an FMRI study. J Cogn Neurosci, 22, 203-211.

Lomber, SG, Malhotra, S, 2008. Double dissociation of 'what' and 'where' processing in auditory cortex. Nat Neurosci, 11, 609-616.

Malhotra, S, Hall, AJ, Lomber, SG, 2004. Cortical control of sound localization in the cat: Unilateral cooling deactivation of 19 cerebral areas. J Neurophysiol, 92, 1625-1643.

Malhotra, S, Lomber, SG, 2007. Sound localization during homotopic and heterotopic bilateral cooling deactivation of primary and nonprimary auditory cortical areas in the cat. J Neurophysiol, 97, 26-43.

Nasr, S, Tootell, RB, 2012. Role of fusiform and anterior temporal cortical areas in facial recognition. Neuroimage, 63, 1743-1753.

Ohayon, S, Freiwald, WA, Tsao, DY, 2012. What makes a cell face selective? The importance of contrast. Neuron, 74, 567-581.

Peelle, JE, Eason, RJ, Schmitter, S, Schwarzbauer, C, Davis, MH, 2010. Evaluating an acoustically quiet EPI sequence for use in fMRI studies of speech and auditory processing. Neuroimage, 52, 1410-1419.

Pernet, CR, McAleer, P, Latinus, M, Gorgolewski, KJ, Charest, I, Bestelmeyer, PE, Watson, RH, Fleming, D, Crabbe, F, Valdes-Sosa, M, Belin, P, 2015. The human voice areas: Spatial organization and inter-individual variability in temporal and extra-temporal cortices. Neuroimage.

Petkov, CI, Kayser, C, Augath, M, Logothetis, NK, 2006. Functional imaging reveals numerous fields in the monkey auditory cortex. PLoS Biol, 4, 1213-1226.

Petkov, CI, Kayser, C, Augath, M, Logothetis, NK, 2009. Optimizing the imaging of the monkey auditory cortex: sparse vs. continuous fMRI. Magn Reson Imaging, 27, 1065-1073.

Petkov, CI, Kayser, C, Steudel, T, Whittingstall, K, Augath, M, Logothetis, NK, 2008. A voice region in the monkey brain. Nat Neurosci, 11, 367-374.

Poeppel, D, Guillemin, A, Thompson, J, Fritz, J, Bavelier, D, Braun, AR, 2004. Auditory lexical decision, categorical perception, and FM direction discrimination differentially engage left and right auditory cortex. Neuropsychologia, 42, 183-200.

Poremba, A, Malloy, M, Saunders, RC, Carson, RE, Herscovitch, P, Mishkin, M, 2004. Species-specific calls evoke asymmetric activity in the monkey's temporal poles. Nature, 427, 448-451.

Rauschecker, JP, Tian, B, 2000. Mechanisms and streams for processing of "what" and "where" in auditory cortex. Proc Natl Acad Sci U S A, 97, 11800-11806.

Recanzone, GH, 2001. Spatial processing in the primate auditory cortex. Audiol Neurootol, 6, 178-181.

Recanzone, GH, Cohen, YE, 2010. Serial and parallel processing in the primate auditory cortex revisited. Behav Brain Res, 206, 1-7.

Recanzone, GH, Guard, DC, Phan, ML, Su, TK, 2000. Correlation between the activity of single auditory cortical neurons and sound-localization behavior in the macaque monkey. J Neurophysiol, 83, 2723-2739.

Schmidt, CF, Zaehle, T, Meyer, M, Geiser, E, Boesiger, P, Jancke, L, 2008. Silent and continuous fMRI scanning differentially modulate activation in an auditory language comprehension task. Hum Brain Mapp, 29, 46-56.

Sergent, J, Ohta, S, MacDonald, B, 1992. Functional neuroanatomy of face and object processing. A positron emission tomography study. Brain, 115 Pt 1, 15-36.

Singhal, A, Monaco, S, Kaufman, LD, Culham, JC, 2013. Human fMRI reveals that delayed action re-recruits visual perception. PLoS One, 8, e73629.

Spitsyna, G, Warren, JE, Scott, SK, Turkheimer, FE, Wise, RJ, 2006. Converging language streams in the human temporal lobe. J Neurosci, 26, 7328-7336.

Stecker, GC, Mickey, BJ, Macpherson, EA, Middlebrooks, JC, 2003. Spatial sensitivity in field PAF of cat auditory cortex. J Neurophysiol, 89, 2889-2903.

Sugase-Miyamoto, Y, Matsumoto, N, Ohyama, K, Kawano, K, 2014. Face inversion decreased information about facial identity and expression in face-responsive neurons in macaque area TE. J Neurosci, 34, 12457-12469.

Tsao, DY, Freiwald, WA, Tootell, RB, Livingstone, MS, 2006. A cortical region consisting entirely of face-selective cells. Science, 311, 670-674.

Woods, DL, Stecker, GC, Rinne, T, Herron, TJ, Cate, AD, Yund, EW, Liao, I, Kang, XJ, 2009. Functional maps of human auditory cortex: effects of acoustic features and attention. PLoS One, 4, e5183.

Appendix A: AUS Approval

Western

AUP Number: 2009-016
PI Name: Lomber, Stephen
AUP Title: Plasticity In Auditory Cortex

Approval Date: 04/16/2013

Official Notice of Animal Use Subcommittee (AUS) Approval: Your new Animal Use Protocol (AUP) entitled "Plasticity In Auditory Cortex

" has been APPROVED by the Animal Use Subcommittee of the University Council on Animal Care. This approval, although valid for four years, and is subject to annual Protocol Renewal.2009-016::5

This AUP number must be indicated when ordering animals for this project.
Animals for other projects may not be ordered under this AUP number.
Purchases of animals other than through this system must be cleared through the ACVS office.
Health certificates will be required.

The holder of this Animal Use Protocol is responsible to ensure that all associated safety components (biosafety, radiation safety, general laboratory safety) comply with institutional safety standards and have received all necessary approvals. Please consult directly with your institutional safety officers.

Submitted by: Copeman, Laura
on behalf of the Animal Use Subcommittee
University Council on Animal Care

Curriculum Vitae

AMEE J HALL

Education

2015
Ph.D. Anatomy and Cell Biology
Western University
London, Ontario
Canada

2008
M.Sc. Neuroscience
Centre for Brain and Mind
Western University
London, Ontario
Canada

2005
B.S. Neuroscience
School of Behavioral and Brain Sciences,
The University of Texas at Dallas
Richardson, Texas
USA

2002
A.S. Biology
Collin County Community College
McKinney, Texas
USA

Professional Scientific Accomplishments

Book Chapters

1. Lomber SG, **McMillan AJ** (2010) Functional specialization in primary and non-primary auditory cortex of the cat. In: *The Auditory Cortex*, eds. Winer WA and Schreiner C (New York, NY; Springer-Verlag).

Refereed Published Articles

1. Malhotra S, **Hall AJ**, Lomber SG (2004) Cortical control of sound localization in the cat: Unilateral cooling deactivation of nineteen cerebral areas. *Journal of Neurophysiology* 92:1625-1643.

2. Lomber SG, Malhotra S, **Hall AJ** (2007) Functional specialization in non-primary auditory cortex of the cat: Areal and laminar contributions to sound localization. *Hearing Research* 229:31-45

3. **Hall AJ**, Lomber SG (2008) Auditory cortex projections target the peripheral field representation of primary visual cortex. *Experimental Brain Research* 4:113-130.

4. Meredith MA, Kryklywy J, **McMillan AJ**, Malhotra S, Lum-Tai R and Lomber SG (2011) Crossmodal reorganization in the early-deaf switches sensory, but not behavioral roles of auditory cortex. *Procedings of the National Accademy of Sciences of the United States of America* 108:8856-8861.

5. Chabot N, Mellott JG, **Hall AJ**, Tichenoff EL and Lomber SG (2013) Cerebral origins of the auditory projection to the superior colliculus of the cat. *Hearing Research* 300:33-45.

6. **Hall AJ**, Brown TA, Grahn JA, Gati JS, Nixon PL, Hughes SM, Menon RS and Lomber SG (2014) There's more than one way to scan a cat: Imaging cat auditory cortex, thalamus and midbrain with high-field fMRI using sparse or continuous sampling. *Journal of Neuroscience Methods* 225:96-106.

7. **Hall AJ**, Lomber SG (2015) High-field fMRI reveals tonotopically organized and core auditory cortex in the cat. *Hearing Research* 325:1-11.

8. Butler BE, **Hall AJ**, Lomber SG (2015) High-field functional imaging of pitch processing in auditory cortex of the cat. *PLoS One*, In Press.

Invited Presentations

1. **Hall AJ** (2007) Multisensory convergence in the peripheral field representation in primary visual cortex of the cat. *Group on Action and Perception (GAP) conference*.

2. **Hall AJ** (2008) Influence of auditory cortex on visual detection. *Group on Action and Perception (GAP) conference*.

3. **McMillan AJ** (2011) Hierarchical Organization within auditory cortex of the cat. *Current topics in cell biology and neurobiology course.* Western University.

4. **McMillan AJ** (2012) There's more than one way to scan a cat: Imaging cat auditory cortex with high-field fMRI using sparse or continuous sampling. *Current topics in cell biology and neurobiology course.* Western University.

5. **Hall AJ** (2013) Hierarchy within auditory cortex. *Department of Anatomy and Cell Biology's seminar series.* Western University.
6. **Hall AJ** (2014) Hierarchy of auditory cortex using high-field fMRI. *National Center for Audiology*, London, Ontario.

Abstracts

1. **Hall AJ**, Malhotra S, Barnes WH, Woller EM, Mellot JG, Hawksworth G, Bolinger M, Lomber SG (2003) Be prepared: What high school students really want to know about the brain. *Society for Neuroscience*, New Orleans, LA. Program No. 26.6.

2. Malhotra S, **Hall AJ**, Manafov E, Woller EM, Lomber SG (2003) Cerebral areas mediating sound localization in the cat: Cooling deactivation of 19 cortical loci. *Society for Neuroscience*, New Orleans, LA. Program No. 183.8.

3. Malhotra S, **Hall AJ**, Lomber SG (2004) Cerebral control of sound localization in the cat: Unilateral and bilateral reversible deactivation of primary and non-primary auditory cortical areas. *Association for Research in Otolaryngology.*

4. Malhotra S, **Hall AJ**, Middlebrooks JC, Lomber SG (2004) Sound Localization deficits during individual or combined reversible deactivation of cat primary auditory cortex and the dorsal zone. *Society for Neuroscience*, San Diego, CA. Program No. 486.8.

5. **Hall AJ**, Malhotra S, Lomber SG (2004) Cerebral control of sound localization in the cat: Unilateral and bilateral deactivation of ten auditory areas. *Society for Neuroscience*, San Diego, CA. Program No. 529.8

6. Malhotra S, **Hall AJ**, Stecker GC, Harrington IA, Macpherson JC, Middlebrooks JC, Lomber SG (2005) Sound localization deficits during unilateral or bilateral reversible deactivation of primary auditory cortex and/or the dorsal zone. *Association for Research in Otolaryngology*, Program No. 118.

7. Lomber SG, Payne BR, **Hall AJ**, Malhotra S, Mellott JG (2006) Adaptive cortical plasticity underlying recovery from cerebral damage induced visual neglect. *Vision Sciences Society*, Sarasota, FL. Program No. 118.

8. **Hall AJ**, Mellot JG, and Lomber SG (2007) Audiovisual interactions in the cat: Direct cortical projections from the posterior auditory field to primary visual cortex. *Vision Sciences Society*, Sarasota, FL. Program No. 664.

9. **Hall AJ**, Mellott JG, Lomber SG (2007) Multisensory convergence in the peripheral field representation of primary visual cortex of the cat. *Canadian Association for Neuroscience*.Toronto, ON.

10. Lomber SG, Woller E, **Hall AJ** and Payne B (2008) Neglected sight: Preserved visual functions within a neglected hemifield. Vision Sciences Society, Sarasota, FL. Program No. 1006.

11. Stevenson SA, **Hall AJ**, Lomber SG, Corneil BD (2008) Using reversible cooling inactivation to assess the oculomotor contributions of the primate superior colliculus. *Society for Neuroscience*, Washington, DC Program No. 167.12

12. Lomber SG, Kryklywy J, **Hall AJ**, Lum-Tai R, Malhotra S and Meredith MA (2009) Crossmodal reorganization in the auditory field of the anterior ectosylvian sulcus (fAES) of postnatally deafened cats. *Society for Neuroscience*, Chicago, IL. Program No. 260.12

13. Birtch K-AH, Degagne B, Carassco A, **McMillan AJ**, Lomber SG (2010) Rapid recovery of sound localization function following ablation of the posterior auditory field: Comparison with reversible deactivation, *Canadian Association for Neuroscience*. Montreal, QC.

14. **McMillan, AJ**, Lomber SG (2011) Increasing specificity for complex acoustic stimuli along a "what" processing pathway in auditory cortex. *Society for Neuroscience*, Washington, DC. Program No. 173.16.

15. Lomber, SG, **McMillan, AJ** (2011) Increasing specificity for complex acoustic stimuli towards the temporal pole of cat auditory cortex. *European Brain and Behaviour Society*, Seville, Spain. Program No. D10-014.

16. **McMillan, AJ**, Brown, TA, Joanisse, MF, Grahn, JA, Lomber, SG (2012) There is more than one way to scan a cat: An assessment of two imaging techniques for optimal auditory cortex activation in the cat. *Association for Research in Otolaryngology*. San Diego, CA. Program Number 511

17. Chabot, N, **McMillan, AJ**, Lomber, SG (2012) Cortical projections from auditory and visual cortex to the superior colliculus of the cat. *Association for Research in Otolaryngology*, San Diego, CA. Program Number 478.

18. **McMillan, AJ**, Brown, TA, Grahn, JA, Gati JS, Nixon, PL, Hughes, SM, Lomber, SG (2012) There's More Than One Way to Scan a Cat: Imaging Cat Auditory Cortex with High-Field fMRI using Sparse or Continuous Sampling. London Health Research Day. London, ON

19. Lomber, SG, **McMillan, AJ**, Carrasco, A, Cornwell, P (2012) A Hierarchically organized sound discrimination pathway in auditory cortex. Federation of European Neuroscience, Barcelona, Spain.

20. Lomber, SG, **McMillan, AJ**, Carrasco, A, Cornwell, P (2012) A Hierarchically organized sound discrimination pathway in auditory cortex. Canadian Association for Neuroscience. Vancouver, B.C.

21. **McMillan, AJ**, Lomber, SG, (2012) Tonotopy of auditory cortex in the cat using high-field fMRI. *International Auditory Cortex Conference*. Lausanne, Switzerland.

22. **McMillan, AJ**, Hall, CL, Lomber, SG (2012) Core auditory cortex of the cat revealed using high-field fMRI. *Society for Neuroscience*, New Orleans, LA.

23. **Hall, AJ**, Lomber, SG (2013) Core auditory cortex of the cat revealed using high-field fMRI. *Canadian Association for Neuroscience*. Toronto, ON.

24. **Hall, AJ**, Lomber, SG (2013) Core auditory cortex of the cat revealed using high-field fMRI. *London Health Research Day*. London, ON.

25. **Hall AJ** and Lomber SG (2014) Deliniation of tonotopically organized core and non-primary auditory cortex of the cat using high field fMRI. *Sothern Ontario Neuroscience Association*. London, ON.

26. Butler BE, **Hall AJ**, Lomber SG (2014) Imaging pitch processing in the cat auditory cortex with high field fMRI. Gordon Research Conference: Auditory System. Lewiston, Maine.

26. Butler BE, **Hall AJ**, Lomber SG (2014) Functional imaging of pitch perception in the auditory cortex of the cat. *International Auditory Cortex Conference*. Magdeburg, Germany.

27. **Hall AJ** and Lomber SG (2014) Activation patterns in non-primary auditory cortex using complex acoustic stimuli and high field fMRI. *International Auditory Cortex Conference*. Magdeburg, Germany.

Honors and Awards

2014 Western Graduate Research Scholarship (WGRS) providing tuition for the Fall 2014 academic term at the University of Western Ontario

2013 Western Graduate Research Scholarship (WGRS) providing tuition for the 2013 academic year at the University of Western Ontario.

2012 Advances and Perspectives in Auditory Neurophysiology (APAN) travel award. $500.

Women in Neuroscience travel award to attend the 2012 Society for Neuroscience meeting. $1000

Association for Research in Otolaryngology (ARO) Graduate student travel award to attend the 2012 annual meeting. $500

2011 Western Graduate Research Scholarship (WGRS) providing tuition for the 2011 academic year at the University of Western Ontario.

2010 Western Graduate Research Scholarship (WGRS) providing tuition for the 2010 academic year at the University of Western Ontario.

2008 Graduate Research Award from the School of Graduate and Postdoctoral Studies at the University of Western Ontario providing financial support for completion of master's thesis.

2007 Western Graduate Research Scholarship (WGRS) providing tuition for the 2007 academic year at the University of Western Ontario.

2006 Western Graduate Research Schoarship (WGRS) providing tuition for the 2006 academic year at the University of Western Ontario.

2005 University of Texas Graduate Scholarship providing tuition for the 2005 academic year at the University of Texas at Dallas.

Cold Spring Harbor Laboratories Scholarship to attend the *Structure, Function, and Development of the Visual System* two week course. $1000

Dean of Behavioral and Brain Sciences award providing additional support to attend the Cold Spring Harbor Laboratories course. $1000

2004 Faculty of Undergraduate Neuroscience (FUN) travel award to attend the 2004 Society for Neuroscience (SfN) conference.

Dean of Behavioral and Brain Sciences list for academic excellence.

Research Experience and Training

2006 – Present
Dr Stephen G. Lomber, PI
Cerebral Systems Laboratory
Department of Physiology and Pharmacology,
Western University
London, Ontario

2003-2006
Dr Stephen G. Lomber, PI
Cerebral Systems Laboratory
School of Behavioral and Brain Sciences,
The University of Texas at Dallas
Richardson, Texas

Relevant Work Experience

July 2008 – August 2010
Research Assistant
P.I. – Stephen G Lomber
Cerebral Systems Laboratory

Duties Included: Writing and editing of manuscripts for publication; Designing and creating figures for publication and presentation; Preparation for and assisting during surgical procedures; Post-surgery monitoring and recovery; Collection of data in behavioral, anatomical, and electrophysiological experiments; Preparation of institutional protocols; Management of all aspects of the laboratory environment including maintenance of equipment and ensuring that necessary supplies are available; Manufacturing cryo-loops for implantation; Research into, and implementation of, new techniques to be used; Designing and producing posters for conferences; Training students on techniques used within the lab; Monitoring of student progress; Maintenance of personnel information; Literature research.

Professional Societies

Society for Neuroscience (SfN)
Association for Research in Otolaryngology (ARO)
Canadian Association for Neuroscience (CAN)

Professional Training

May 2014
Evaluation and Feedback
Continuing Professional Development
Schulich School of Medicine and Dentistry
Western University
London, Ontario
Canada

February 2014
Time Management: Improving Professional and Personal Productivity
Continuing Professional Development
Schulich School of Medicine and Dentistry
Western University
London, Ontario
Canada

July 2011
fMRI Image Acquisition and Analysis Course
The Mind Research Network for Neurodiagnostic Descovery
The University of New Mexico
Albuquerque, New Mexico
USA

June 2005
Structure, Function, and Development of the Visual System
Cold Spring Harbor Laboratories
Cold Spring Harbor, New York
USA

Educational Training and Experience

Certifications

April 2014
Western Certificate in University Teaching and Learning
The Teaching Support Center
Western University
London, Ontario
Canada

Training

January 2014
Education Research and Scholarship: Tips for Clinicians and Teachers
Continuing Professional Development
Schulich School of Medicine and Dentistry
Western University
London, Ontario
Canada

October 2013
Designing Your Teaching Road Map
Continuing Professional Development
Schulich School of Medicine and Dentistry
Western University
London, Ontario
Canada

Fall 2012
The Theory and Practice of University Teaching graduate course
The Teaching Support Center
Western University
London, Ontario
Canada

Guest Lecturer

April 10, 2013
Guest Lecturer – Mental Illness
Introduction to Neuroscience (NEURO 2000)
Western University

February 14, 2012
Guest Lecturer – Perception and Action
Sensation and Perception (PSY 2115)
Western University

January 16, 2012
Guest Lecturer – Oral Mucosa: Hard Palate and Tongue
Dental Histology (DENT 5140)
Western University

Teaching Experience

Fall 2014
Teaching Assistant
Introduction to Neuroscience (NEURO 2000)
Western University

2013 academic year
Teaching Assistant
Introduction to Neuroscience (NEURO 2000)
Western University

2012 academic year
Teaching Assistant
Introduction to Neuroscience (NEURO 2000)
Western University

2012 academic year
Teaching Assistant
Systemic Human Anatomy (ACB 3319)
Western University

Fall 2011
Teaching Assistant
Physiology of the Senses (PHYS 4710)
Western University

Fall 2011
Teaching Assistant
Dental Histology (DENT 5140)
Western University

Fall 2010
Teaching Assistant
Dental Histology (DENT 5140)
Western University
Fall 2010
Teaching Assistant
Neuroscience for Rehabilitation Sciences (ANA 9551)
Western University